Growth factor independence 1b –

A novel tumor suppressor in acute myeloid leukemia

Inaugural – Dissertation

zur

Erlangung des Doktorgrades

Dr. rer. nat.

an der Fakultät für

Biologie

der Universität Duisburg-Essen

vorgelegt von

M.Sc. Molekularbiologie

Aniththa Thivakaran

aus Essen

Februar 2018

Die der vorliegenden Arbeit zugrundeliegenden Experimente wurden in der Abteilung für Hämatologie des Universitätsklinikums Essen durchgeführt.

1. Gutachter: PD Dr. med. Cyrus Khandanpour, MBA

2. Gutachter: Prof. Dr. med. Jürgen Becker

3. Gutachter: Prof. Dr. med. Christoph Schliemann

Vorsitzender des Prüfungsausschusses: Univ.- Prof. Dr. Ralf Küppers

Tag der mündlichen Prüfung: 30.08.2018

Table of Contents

Abbreviations

2-HG	2-hydroxyglutarate
ALL	Acute lymphoblastic leukemia
AMG	Aorta-gonad-mesonephro
AML	Acute myeloid leukemia
APL	Acute promyelocytic leukemia
Bonemarrow	BM
BSA	Bovine serum albumin
CD	Common differentiation
CLL	Chronic lymphocytic leukemia
CLP	Common lymphoid progenitor
CML	Chronic myeloid leukemia
CMP	Common myeloid progenitor
CN-AML	Cytogenetically normal AML
DCDFA	2'.7'–dichlorofluorescin diacetate
EFS	Event-free survival
EMP	Erythromyeloid lineage
ERK	Extracellular signal-regulated kinase
FBS	Fetal bovine serum
Fl/fl	Flox/flox
FoXO	Forkhead box subgroup O
Gfi1	Growth factor independence 1
Gfi1b	Growth factor independence 1b
GFP positive	GFP^+
GLFG	Glycine-lysine-phenylalanine-glycine
Green fluorescence protein	GFP
GSEA	Gene set enrichment analysis
H	Hour
H_2O_2	hydrogen peroxide
HGB	Hemoglobin
HSC	Hematopoietic stem cell
IDH1	Isocitrate dehydogenase 1
IDH2	Isocitrate dehydogenase 2
JNK	Jun N-terminal kinase
Ko	Knock-out
Kras	Kirsten rat sarcoma viral oncogene homolog
Lin^-	Lineage negative
LMPP	Lymphoid-primed multipotent progenitor
LPS	Lipopolysaccharide
LSC	Leukemic stem cell
LSD1	Lysine-specific demethylase
MAPK	Mitogen-activated protein kinase
MAPKK	Mitogen-activated-protein kinase kinase
MAPKKK	Mitogen-activated-protein kinase kinase kinase

MDS	Myelodyplastic syndrome
MEP	Megakaryocyte/erythrocyte progenitor
Min	Minute
MLL	Mixed lineage leukemia
MPP	Multipotent progenitor
MRP1	MDR –related protein1
MSigDB	Molecular signatures databases
NAC	N-Acetyl L-Cystein
NES	Normalized enrichment score
$O2^-$	superoxide anions
$OH^·$	hydroxyl radicals
OS	Overall survival
P/S	Penicillin/Streptomycin
PB	Peripheral blood
PBS	Phosphate buffered saline
PKB	Protein kinase B
PLT	Platelets
Poly (I: C)	polyinonsinic-polycytidylic acid sodium salt
RBC	Red blood counts
ROS	Reactive oxygen species
RT	Room temperature
RT-PCR	Real-Time PCR
Scf	Stem cell factor
Snail/Gfi	SNAG domain
Spleen	SPL
TF	Transcription factor
Tg	Transgene
VLA	Very late antigen
WBC	White blood counts
Wt	Wildtype

List of Figures

List of Tables

1 Introduction

1.1 Hematopoesis

Hematopoiesis is the dynamic process of blood cell formation. It was first described by Till and McCulloch (Till and Mc 1961). The development of hematopoietic stem cells (HSCs) begins during embryogenesis and proceeds in various hematopoetic organs, such as the yolk sac, the placenta, the fetal liver and the aorta-gonad-mesonephros (AGM) region. Lifelong blood cell production depends on (HSCs) and their ability to replenish their own compartment (“capacity of selfrenewal”) and to differentiate into progenitor cells and mature blood cells of multiple lineages (Seita and Weissman 2010). A current text book model of hematopoiesis is a simplified model highlighted like a hierarchical pyramid (Seita and Weissman 2010). HSCs reside in a “quiescent” state at the top of the hematopoietic hierarchy and give rise to functional mature effector cells (Bryder, Rossi et al. 2006). Initially, HSCs give rise to multipotent progenitors (MPPs) and lymphoid-primed multipotent progenitors (LMPPs) both lose the self-renewal capacity but gain full lineage differentiation potential. Further downstream, MPPs can differentiate into common lymphoid progenitor (CLP) and the common myeloid progenitor (CMP). CMP give rise to megakaryocyte/erythrocyte progenitors (MEPs) and granulocyte/macrophage progenitors (GMPs). Finally, these committed progenitor cells in turn give rise to the terminally differentiated cells of the hematopoietic system, such as erythrocytes, platelets, macrophages, granulocytes, lymphocytes, and natural killer (NK) cells (Seita and Weissman 2010). Recently it was published that MPP fraction can divide asymmetric to lymphomyeloid and erythromyeloid lineages (EMP) daughter cells (Görgens, Ludwig et al. 2014) (Figure 1). This out-differentiation of HSC into such very differently specialized functional hematopoietic cells is a very complex process which is regulated by a multitude of factors, for example, transcription factors (TFs ((later on:

GFI1B))), so at many levels dysregulation can occur, resulting in worst case in full-blown leukemia.))

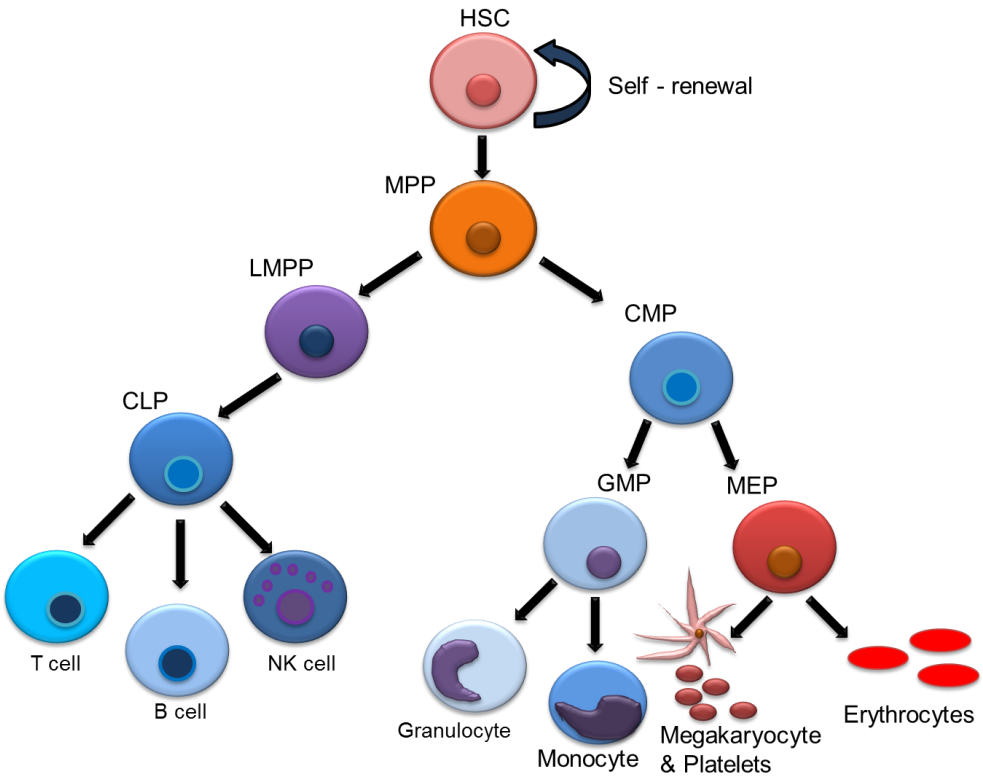

Figure 1: Simplified hierarchical hematopoietic system.

HSCs remain at the top level and possess two fundamental functions, namely self-renewal and differentiation, e.g., MPPs, which no longer have the ability to self-renew but keep the ability to differentiate into multiple progenitor cells, such as LMPPs and CMPs. LMPPs give arise to CLPs. CLPs can differentiate to T-, B-, and NK cells. In parallel, CMPs give rise to GMPs and MEPs. Further downstream, GMPs differentiate into granulocytes and monocytes, and MEPs give rise to erythrocytes and platelets. Adapted from (Görgens, Ludwig et al. 2014).

1.1.1 Myelodysplastic syndromes and acute myeloid leukemia

Myelodyplastic syndrome (MDS) is well characterized as a clonal hematopoietic disorder with an impaired function of HSC (Warlick, Cioc et al. 2009) and blood formation. Mostly, this disease is diagnosed in older patients. The patients suffer from anemia, thrombocytopenia, leukopenia, or pancytopenia, or they have recurrent infections (Hamblin 1992). Mainly, it affects hematopoiesis at the stem cell level as indicated by cytogenetic abnormalities, molecular mutations, and alterations of morphological and physiological features in the maturation and differentiation of one or several of the cell lineages. In the clinic, MDS patients are categorized into two different subgroups: lower-risk and higher-risk. The two subclasses are characterized by pathological and clinical features and by the probability of transforming into AML. Lower-risk MDS patients have severe cytopenias, and higher-risk MDS patients carry a major risk of transformation into AML (Fenaux and Ades 2013). About 33% of MDS cases can transform into acute myeloid leukemia (Barzi and Sekeres 2010).

Leukemia comprises different classification models, based on acute leukemia or chronic leukemia, the affected blood cell type (lymphoblastic and myeloid), the maturity stage of the blood cells and phenotypic appearance of the disease. There are five major types of leukemia: acute myeloid leukemia (AML), acute lymphoblastic leukemia (ALL), chronic myeloid leukemia (CML), chronic lymphocytic leukemia (CLL) and acute promyelocytic leukemia (APL) (Cook and Pardee 2013). AML is an aggressive neoplastic disease characterized by enhanced proliferation of immature cells, blocked differentiation mature cells, and dysregulated apoptosis (Smith, Beach et al. 2014). HSCs reside at the top of the hierarchical system and differentiate into mature cells. In acute myeloid leukemia, leukemia-initiating cells (LICs) are resided at the top of the hierarchical system (Bonnet and Dick 1997). There are at present two most commonly used classification systems for AML, the French-American-British (FAB) and the World Health Organization (WHO). The FAB classification system was defined in 1976 by a group of French, American and

British leukemia experts. They decided to classify AML into several subtypes, M0 through M7, based on the cell type from which the leukemia develops (Bennett, Catovsky et al. 1976) (Table 1).

Table 1: FAB classification.

Subtype	Description	Cytogenetics
M0	Undifferentiated acute myeloid leukemia	
M1	Acute myeloid leukemia without maturation	
M2	Acute myeloid leukemia with maturation	t(8;21)(q22;q22), t(6;9)
M3	Acute promyelotic leukemia	t(15;17)
M4	Acute myelomonocytic leukemia	inv(16)(p13q22), del(16q)
M4 Eos	Acute myelomonocytic leukemia with eosionophilia	inv(16), t(16;16)
M5	Acute monocytic leukemia	Monocytic leukaemia (M5b) del (11q), t(9;11), t(11;19)
M6	Acute erythroid leukemia	
M7	Acute megakaryoblastic leukemia	t(1;22)

In 2008, the WHO classification was updated to replace the FAB classification (Vardiman, Thiele et al. 2009). The novel classification distinguishes seven AML subtypes, (1) AML with the recurrent genetic abnormalities are RUNX1-RUNX1T1 t(8;21)(q22;q22); CBFB-MYH11 inv(16)(p13.1q22) t(16;16)(p13.1;q22); PML-RARA t(15,17)(q22;q12), MLL 11q23 abnormalities, etc.), and AML with gene mutations (Nucleophosmin 1 (NPM1) and CEBPA mutated gene); (2) AML with myelodysplasia-related changes; (3) therapy related myeloid neoplasms; (4) AML not otherwise specified (NOS) (similar to the FAB classification M0–M7 with others such as acute megakaryoblastic leukemia, acute panmyelosis with myelofibrosis, and pure erythroleukemia); (5) Myeloid sarcoma; (6) Myeloid proliferations related to Down syndrome; and (7) Blastic plasmocytoid dendritic cell neoplasm (Vardiman, Thiele et al.

2009; Saultz and Garzon 2016). Recently the WHO classification was updated with a new category called “myeloid neoplasms with germ line predisposition” (Dohner, Estey et al. 2017).

1.1.2 Morphology of leukemic cells

Leukemia subgroups were characterized based on the morphology of leukemic cells. Cytological characterization was subdivided into several groups, such as cytoplasm ratio, cell size, presence of nucleoli, and characteristics of the nuclear membrane (Miller, Leikin et al. 1981). In addition immunophenotype characterization was performed by using common differentiation (CD) markers. Both, AML blast cells or non-malignant immature myeloid cells express CD13, CD33, and CD34. Depending on the type of leukemia, monocytic differentiation markers such CD4, CD14 and CD11b, erythroid markers CD36 and CD71, and megakaryocytes markers (CD41 and CD61) (Saultz and Garzon 2016) are available. Bone marrow cells derived from M1-M5 AML patients were tested for antigen expression (Dubosc-Marchenay, Lacombe et al. 1992, Döhner, Estey et al. 2017) (Table 2), bold arrow= more frequent expression, normal arrow=less frequent expression).

Table 2: Expression of cell surface markers for the FAB classification.

FAB classification	Antigen expression
M1	CD14 ↑; CD34 ↑; CD15 ↑
M2	CD14 ↑; CD34 ↑; CD15 ↑
M3	CD14 ↑; CD34 ↑; CD15 ↑
M4	CD14 ↑; CD34 ↑; CD15 ↑
M5	CD14 ↑; CD34 ↑

1.1.3 Chromosomal translocations in AML

Animal models are used to study the AML development. At present, many murine leukemia models are available, such as carcinogen-induced models, viral and transposon models, transgenic models, and knocked-out models (Cook and Pardee 2013).

In the current study, I used three different mouse models containing different transgenetically different chromosomal translocations and thus represent models for the development of MDS/AML. Very common in hematologic malignancies is the *NUP98* gene, which can fuse to 15 different partner genes and is located on chromosome 11p15.5. It encodes a 98 kD protein that is important for the transport of RNA and proteins across the membrane (Slape and Aplan 2004). NUP98 possesses two major domains: N-terminal GLFG (glycine-lysine-phenylalanine-glycine), which facilitates the forming of a docking site for karyopherins, family members of nuclear transport signal receptor proteins (Rosenblum and Blobel 1999; Bayliss, Littlewood et al. 2002); and a C-

terminal auto-proteolytic domain (Rosenblum and Blobel 1999). The fusion proteins of NUP98 can be subdivided into two classifications, homeobox genes and nonhomeobox genes (Rosenblum and Blobel 1999). Yin-Wei Lin and colleagues found the fusion of *NUP98* with *HOXD11* or *HOXD13* in the malignant cells of patients with hematopoietic malignancies with the translocation t(2;11)(q31;p15), and they generated a transgenic mouse model to study the role of the *NUP98/HOXD13* gene in MDS/AML development (Lin, Slape et al. 2005).

A second mouse model used in this study is the conditional mouse model with mutated *Kras* oncogene. The protein belongs to the RAS pathway and has been implicated as a key component of the proliferative drive in AML. In general there are three members of the *RAS* genes containing four exons, N- (neuroblastoma cell line), K-(Kirsten) and H-(Harvey) *RAS (Cox and Der 2010).* These oncogenes were first discovered in human solid tumors more than 30 years ago, along with the gene mutations at codons 12, 13, and 61, which cause activation of the RAS protein (Janssen, Steenvoorden et al. 1987). Clinical case studies also implicated RAS mutations found in 12% to 27% of AML patients (Neubauer, Maharry et al. 2008).

The third AML model investigated in this study is the common mixed lineage leukemia (MLL), whose expression has been linked to inducing AML (Krivtsov, Feng et al. 2008). The *MLL* gene encodes a DNA-binding protein (H3K4) for regulating gene expression (Nakamura, Mori et al. 2002). The MLL protein is characterized for the maintenance and development in the hematopoiesis (Jude, Climer et al. 2007). Most common chromosomal rearrangements involving the *MLL* gene are *AF4*, *AF9*, *ENL*, *AF10*, *AF6,* and tandem duplications of the *MLL* gene are also found (*MLL-PTD*) (Quentmeier, Reinhardt et al. 2003).

The translocation t(9;11)(p2;q23), which encodes the oncogene MLL-AF9 fusion protein, is the most common chromosomal rearrangement in AML (Krivtsov and Armstrong 2007).

1.2 Transcription factor

Gene regulation is a fundamental process in each cell. Transcription factors are proteins that can activate or repress gene expression by binding to the DNA regulatory sequences of target genes (Lelli, Slattery et al. 2012). Many transcription factors are characterized in structure motifs that serve for binding to DNA. Such motifs are the helix-turn-helix motif, helix-loop-helix-motif, leucine zipper, homeodomain, and zinc-finger motifs.

Zinc finger proteins are one of the largest families of nucleic-acid –binding proteins in eukaryotic genomes (Laity, Lee et al. 2001). It is a simplified structure, containing one α helix and a β sheet held by a zinc molecule (Matharu, Hussain et al. 2010) (Figure 2). Many molecular functions such as DNA recognition, RNA packaging, transcriptional activation, and regulation of apoptosis are found in the zinc-finger family (Laity, Lee et al. 2001). Family members are subdivided into different classes based on their zinc-chelating residues, such as C_2H_2, CCHC and CCCC motifs. The snail superfamily transcription factor belongs to the C_2H_2 zinc-finger type; it acts as a transcriptional repressor (Hemavathy, Guru et al. 2000) and contains the SNAG domain (Snail/Gfi) for the repressor activity (Grimes, Chan et al. 1996).

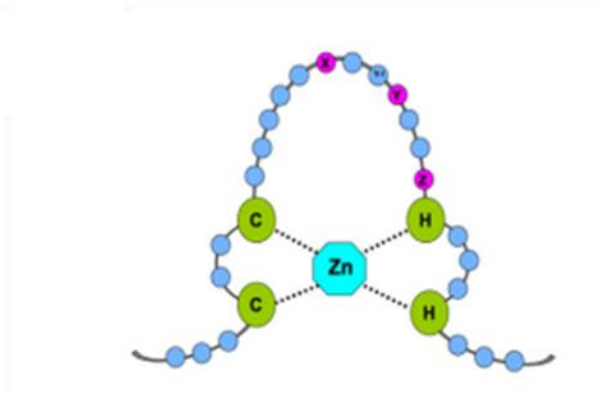

Figure 2: Structure of a C_2H_2 zinc finger.

Structurally, C_2H_2 are conversed with two cysteines and two histidines and are centered with one Zn-ion molecule. Adapted from (Matharu, Hussain et al. 2010).

1.2.1 Growth factor independence 1b

Growth factor independence 1b (Gfi1b) belongs to the zinc finger protein family and is important for the development of mature blood cells. The gene encoding Gfi1b was identified by its sequence homology with *GFI1*, which is a paralog to *GFI1B*, by its sequence homology with *Gfi1* and was mapped to chromose 9 of the human genome (9q34.13) (Rodel, Wagner et al. 1998; Tong, Grimes et al. 1998) . GFI1B contains three respective functional domains. The Snag domain is located at the N-terminus it possesses a recruiting element for histone-modifying enzymes, which act through the binding of cofactors lysine-specific demethylase (LSD1) and RCOR1/2 (COREST). In the middle, an intermediate domain is located, which is less well characterized by its functions. The C-terminal domain has a zinc finger DNA binding domain with six highly conserved C_2H_2-type zinc fingers. Especially fingers like 1, 2, and 6 are responsible for the protein interaction, while fingers from position 3 through 5 are necessary to bind at the DNA motif AATC (Moroy, Vassen et al. 2015). The short GFI1B isoform lacks the first two zinc fingers and consists of 284 amino acids, compared to the normal form of GFI1B with 330 amino acids (Figure 3).

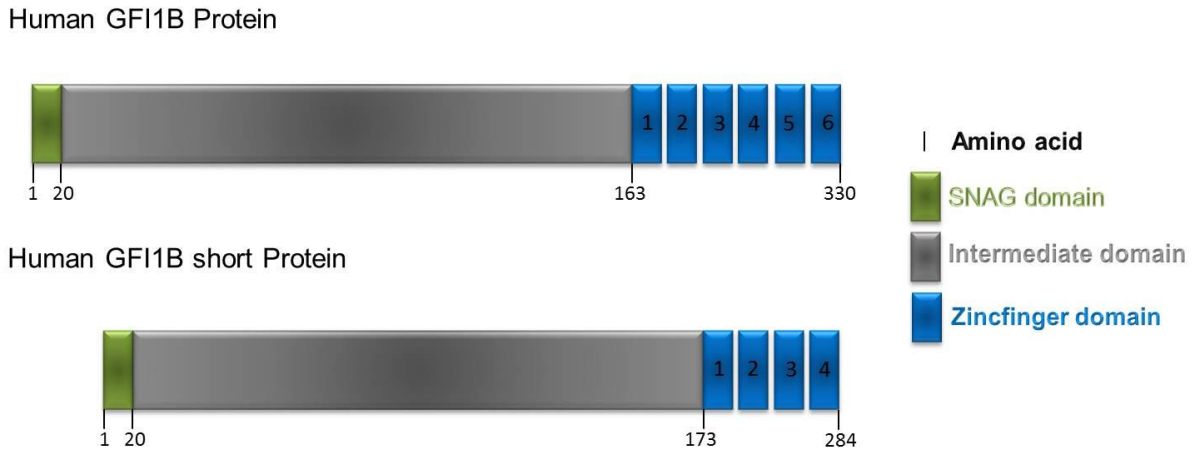

Figure 3: Structure of GFI1B.

The human GFI1B protein has two isoforms: The full-length protein has three domains with 330 amino acids, and the short form of GFI1B possesses 284 amino acids. Both isoforms share three functional domains: At the N-Terminus there is a snag domain (green), in the middle an intermediate domain and at the C-terminus a zinc-finger domain, whereby the short GFI1B protein has only four zinc fingers compared to the normal GFI1B protein (Adapted from (Moroy, Vassen et al. 2015).

The transcriptional regulation of GFI1B and its network is well characterized (Figure 4). The figure displays the function of GFI1B (repression or direct/indirect activation) and the target genes at the DNA– and protein levels (Anguita, Candel et al. 2017).

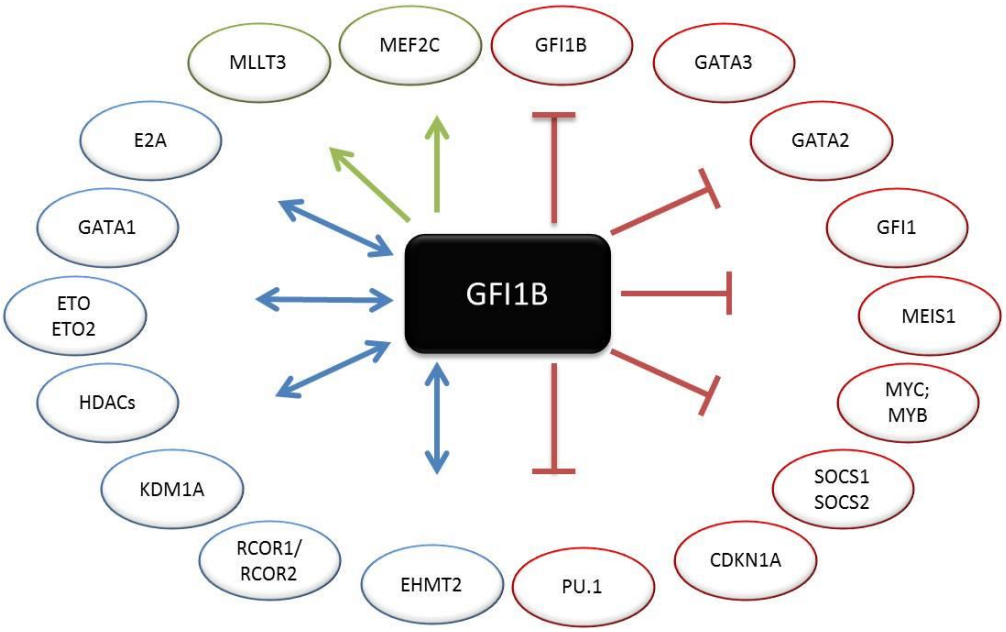

Figure 4: GFI1B functional network.
The transcription factor GFI1B can act as an activator or repressor, both directly or indirectly. In red are shown genes repressed by Gfi1b. Green arrows indicate the activation of genes by GFI1B which also interacts with other TFs and corepressors highlighted in blue. Abbreviations: Growth factor independence 1b (Gfi1b), Growth factor independence 1 (Gfi1), euchromatic histone lysine methyltransferase (Ehmt2) e, Rest corepressor1 (RCOR1), Rest corepressor2 (RCOR2), K-specific demethylase (KDM1A), Histone deacetylase (HDAC), Eight twenty one (ETO) , Eight twenty two (ETO2), Immunoglobin enhancer binding factor E12/E47 (E2a), Super elongation complex subunit (MLLT3), Myocyte enhancer factor 2c (MEF2C), cyclin dependent kinase 1A (CDKN1A), Suppressor of cytokine signaling 1(SOCS1), Suppressor of cytokine signaling 2(SOCS 2).(Adapted from (Anguita, Candel et al. 2017)).

Also *GFI1B* cis regulatory elements are well characterized. *GFI1B* possesses four cis regulatory elements; the first element lies in the first intron of the *GFI1B* gene (CNEi), and three lie downstream of the *GFI1B* gene: CNE+1, CNE+2 and CNE+3. These cis regulatory elements are conserved and contain erythroid/megakaryotic- specific transcription factor binding sites. Two of these sites, CNE+1 and CNE+2, are

characterized as an open chromatin conformation, which means it is an active chromatin site for gene regulation (Anguita, Villegas et al. 2010). A recent publication revealed that GFI1B represses its own gene expression by binding to its own promoter and recruiting the CoREST/LSD1 repressive complex (Anguita, Villegas et al. 2010). By examining of Gfi1-like binding sites at the *Gfi1b* promoter region, two tandem like sequences (AATC) at positions -59/-56 and -47/-44 were found as well (Huang, Kuo et al. 2005). Gfi1 and Gfi1b are both expressed in a complementary and partially overlapping manner in HSCs (Vassen, Okayama et al. 2007). By chromatin immunoprecipitation it was found that, the, Gfi1b/Lsd1/CoREST complex binds to the *Meis1* promoter in erythropoiesis, but not in megakaryopoiesis (Chowdhury, Ramroop et al. 2013). In a recent publication about Gfi1b, Tsukada and colleagues show over expression of murine *Gfi1b* in combination with two other TFs induces the formation of HSCs from iPSCs during teratoma formation *in vivo* (Tsukada, Ota et al. 2017). Overall the structure of GFI1B/Gfi1b is well characterized, as is the functional role of Gfi1b in hematopoiesis, bleeding disorders, and lymphoma (Xu and Kee 2007; Khandanpour, Sharif-Askari et al. 2010; Anguita, Candel et al. 2017). However, the role of GFI1B/Gfi1b in context of leukemia development is still unclear.

1.3 Reactive oxygen species

Reactive oxygen species (ROS) are by–products of aerobic organisms. ROS are defined as free oxygen radical molecules with one or more unpaired electrons in atomic or molecular orbitals (Karihtala and Soini 2007), superoxide anions ($O2^{-}$), hydrogen peroxide (H_2O_2), and hydroxyl radicals ($OH^{\cdot}$) (Trachootham, Alexandre et al. 2009). ROS molecules possess the ability to react easily with other molecules to form new compounds, because of the unpaired electrons. However, ROS are often linked with oxidative stress, which means that ROS induce pathology by damaging lipids, proteins

and DNA (Cross, Halliwell et al. 1987). ROS overproduction is implicated with numerous disorders such as age-related diseases, inflammatory conditions, cancer, cardiovascular and neurodegenerative diseases. The cause of the diseases is the imbalance between excessive formation of ROS and limited presence of antioxidants. ROS also act as second messengers for the expression of several TFs and signaling transduction molecules (Winterbourn and Hampton 2008). Most cancer cells try to counterbalance the level of ROS production in counterbalance, by holding the level of antioxidant activity in order to maintain redox balance (Gorrini, Harris et al. 2013).

1.3.1 The influence of ROS in HSC and LSC

Stem cells are important for the maintenance of functional tissues and organs. Functionally, stem cells have the ability to self-renew and replace damaged cells (Insinga, Cicalese et al. 2014). Low level of ROS control stem cells self-renewal and proliferative capacity (Ludin, Gur-Cohen et al. 2014). Principally, HSC are found in a quiescent state in the bone marrow stem cell niche (Yahata, Muguruma et al. 2008). If the ROS levels are increased, HSCs mobilize to more oxygen-containing areas of the BM niche, and they facilitate cell differentiation. An excessive amount of ROS alters the phenotype of HSCs (Yahata, Takanashi et al. 2011). However, immature leukemia blood cells are produce higher levels of ROS compared to normal leukocytes. Maintaining the redox homeostasis, the balance between ROS and the activity of antioxidant enzymes, is important for leukemia cells. As mentioned above, low levels of ROS act as second messengers and promote a number of molecules in several signaling cascades (Figure 6) (Finkel 2003). In leukemia, elevated levels of ROS induce genomic instability, survival and growth signaling, and motility (Finkel 2011). A moderate increase in ROS can promote cell proliferation and differentiation, but excessive level of ROS facilitates the activation of oxidative damage, as a result, DNA damage (Trachootham, Lu et al. 2008)

and oncogenes can transform normal cells to leukemic cells and promote leukemogenesis (Irwin, Rivera-Del Valle et al. 2013).

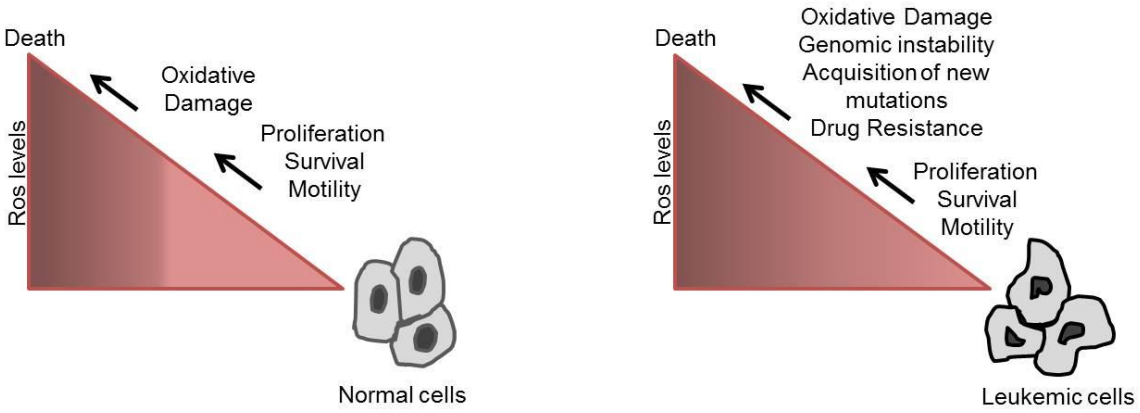

Figure 5: ROS level and different biological outcomes in normal and leukemic cells. /Adapted from (Irwin, Rivera-Del Valle et al. 2013)).
Normal cells have low basal levels of ROS. In non-leukemic cells (left panel), low levels of ROS are basically produced (bright triangle), which afford cell proliferation, survival and motility. When ROS levels are increased (darker shading), oxidative damage can appear in cells as a result of cell death. In contrast to normal cells, leukemic cells have permanent high ROS levels (darker shading in the filled triangle), because of alterations in redox control. Usually elevated ROS contributes the same benefits as low ROS levels in normal cells, but additionally causes genomic instability and drug resistance.

A relation between an increased level of ROS and AML relapse may be a critical factor for AML initiation and progression. Leukemic stem cells (LSCs) are characterized as a subpopulation of leukemia cells and possess stem cell–like characteristics. These rare subpopulations in leukemia cells are mostly located in an osteoblast-rich area of low oxygen pressure, and they have escaped from chemotherapy. Moreover, the LSCs have a less quiescent cycling activity, and they express P-glycoprotein, MDR –related protein1 (MRP1) and other proteins, which effects the drug efflux capacity on LSC and thus they are making them immune to chemotherapy (de Figueiredo-Pontes, Pintao et

al. 2008). Basically, genetic mutations or epigenetic alterations are directly relevant to ROS metabolism. These abnormalities can interrupt the balance between pro-oxidative and anti-oxidative states, which facilitates the excessive amount of ROS production (Wang, Jiao et al. 2010). Another study identified AML patients with 7% mutations of isocitrate dehydogenase 1 (IDH1) and 8% isocitrate dehydogenase 2 (IDH2). These driver mutations influence the normal enzymatic activity of IDHs, followed by decreased production of NADPH, alpha-KG, and glutathione and an increased level of oncometabolite 2-hydroxyglutarate (2-HG) (Hole, Pearn et al. 2010). AML patients with rate of 30% FLT3 mutations also present increased ROS productions (Zhang, Fang et al. 2014). Overall genetic abnormalities play an important role to control the imbalance between normal and increased ROS levels.

1.4 MAPK signaling and the function of p38

Mitogen-activated protein kinase (MAPK) cascades are key players in the transduction of extracellular signals to cellular responses. The family members belong to the class of serine/threonine kinases and are involved in a variety of cellular functions like cellular proliferation, differentiation, migration and apoptosis (Davis 2000, Kyriakis and Avruch 2001, Wada and Penninger 2004). MAPK signaling is stimulated by three kinase protein serine/threonine kinases, whereby MAPK is activated by phosphorylation by a mitogen-activated-protein kinase kinase (MAPKK) which rise the activation of mitogen-activated-protein kinase kinase kinase (MAPKKK) by phosphorylation (Dhillon, Hagan et al. 2007). Publications have validated six characterized groups of MAPK in mammalians, namely extracellular signal-regulated kinase (ERK)1/2, ERK3/4, ERK5, ERK7/8, Jun N-terminal kinase (JNK)1/2/3 and the p38 isoforms α/β/γ (ERK6)/δ (Schaeffer and Weber 1999). In this study I focused on the p38 MAPK module, which is activated by cellular stresses and responds to inflammatory stress. Family members are p38α (MAPK14), p38β

(MAPK11), p38γ (MAPK12) and p38 δ (MAPK13). All four protein kinases possess 60% amino acids sequence homology. The well-known characterized isoform in the family was p38 α (Cuenda and Rousseau 2007). It was independently identified by four groups as a 38 kDa protein (p38), in response to LPS (lipopolysaccharide) stimulation by phosphorylation on tyrosine residues (Han, Lee et al. 1994). p38 was found to be the homologue of *Saccharomyces cerevisisae* Hog1 (Brewster, de Valoir et al. 1993). At the same time two different groups identified that p38α functioned as a kinase-activated stress response (Rouse, Cohen et al. 1994) and as IL-10 (Freshney, Rawlinson et al. 1994). p38α and p38β are 75% homogeneous based on the amino acid sequence, while p38γ and p38δ share 62% identity. Four groups are encoded by different genes and have different tissue expression patterns. Frequently p38α is expressed in all cell types, whereas the expression of p38 β will be found in the brain, p38γ in skeletal muscle and p38δ in endocrine glands (Cuenda and Rousseau 2007). Activated MAPK kinases are responsible for various cell activities, like apoptosis, cell-cycle arrest, cytokine production, cell differentiation, cell senescence and tumor suppression, by activation or inhibition of several TFs or stimulators. The role of p38 and apoptosis in cancer cells is well distinguished, among others the ROS mediated stimulation of p38. For example in melanoma patients treated with betulinic acid, acts an inhibitor, induce apoptosis by ROS mediated activation of p38 (Tan, Yu et al. 2003). Another group showed that ROS-mediated activation of p38 induced differentiation of glioma-initiating cells from human glioblastomas (Sato, Okada et al. 2014). Ito et al. showed that ROS-associated p38 MAPK activation limited the lifespan of HSCs (Ito, Hirao et al. 2006). In contrast, another group tested activation of the ROS-p38 signaling pathway in AML patients and concluded that the level of p38 was low or even undetectable (Hole, Zabkiewicz et al. 2013).

1.5 Akt signaling and FoXO3

Akt, also known as protein kinase B (PKB) is a critical regulator of cell survival and proliferation. It is a serine/ threonine protein kinase and contains three family members, namely AKT1, AKT2 and AKT3 in mammalian cells (Song, Ouyang et al. 2005). AKT kinase acts as a mediators of a downstream signaling pathway by activating cytokine receptor, growth factor and PI3K in mammalian cells (Testa and Tsichlis 2005). AKT has been described in many human diseases (Nicholson and Anderson 2002). A mouse study showed that the constitutive activation of *Akt* accelerated AML progression (Kharas, Okabe et al. 2010). In AML, PI3K/AKT signaling pathways are activated in the more immature leukemic populations in AML patients (Park, Chapuis et al. 2010). Akt also regulates the forkhead box subgroup O (FoXO) family members; FoXO1, FoXO3, and FoXO4. FoXO proteins are important for the regulation of apoptosis, quiescence and oxidative stress response. FoXO3 can be phosphorylated by Akt at three conserved sites such as Thr32, Ser253 and Ser315 and the FoXO3 can exports to the cytoplasm, whereby dephosphorylated FoXO3 remain in the nucleus and induce the transcription of target genes (Park, Chapuis et al. 2010). The interface between AKT/FoXOs was studied in AML patients, and it described that AKT is repressed; thus FoXOs are activated in AML patient samples and act as an oncogene (Sykes, Lane et al. 2011).

1.6 Aim of the thesis

AML is characterized by an abnormal, uncontrolled proliferation of myeloid cells (Crans and Sakamoto 2001). TFs play a major role in the development of mature BM cells. Various TFs have been studied that are important regulators for hematopoiesis. The effect of disturbance of certain TFs has been studied in AML. Gfi1b is a TF that plays a critical role in HSC and erythroid/platelets differentiation. Gfi1b regulates function of normal HSC and I was interested whether it might also be involved in the regulation of leukemic stem cells (LSCs).

The following questions were specifically addressed in this thesis:

- Does the level of Gfi1b protein play a role in AML development?
- Does Gfi1b regulate number of LSCs?
- Which signaling pathways are altered and influence the emergence of LSC in cells with reduced Gfi1b level?
- Is Gfi1b an attractive option/ therapeutic target in the treatment of myeloid disease?

2 Materials and Methods

2.1 Material

2.1.1 Chemicals and Reagents

Table 3: Suppliers of reagents utilized in this study. Abbreviations are given in brackets.

Chemical/Reagent	Cat. No.	Suppliers
25mM $MgCl_2$	A3511	Promega, Mannheim, Germany
5X Green GoTaq® Reaction Flexi Buffer	M891A	Promega, Mannheim, Germany
Anisomycin	A9789	Sigma Aldrich, Taufkirchen, Germany
Annexin V Binding Buffer	556454	BD Biosciences, Heidelberg , Germany
Aqua	172328001	B. Braun, Melsungen, Germany
Baytril		Bayer, Leverkusen, Germany
BD Phosflow Fix Buffer I	557870	BD Biosciences, Heidelberg , Germany
BD Phosflow Perm Buffer III	558055	BD Biosciences, Heidelberg , Germany
Bovine serum albumin (BSA)	B9000S	New England Biolabs, Frankfurt am Main, Germany
Coulter Clenz Cleaning Agent	8546929	Beckmann Coulter, Krefeld, Germany
Deoxynucleotide Adenosin Triphosphates (dATP)	U1205	Promega, Mannheim, Germany
Deoxynucleotide Cytosin Triphosphates (dCTP)	U1225	Promega, Mannheim, Germany
Deoxynucleotide Guanin Triphosphates (dGTP)	U1215	Promega, Mannheim, Germany
Deoxynucleotide Thymin	U1235	Promega, Mannheim,

Triphosphates (dGTP)		Germany
Development Concentrate	00009	Adefo Chemie, Neu Isenburg, Germany
Dimethylsulfoxid (DMSO)	472301	Sigma Aldrich, Taufkirchen, Germany
EDTA	E9884-100G	Sigma Aldrich, Taufkirchen, Germany
Ethanol absolute	32205	Sigma Aldrich, Taufkirchen, Germany
Ethanol Solution 70%	02877	Sigma Aldrich, Taufkirchen, Germany
FACS Clean	340345	BD Biosciences, Heidelberg , Germany
FACS Flow	1716502821	BD Biosciences, Heidelberg , Germany
FACS Rinse	340346	BD Biosciences, Heidelberg , Germany
Fetal bovine serum	P30-3702	PAN^{TM} BIOTECH, Aidenbach, Germany
Fixation Concentrate	00062	Adefo Chemie, Neu Isenburg, Germany
FORENE 100% (V/V) (Isoflurane)		Abb Vie
Formaldehyde solution	F1635-500ML	Sigma Aldrich, Taufkirchen, Germany
Glycine	50046	Sigma Aldrich, Taufkirchen, Germany
Glycine	G8898-500G	Sigma Aldrich, Taufkirchen, Germany
GoTaq® Hot Start Polymerase	M5008	Promega, Mannheim, Germany
Leupeptin hemisulfate salt	L2884-5MG	Sigma Aldrich, Taufkirchen, Germany
Lineage cell depletion cocktail biotin	130-090-858	MLtenyi Biotec, Bergisch Gladbach, Germany
Marrow Max Bone Marrow Medium	12260-014	Life Technologies, Darmstadt, Germany
Murine IL-3	130-096-687	MLtenyi Biotec, Bergisch Gladbach, Germany
Murine IL-6	130-094-065	MLtenyi Biotec, Bergisch Gladbach, Germany

Murine SCF	130-094-079	MLtenyi Biotec, Bergisch Gladbach, Germany
Nonfat dried milk powder	A0830	AppliChem, Darmstadt, Germany
NuPAGE Antioxidant	NP0005	Novex, Life Technologies
NuPAGE LDS Sample Buffer 4x	NP0007	Novex, Life Technologies
NuPAGE MES SDS Running Buffer 20x	NP0002	Novex, Life Technologies
NuPAGE Sample Reducing Agent 10x	NP0004	Novex, Life Technologies
Oil Red O	SLBH1073V	Sigma Aldrich, Taufkirchen, Germany
Penicillin-Streptomycin	P4333	Sigma Aldrich, Taufkirchen, Germany
PharmLyse Lysis Buffer 10x	555899	BD Biosciences, Heidelberg , Germany
PMSF ≥99,0% (T)	78830-1G	Sigma Aldrich, Taufkirchen, Germany
Polybrene	TR-1003-G	Merck Millipore, Billerice, U.S.A
Polyinonsinic-polycytidylic acid sodium salt	P0913-50mg	Sigma Aldrich, Taufkirchen, Germany
Power SYBR®Green PCR Master Mix	4367659	Gibco, Life Technologies, Darmstadt, Germany
Protein G Agarose (2mL)	11719416001	Roche
Proteinase K	P6556-5MG	Sigma Aldrich, Taufkirchen, Germany
Retronectin Recombinant Human Fibronectin Fragment	T100B	Clontech, Saint-German-en-Laye, France
RNase A	R6513-10MG	Sigma Aldrich, Taufkirchen, Germany
Sodium bicarbonate ($NaHCO_3$)	S6014-500G	Sigma Aldrich, Taufkirchen,Germany
Sodium butyrate (NaBu)	B5887-1G	Sigma Aldrich, Taufkirchen, Germany
Sodium chloride (NaCl)	S9888-500G	Sigma Aldrich, Taufkirchen, Germany
Sodium deoxycholate monohydrate	D5670-5G	Sigma Aldrich, Taufkirchen, Germany

Tergitol® solution (Type NP-40)	NP40S-100ML	Sigma Aldrich, Taufkirchen, Germany
TrisCL	T5941	Sigma Aldrich, Taufkirchen, Germany
Trizma® Base (Tris)	T1503-100G	Sigma Aldrich, Taufkirchen, Germany
Trypan blue solution	T8154	Sigma Aldrich, Taufkirchen, Germany
Trypsin-EDTA	1848040	Gibco, Life Technologies, Darmstadt, Germany
Tween 20	P9416	Sigma Aldrich, Taufkirchen, Germany
β-Mercaptoethanol	M3148	Sigma Aldrich, Taufkirchen, Germany

2.1.2 Kits

Table 4: List of kits used in this study.

Kit	Cat. No.	Supplier
Advantage RT-for-PCR Kit	639505	Clontech, Saint-German-en-Laye, France
Amersham ECL Prime Western Blotting Detection Reagent	RPN2232	GE Healthcare, Solingen, Germany
Cellular Reactive Oxygen Species Detecton Assay Kit	ab113851	Abcam, Cambridge, United Kingdom
EndoFree© Plasmid Maxi Kit from QIAGEN	12362	Qiagen, Hilden, Germany
Lineage Cell Depletion Kit	552598	Miltenyi Biotec, Bergisch Gladbach, Germany
NE-PER Nuclear and Cytoplasmic Extraction Reagents	78833	Thermo Scientific, Schwerte, Germany
Pierce BCA Protein Assay Kit	23225	Thermo Scientific, Schwerte Germany
QIAamp DNA Blood Mini Kit	51106	Qiagen, Hilden, Germany
Qiagen PCR purification kit (50)	28104	Qiagen, Hilden, Germany
RNeasy Mini Kit	74104	Qiagen, Hilden, Germany

Taqman Master Mix	4369016	Applied Biosystems, Darmstadt, Germany

2.1.3 Instruments

Table 5: List of instruments used for this study.

Instrument	Supplier
BD FACSVantage SE	BD Biosciences, Heidelberg, Germany
Beckman Coulter counter Z2	Beckman Coulter, Krefeld, Germany
Biological safety cabinet classII	NuAire, Plymouth, U.S.A
Bioruptor® Plus sonication device	Diagenode, Belgien
Cellsorter FACSAria II	BD Biosciences, Heidelberg, Germany
Cellsorter FACSDiva	BD Biosciences, Heidelberg, Germany
Centrifuge 5415C	Eppendorf, Hamburg, Germany
Centrifuge 5415R	Eppendorf, Hamburg, Germany
Centrifuge Allegra 21R	Beckman Coulter, Krefeld, Germany
Centrifuge Rotana 460R	Hettich, Kirchlengern, Germany
Centrifuge Rotana 50RS	Hettich, Kirchlengern, Germany
CO2 incubator , Water- jacketted	Thermo Scientific, Braunschweig, Germany
Cytospin 2, Shandon	Thermo Scientific, Braunschweig, Germany
Flowcytometer BD FACScan	BD Biosciences, Heidelberg, Germany
Flowcytometer BD LSRII	BD Biosciences, Heidelberg, Germany
Freezing container, Nalgene® Mr.Frosty	Sigma Aldrich, Taufkirchen, Germany
Hirschmann automatic pipettes	Hirschmann Laborgeräte GmbH & Co. KG, Eberstadt, Germany
Incubator 1000	Heidolph, Schwabach , Germany
Micro-centrifuge	Hettich, Kirchlengern, Germany
Microplate reader, iMark	Bio-Rad, München, Germany
Microscope DFC 450C	Leica Biosystems, Wetzlar, Germany
Microscope DM1000LED	Leica Biosystems, Wetzlar, Germany
Microscope Olympus CK2	Olympus, Hamburg, Germany
Min Elute ® reaction Clean up Kit(50)	Qiagen, Hilden, Germany
Mini-centrifuge	Bio-Rad, München, Germany

Multi-tips Micro-pipet, 300 µL	Eppendorf, Hamburg, Germany
Nanophotometer P330	Implen, Germany
Neubauer Chambers 0,1 mm	Assistent, Sondheim, Germany
Pipets 10 µL, 100 µL , 200 µL and 1 mL	Eppendorf, Hamburg, Germany
StepOne Plus Real-Time PCR System	Applied Biosystems, Darmstadt, Germany
Sysmex XE-2100 blood analyzer	Sysmex Europe GmbH, Norderstedt, Germany
Thermocycler Flex Cycler	Analytik Jena, Jena, Germany
Thermomixer comfort	Eppendorf, Hamburg, Germany
Vortexer Genius 3	IKA, Staufen, Germany
x-Ray machine X-RAD 320	Precision X-ray Inc.

2.1.4 Consumables

Table 6: List of consumables used in this study.

Article	Cat. No.	Supplier
BD Eclipse Needle (0,5mm x 25mm(25G x 1))	305891	BD Biosciences, Heidelberg, Germany
BD Eclipse Needle (0,9mm x 40mm(20G x ½ TW))	305888	BD Biosciences, Heidelberg, Germany
Cell Container with cover	5515040	Ratiolab, Dreieich, Germany
Cell culture flask, 25 cm^2 with filter cap	90025	Greiner Bio-One, Solingen, Germany
Cell culture insert 12 well-plate	353090	Greiner Bio-One, Solingen, Germany
Cell filters 100 µm (Nylon)	542000	BD Biosciences, Heidelberg, Germany
Cell filters 40 µm (Nylon)	542040	BD Biosciences, Heidelberg, Germany
Centrifuge tube Falcon, 50 mL, sterile	227261	Greiner Bio-One, Solingen, Germany
Centrifuge tubes Falcon, 15 mL, sterile	188271	Greiner Bio-One, Solingen, Germany

Cytospin slide	27157	Thermo Scientific, Braunschweig, Germany
Disposable scalpel, sterile		Medi-ware, Wesel, Germany
Graduated pipettes, 10 mL sterile, single use	607180	Greiner Bio-One, Solingen, Germany
Graduated pipettes, 5 mL sterile, single use	606180	Greiner Bio-One, Solingen, Germany
Microcentrifuge tube, 1.5 mL, single use	S1615-5510	STARLAB GmbH, Hamburg, Germany
Micro-Hematocrit-capillaries, CE, heparinized	180950	BRAND GmbH; Wertheim, Germany
Mini-Collect-blood collection tubes, K3EDTA, 0.25 mL	450476	Greiner Bio-One, Solingen, Germany
Multiwell™ plate 12 well, Non-tissue culture treated	353043	BD Biosciences, Heidelberg, Germany
Multiwell™ plate 24 well, Non-tissue culture treated	351147	BD Biosciences, Heidelberg, Germany
Multiwell™ plate 6 well, Non-tissue culture treated	353046	BD Biosciences, Heidelberg, Germany
Pipette tips 1 mL	S1126-7810	STARLAB GmbH, Hamburg, Germany
Pipette tips 10 µL	S1121-3810	STARLAB GmbH, Hamburg, Germany
Pipette tips 100 µL	S1123-1840	STARLAB GmbH, Hamburg, Germany
Pipette tips 200 µL	S1120-8810	STARLAB GmbH, Hamburg, Germany
Syringe 1 mL	303173	BD Biosciences, Heidelberg, Germany
Syringe 5 mL	309050	BD Biosciences, Heidelberg, Germany
Whatman gel blotting paper Grade GB003	WHA10547922	Sigma Aldrich, Taufkirchen, Germany

2.1.5 Primers used in this study

Table 7: Primers for genotyping of mice.

Primer	Sequence
Forward primer	5‘- GGT TTC TAC CAG TCT GGC CCT GAA CTC -3’
Reverse primer (*Gfi1b* WT)	5‘- TAC ATT CAT GCT TAG AAA CTT GAG TC -3’
Reverse primer (*Gfi1b* KO)	5‘- CTC ACC TCT CTG TGG CAG TTT CCT ATC -3’

Table 8: Taqman primers used in this study.

Gene	Gene Product	Primer ID	Suppliers
Atm	murine *Atm*	Mm01177457_m1	Life Technologies, Darmstadt, Germany
Cdknb1	murine *Cdknb1*	Mm00438168_m1	Life Technologies, Darmstadt, Germany
Hrpt	murine *Hrpt*	Mm03024075_m1	Life Technologies, Darmstadt, Germany
Meis1	murine *Meis1*	Mm00487664_m1	Life Technologies, Darmstadt, Germany

Table 9: Primers for SYBR Green assay used in this study.

Gene	Sequence
***Gfi1b* forward**	5‘- CTGGCCTCCTGCTGTAATTC-3‘
***Gfi1b* reverse**	5‘- GGGGGTCTGTGTGTAGCTGT-3‘
***Hprt* forward**	5‘- AGTGTTGGATACAGGCCAGAC-3‘
***Hprt* reverse**	5‘- CGTGATTCAAATCCCTGAAGT-3‘

2.1.6 Antibodies

Table 10: List of antibodies used for Western Blots.

Antigen	Cat. No.	Species	Dilution	Supplier
primary antibodies				
Gfi1b (D-19)	sc-8559	goat	1:400	Santa Cruz Biotechnology, Heidelberg Germany
Pcna	9466	rabbit	1:500	Santa Cruz Biotechnology, Heidelberg Germany
secondary antibodies				
Chicken anti-rabbit	sc-516087		1:5000	Santa Cruz Biotechnology, Heidelberg Germany
Donkey anti-goat	sc-2020		1:5000	Santa Cruz Biotechnology, Heidelberg Germany

Table 11: List of antibodies used for Chromatin Immunoprecipitation.

Antigen	Cat.No.	Used volume/reaction	Supplier
H3K9acetyl	ab4441 (50µl)	1 µL	Abcam, Cambridge, United Kingdom
Rabbit IgG	15006	1 µL	Sigma Aldrich, Taufkirchen, Germany

Table 12: List of antibodies used for flow cytometry. All antibodies were anti-mouse.

FACS Antibody	Conjugate	Cat. No.	Supplier
Akt (pS473)	PE	561671	BD Biosciences, Heidelberg, Germany
Annexin V	FITC	640906	Biolgend, Koblenz, Germany
Annexin V	APC	640920	Biolgend, Koblenz, Germany
B220	PerCP	RA3-6B2	Biolgend, Koblenz, Germany
CD117	PE	135106	Biolgend, Koblenz, Germany
CD117	Brilliant Violet 421	105827	Biolgend, Koblenz, Germany
CD11b	PerCP	101228	Biolgend, Koblenz, Germany
CD16/32	PE/Cy7	93	Biolgend, Koblenz, Germany
CD4	PerCP	100433	Biolgend, Koblenz, Germany
CD45	PE	103106	Biolgend, Koblenz, Germany
CD45	PerCP	103113	Biolgend, Koblenz, Germany
CD8	PE	100708	Biolgend, Koblenz, Germany
Fixable viability dye	eFluor 780	65-0865-14	eBioscience
Gr1	PE	108408	Biolgend, Koblenz, Germany
IgG1 κ Isotype control	PE	551436	BD Biosciences, Heidelberg, Germany
p38 MAPK (pT180/pY182)	PE	612565	BD Biosciences, Heidelberg, Germany
Ter119 murine	PE	116208	Biolgend, Koblenz, Germany

2.1.7 Buffers

Table 13: List of buffers with components used in this study.

Buffer	Components	Supplier
Annexin binding buffer	Stock solution; Cat. No. 5281679, Diluted 1:10 in H_2O	Bioscience, Franklin Lakes, United States of America (U.S.A.)
PD Cytofix/Cytoperm buffer	Ready to use, Cat. No. 51-2090KE	BD Pharmingen™, Heidelberg, Germany
PD Cytoperm permeabilization buffer plus	Ready to use, Cat. No. 51-2356KC	BD Pharmingen™, Heidelberg, Germany
FACS buffer	PBS +2.5% FCS +1% Penicillin/Streptomycin	
Perm/ wash buffer	Ready to use Cat. No.51-2091KE	BD Pharmingen™, Heidelberg, Germany
RLT lysis buffer	Ready to use, Cat. No. 151042586	Qiagen, Hilden, Germany
MACS buffer	PBS pH 7.2 0.5% BSA 2mM EDTA	
1x SDS-Running buffer	950 mL H_2O 50 mL NuPage™ MES SDS Running buffer 20X	
10x TG buffer	30g Tris base 144g Glycine 1L VE H_2O	
1x TG buffer	200 mL absolute Ethanol 100 mL TG buffer 700 mL VE H_2O	
10x TBS	200 mM Tris 1.5 M NaCl dissolve in H_2O pH=7.2	
1x TBS-T	900 mL H_2O 100 mL 10x TBS 1 mL (0.1%) Tween 20	

2.1.8 Software programs

Table 14: List of programs used in this study.

Program	Manufacturer	Function
BD Diva	BD Biosciences	Software for compensation tool at LSRII
FlowJo-Software	Miltenyi Biotec,	Analysis of flow cytometry results
GraphPad Prism 6	GraphPad Software	Analysis of all results
Microplate Manager 6 Software	Biorad	Analysis for protein estimination
StepOnePlus	Applied Biosystems	Calculation and analysis of RT-PCR results

2.2 Methods

2.2.1 Nucleic acid procedures

2.2.1.1DNA extraction

DNA from bone marrow (BM) cells was purified using the QIAmp DNA Blood Mini Kit from QIAGEN, following the manufacturer's instructions see Table 3 and Table 4. Briefly, 5x106 BM cells were taken in 200 µL PBS and 20 µL protease. For a cell lysis buffer AL was added to the sample and mixed by pulse-vortexing; it was incubated at 56 °C for 10 min. In the next step, 200 µL absolute ethanol was added to the sample and was again mixed by pulse-vortexing. The mixture was transferred to the QIAmp Mini spin column and was centrifuged. In order 500 µL of AW1 and AW2 buffers were applied to the column and were centrifuged at 6000 x *g* for 1 min by using a micro centrifuge (Table 5). Finally, DNA elution was performed with buffer AE and DNA was stored for further experiments.

2.2.1.2Plasmid DNA preparation

Bacteria were grown as described in 2.2.5.2. Extraction of plasmid DNA was performed by using an EndoFree© Plasmid Maxi Kit from QIAGEN according to the supplier's recommendations (see in Table 3,Table 4,Table 5).

2.2.1.3RNA extraction

RNA extraction was performed using the RNeasy Mini Kit from QIAGEN following the manufacturer's recommendations (Table 4). Briefly, $5x10^6$ BM cells were washed with

500 µL PBS and centrifuged at 338 x *g* for 5 min. BM pellet was resuspended with a 1 mL syringe attached to a 20G needle with 350 µL RLT-buffer containing 3.5 µL ß-Mercapthoethanol and was centrifuged at 14000 rpm for 3 min by using a micro centrifuge. The supernatant was applied in a new Eppendorf tube and was resuspended with 350 µL of 70% ethanol. The mixture was applied to the RNeasy spin column and was centrifuged at 10.000 rpm for 15 seconds. The flow-through was discarded and 700 µL of RW1 buffer was pipetted on the column. In the following steps 500 µL RPE buffer was applied twice to the column and centrifuged at 10000 rpm for 2 min. The column was placed in a new eppendorf tube and RNA was eluated with 30 µL RNAse-free H_2O.

2.2.1.4 cDNA synthesis

For Real Time PCR 0.5 µg of RNA was converted to cDNA. Briefly, a master-mix was prepared as mentioned in Table 15 by using reagents from the Advantage RT-for –PCR Kit (Table 4). All tubes were briefly spun down and afterwards placed on ice. A total of 0.5 µg RNA was added in a 0.5 mL microcentrifuge tube (Table 6) and was filled up to 12.5 µL with DEPC-H_2O. 1 µL of oligo dT was added and the tube was incubated at 70°C for 2min. The tube was then cooled on ice and 6.5 µL of the mastermix was added to the same tube. The reaction was incubated at 42 °C for 1 h. After cDNA synthesis 80 µL of DEPC-H_2O was added to the microcentrifuge tube.

Table 15: Reagents for cDNA synthesis.

Component	Volume pro reaction
5 x RT buffer	4 µL
dNTP Mix	1 µL
RNase Inhibitor	0.5 µL
MMLV Reverse Transcriptase	1 µL
Total volume/tube	6.5 µL

2.2.1.5Nucleic acid quantification

For the purity and the concentration of the nucleic acid 1 µL of sample was taken for the measurement. Initially the machine was blanked either with AE buffer for the DNA sample, RNAse-free H_2O for the RNA sample and TE buffer for the plasmid sample. Measurement was performed with a nanophotometer (Implen).

2.2.1.6Genotyping Polymerase Chain Reaction (PCR)

For the genotyping of the *Gfi1b* gene in our mice (see 2.2.7.2) PCR was performed. This technique was described by Kary B. Mullis in 1990 (Mullis 1990) and allows amplification of a specific DNA fragment in three reaction steps denaturation, annealing, and extension. To apply this method, components are needed such as template DNA, nucleotides, designed forward and reverse primer and the DNA polymerase enzyme (Garibyan and Avashia). Following the designed primers (Table 7) and reaction set up (Table 16) were used for the PCR.

Table 16: PCR reaction mix.

Component	Amount	Final Concentration
Forward primer	0.6 µL	20 µM
Reverse primer (*Gfi1b* WT)	0.6 µL	20 µM
Reverse primer (*Gfi1b* KO)	0.6 µL	20 µM
Deoxynucleotide Mix	0.16 µL	25 mM
Green GoTaq©Reaction Buffer	5 µL	1X
Taq DNA polymerase	0.1µL	5 U/µL
$MgCl_2$	1.4 µL	25 mM
Template DNA	2 µL	
Water	13.29 µL	
DMSO	1.25 µL	
Total volume	25 µL	

All the components were mixed and centrifuged gently in order to collect all the components at the bottom of the PCR tubes. Finally PCR was performed by using the parameters shown in Table 17.

Table 17: PCR cycle step.

Cycle step	Temperature	Time	Number of cycles
Activation of AmpliTaq	95°C	10min	1 x
1 Denaturation	95°C	15 sec	35 x
2 Annealing	58°C	30 sec	
3 Extension	72°C	1 min	
Final extension	72°C	3 min	
	4°C	infinite	

The amplified DNA was separated by 1.5% agarose gel electrophoresis at 90 V for 30-45 min.

2.2.1.7Real Time PCR (RT-PCR)

Real- Time PCR (RT-PCR) was performed to detect and quantify the expression profiles of selected genes (see Table 8). In RT-PCR, the measurement can be detected via fluorescence signal. Based on the principle of method 1 the TaqMan probes are labeled with a fluorescent reporter dye at the 5' end and with a quencher dye at the 3' end. The 5' nuclease activity of Taq polymerase cleaves the probe, resulting in an increase of fluorescence signal in each cycle because the quencher is distant from the 5' label, proportional to the amount of probe cleaved (Huggett, Dheda et al. 2005). In contrast, in method 2, SYBR Green binds to double - stranded DNA, and the fluorescence signal increases by accumulation of PCR products. In this study, I used both applications. For detection of the different expression levels of *Gfi1b* in BM cells, we used designed primers and SYBR Green dye (Table 9). Mastermix was prepared according to Table 18.

Table 18: Mastermix for Real-Time PCR.

Reagent	Pro reaction
TaqMan Gene Expression Master-Mix 2x	10 µL
TaqMan Gene Expression assay	1 µL
H_2O	4.5 µL
Total volume	15.5 µL

For RT-PCR, 15.5 µL of master-mix was added in each well of a 96-well plate and 1 µL of synthesized cDNA sample was added to the respective wells. The reaction was run by using the StepOnePlus thermocycler and the analysis was performed by using the ddCt method in Excel (Rao, Huang et al. 2013). I used *Hprt* as a housekeeper gene.

2.2.2 Protein procedures

2.2.2.1Protein extraction

Protein extraction was performed with NE-PER Nuclear and Cytoplasmic Extraction Reagents from Thermo Fisher Scientific. $3x10^7$ BM cells were prepared, and proteins were isolated according to the suppliers' recommendations.

2.2.2.2Protein concentration measurement

Protein concentrations were determined using a bovine serum albumin (BSA) stock (200 µg/ mL) for standardization, and the working reagents were used from the Pierce BCA Protein Assay Kit. BSA was serially diluted in order to determine the concentration of nuclear or cytoplasmic proteins (Table 19). Depending on where the protein of interest was localized in the cell, CER or NER buffers were used for the dilutions.

Table 19: BSA standard serial dilutions for protein concentration estimations.

Vial	BSA concentration [µg/mL]	Dilution
A	2000	300 µL BSA stock (2000 µg/mL)
B	1500	375 µL BSA stock + 125 µL NER/CER
C	1000	325 µL BSA stock + 325 µL NER/CER
D	750	175 µL of vial B + 175 µL NER/CER
E	500	325 µL vial C + 325 µL NER/CER
F	250	325 µL vial E + 325 µL NER/CER
G	125	325 µL vial F + 325 µL NER/CER
H	25	100 µL vial G + 400 µL NER/CER

According to Pierce's recommendation, working reagents A and B from the BSA Protein Assay Kit were mixed in a 1:50 ratio. 200 µL of the mixed reagent were added to each well of a 96-well non-tissue culture treated plate with a flat bottom. 10 µL of the various standard dilutions were added to the corresponding wells. The protein samples were diluted in a ratio of 1:5 either with NER buffer for nuclear-extracted proteins or CER buffer for cytoplasmic-extracted proteins. For each sample, replicates were performed. To measure the background signal, NER buffer or CER buffer were used. The covered plate was briefly shaken and then incubated for 30 min at 37 °C using an Incubator 1000 Platform Shaker (Heidolph). The plate was incubated again at RT for another 10 min. Absorbance measurement was performed using the Microplate Manager 6 Software (Version 6.2) and the iMark Microplate Reader (Bio-rad) with an optimal wavelength around 540–590 nm.

2.2.2.3SDS-PAGE and Western Blot analysis

Western Blotting is used to visualize proteins that have been separated by gel electrophoresis. Equal amounts of protein (20- 30µg) were incubated together with NuPAGE LDS sample buffer (4x), NuPAGE Reducing Agent (10x), and deionized water

up to a volume of 35 µL. The sample mix was incubated at 95 °C for 5 min using a Thermocycler. Samples were briefly centrifuged and then loaded into a NuPAGE 4-12%Bis-Tris Mini –gel (Invitrogen). 10 µL of SeeBlue Plus2 Prestained Standard was loaded as a molecular weight control. Inner chamber contains 1x running buffer with 500 µL antioxidant and the outer chamber contains only 1x running buffer. The antioxidant reduces the gel environment to prevent sample reoxidation during electrophoresis. Gel was run for 45 min at 200V. The next step was to transfer the protein from the gel to the PVDF membrane (Invitrogen). The membrane was activated with absolute ethanol and rinsed with 1xTG buffer. The transfer was performed at 25 mA for two hours. After the successful transfer to the membrane it was incubated for 30 min with 5% milk in TBS-0.1% Tween to prevent unspecific binding of antibodies. The membrane was washed for 3 x 5 min with TBS-T 0.1% before and after application of either primary or secondary antibodies. The antibody dilution was received from the suppliers (Table 10) and was diluted either in 5% milk in TBS-T 0.1% or in 5% BSA in TBS-T 0.1% (Table 13). For antibody detection, I used Amersham Hyperfilm ECL (GE Healthcare) Western Blotting detection reagent and bands were estimated by using developing and fixation reagents.

2.2.3 Protein DNA Interaction

2.2.3.1Chromatin immunoprecipitation

Frozen BM cells from liquid nitrogen were used for this approach. Cells were thawed in an incubator at 37°C and transferred in a 15 mL falcon tube filled with FACS buffer. Protein-DNA interaction was performed by using 1% formaldehyde and the cells were stirred at 20 rpm at RT for 8 min. The cross-linking reaction was stopped by adding 0.125M glycine and was incubated for 5 min at RT. Afterwards cells were harvested by centrifugation at 338 x *g* and 4 °C for 7 min and washed with 5 mL ice cold PBS. Cells

were lysed in 600 µL cell lysis buffer (10 mM Tris pH 8.0, 10 mM NaCl and 0.2 % Nonidet P-40) containing protease inhibitors (50 µg/mL PMSF, NaBu and 1µg/mL leupeptin) and were incubated on ice for 10 min. Cells were centrifuged at 338 x *g* and 4 °C for 5 min to recover the nuclei. Supernatant was discarded and the cells were treated with 600 µL nuclei lysis buffer (50 mM Tris pH 8.0, 10 mM EDTA, 1 % SDS) containing protease inhibitors (1 µg/ mL leupeptin, 10 mM NaBu and 50 µg/mL PMSF) and incubated on ice for 10 min. An equal volume of IP dilution buffer (20 mM Tris pH 8.0, 2 mM EDTA, 150 mM NaCl, 1% Triton X-100, 0.01 % SDS) containing protease inhibitors (1 µg/ mL leupeptin, 10 mM NaBu and 50 µg/ mL PMSF) was added. Sonication was run for a total time of 25 min (=25 cycle) using a high power setting for 30 s on followed by 30 s off. DNA fragmentation was performed by using the Diagnode Bioruptor plus. The solution was centrifuged at 676 x *g* at 4°C for 7 min, the supernatant containing chromatin was transferred into a new 15 mL Falcon tube and 1.5 mL IP dilution buffer was added. Chromatin was precleared by adding 1mg/ mL preimmune serum Rabbit IgG with rotation at 4°C for 1h, followed by 100 µL protein A agarose and further rotation at 4 °C for 2h. Agarose was pelleted by centrifugation at 338 x *g* for 2 min. Afterwards the chromatin was transferred to 1.5 mL tubes and an additional tube was used as an input control. Precipitation was performed overnight at 4°C with rotation by using following antibodies, 1 µL of H3K9ac and 2 µg/ µL Rabbit IgG (Table 11). The next day 40 µL of protein A/G sepharose beads were added and rotated with the samples for 2 h. The beads were harvested at x *g* for 2 min and washed twice with 500 µL IP Wash I, once with 500 µL IP Wash 2 and twice with 500 µL TE. DNA-protein-antibody complexes were eluated twice from the beads by adding 150 µL elution buffer. To reverse the cross-linking 1 µg RNase and 0.3 M NaCl and were added to the IP samples and the input and was incubated at 67°C overnight. Finally samples were incubated with 3 µL Proteinase K (20mg/mL) at 45°C for 2h. DNA purification was performed using the MinElute® Reaction Clean up kit (Qiagen) according to the manufacturer's instructions.

Preparation of the library for ChIP sequencing was performed by Dr.Judith Schütte and the ChIP-Seq analysis was carried out by Dr.Lothar Vassen.

2.2.4 Cell culture

2.2.4.1Maintenance

J2E cells were cultured in Gibco™ RPMI 1640 medium containing 10 % fetal bovine serum (FBS) and 1% Penicillin/Streptomycin (P/S). J2E cells double every 24 hours and are cultured at a concentration of 2- 8 x 10^5/mL.

HEK293-T cells were cultured in Gibco™ DMEM (1x) + GlutaMAX™-I, 10% FBS and 1% (P/S) and passaged every 2-3 days as necessary to maintain 50%–80% confluency.

NIH 3T3 cell were cultured in Gibco™ DMEM(1), 10% FBS, and 1% P/S and passaged every 2–3 days as necessary to maintain 50%–80% confluency.

Incubation of all cell lines was carried out at 37 °C, 5 % CO_2 and 100% humidity.

2.2.4.2Freezing and thawing

For further experiments cells were counted and resuspended in freezing medium. The freezing medium was selected according to the cell line as given by DSMZ. For primary BM and spleen (SPL) 3x10^7 cells were frozen in a final volume of 1 mL using 10% DMSO and 90% FBS. Cells were stored in a cryo-freezing container at -80°C overnight to allow slow freezing before they were transferred to liquid nitrogen for long- term storage.

Frozen cells were thawed quickly in a 37 °C water bath and washed with the appropriate medium to remove the remaining DMSO. Cells were kept at 37 °C and 5% CO_2 overnight.

2.2.5 Culture of bacterial cells

2.2.5.1Plasmid transformation

One Shot™ TOP10 chemically competent *E.coli* cells were purchased from Invitrogen. 1µL of plasmid was pipetted into the vial of competent cells and were incubated for 30 min on ice. Afterwards cells were heated for 45 seconds at 42 °C in a Thermomixer and placed on ice. 250 µL of pre-warmed S.O.C medium was added to the vial and the mix was shaken for 1 h at 37 °C and at 225 rpm in a shaker. After 1 h incubation 10 µL of the cell suspension was plated onto a LB agar plate with the appropriate antibiotic selection of ampicillin and incubated overnight at 37 °C.

2.2.5.2Bacterial growth conditions

Bacterial cultures were inoculated from a single colony and grown in LB medium at 37°C with respective antibiotics depending on the plasmid resistance marker. Liquid cultures were grown in an incubator, shaking at 180–200 rpm to allow adequate aeration. Ampicillin was used at 100 µg/mL.

2.2.6 Virus productions

2.2.6.1Retrovirus production by $CaCl_2$

Retroviruses are linear single-stranded RNA with 7–12 kb. Retroviral DNA code three potential protein domains: 1) *gag*, which is important for the synthesis of internal viral DNA proteins that form the matrix, the capsid, and the nucleoprotein structures; 2) *pol*, which possesses the information of the reverse transcriptase enzyme and the integrase enzyme; and 3) *env*, which encodes the surface and transmembrane components of the viral envelope proteins. One day before retrovirus production, $1x10^7$ HEK 293-T cells were seeded in 25 mL Gibco™ DMEM (1x) + GlutaMAX™-I, 10% FBS, and 1% P/S in 140 cm^2 tissue-culture treated dishes. The cells were expected to be 80%–90% confluent the next day, when the media was changed in order to improve transfection efficiency. Next, the transfection mix was prepared by mixing 1 mL H_2O, 20 µg plasmid MSCV-*MLL-AF9*-IRES-*GFP*, 2.25 µg of pCL-Eco (retroviral packaging plasmid), and 2.5 M $CaCl_2$, which was subsequently added dropwise to 1 mL 2x HEBS while vortexing. The resulting precipitate was incubated for 10 min at room temperature. Meanwhile, the media was replaced with fresh 15 mL media, which contains Gibco™ DMEM (1x) + GlutaMAX™-I, 10% FBS, 1% P/S, and 20mM HEPES. Finally, the DNA-transfection mixture was added dropwise to the plate while gently agitating the plate to mix the precipitate with the media. Cells were incubated with the precipitate in the incubator overnight before aspirating the media and carefully replacing it with 15 mL Gibco™ DMEM (1x) + GlutaMAX™-I, 10% FBS, 1% P/S, and 10 mM HEPES. On the following two days, the supernatant containing the viral particles was collected by using a 40 µm filter, and the media was replaced with fresh media. Virus particles were stored at -80 °C for the quantification of the virus titer concentration.

2.2.6.2Virus titer estimation

The virus titer was calculated to determine how much functional virus was produced by $CaCl_2$-mediated transfection. $2x10^4$ NIH 3T3 cells were seeded in a 12-well tissue-culture treated plate containing 1 mL Gibco™ DMEM (1x) + GlutaMAX™-I, 10% FBS, and 1% P/S and incubated overnight at 37 °C, 5% CO_2, and 100% humidity. The retrovirus containing supernatant was serially diluted 1:10, 1:100, and 1:1000 with DMEM/10% + FBS 1% + P/S and 8 µg/mL polybrene. The media was aspirated and replaced with 300 µL serially diluted and undiluted virus. The decreased culture volume during the incubation allows for optimal contact between the virus and the cells. Cells without incubation of the virus were counted to determine the cell number for the calculation of the virus titer. Cells were incubated overnight at 37° C in a humidified incubator in an atmosphere of 5% CO_2. Media containing retroviral particles was removed and replaced by fresh media without viral particles. Importantly, the media was added to the inner wall of the well and not directly onto the cells in order to keep the cells attached to the well. After overnight incubation, cells were prepared for flow cytometry. Cells were trypsinized, transferred into FACS tubes and centrifuged at 300 x *g* for 5 min at 4°C. The supernatant was discarded, and the cell pellet was resuspended in 300 µL FACS buffer. The GFP^+ signal was identified by using BD FACScan, and analysis was performed using the FlowJo Single Cell Analysis Software V10.

2.2.6.3Virus transduction/ RetroNectin

MACS sorted lineage negative (Lin^-) cells were used for virus transduction. To achieve a high transduction efficiency, non-tissue culture treated plates were coated with 20 µg/mL RetroNectin diluted in PBS at least 2 h prior to the addition of the virus. RetroNectin is an excellent enhancer for retroviral gene transfer because it co-localizes target cells and

viruses onto the RetroNectin molecules (Lee, Lee et al. 2009). This reagent is a recombinant human fibronectin fragment that encodes three functional domains: the cell-binding domain, the heparin domain, and the CS-1 sequence domain. The cell-binding domain recognizes the integrin receptor of very late antigen (VLA-5, a5β1) from target cell, and the CS-1 sequence domain will bind to the intregrin receptor of very late antigen (VLA-4, a4 β1). The intermediate domain, which contains the heparin binding domain is responsible for the binding of virus (Han, Shang et al.). After incubation with RetroNectin, the solution was removed and transferred into a new non treated tissue culture plate. The coated wells with RetroNectin were washed with 1 mL FACS buffer and were blocked with 2% BSA in PBS at RT for 30 min. The BSA solution was removed and the wells were washed with 1 mL PBS. 500 µL retrovirus stock solution was added to the RetroNectin coated plate and the plate was centrifuged for 2 h at 32°C and 3500 x *g*. After centrifugation the supernatant was discarded and replaced with fresh retrovirus stock solution for a second round of centrifugation. Meanwhile Lin- target cells were counted and resuspended in Marrow Max medium containing 20 ng/mL of SCF, 10ng/mL of IL6 and 10 ng/mL of IL3 with a density of $1x10^6$ cells/ mL. The virus solutions were removed from the well and the prepared cells were added to the wells. After another centrifugation step at 300 x *g* for 10 min at 4 °C, 2 µg/mL polybrene was added and the cells were incubated overnight at 37°C in a humidified incubator in an atmosphere of 5% CO_2.

2.2.7 Mice

2.2.7.1Husbandry and housing

All mice were housed in specific pathogen-free conditions at the animal facilities of the University Hospital Essen. All animal experiments were conducted after approval of the

ethics committee and local authorities of the University Hospital Essen, Germany, under permission document numbers G 1469/15 and Z 1460/14.

2.2.7.2Strains

All strains are maintained on a pure C57BL/6 background and were purchased from the Jackson Laboratory (Bar Harbor, ME, USA). Gfi1b mouse strains with different expression levels were crossed with *NUP98/HOXD13* (Table 20), Kirsten rat sarcoma viral oncogene homolog (*Kras)* mouse model (Table 21), or by retroviral transduction with *MLL-AF9* oncogene-containing vectors (Table 22) (see 2.1.3). When the mice were around 8 weeks old, *Gfi1b*$^{fl/fl}$ *MxCre*^{tg} (fl/fl = flox/flox, tg = transgene) and *Gfi1b*$^{fl/fl}$ MxCre^{wt} (wt=wildtype) (used as control) were treated every second day with polyinonsinic-polycytidylic acid sodium salt poly (I:C) (2mg/ mL) for a total of 7 days.

Table 20: Characetristics of the NUP98/HOXD13 MDS/AML mouse model.

MDS/ AML mouse model	Genotype	*Gfi1b* expression level
NUP98/HOXD13^{tg}	*Gfi1b*$^{wt/wt}$	100%
	Gfi1b$^{eGFP/wt}$	50%
	Gfi1b$^{fl/fl}$ *MxCre*^{wt}	100%
	Gfi1b$^{fl/fl}$ *MxCre*^{tg}	0-10%

NUP98/HOXD13 mice crossed with *Gfi1b*$^{fl/fl}$ *MxCre*^{wt} (control mice) and *Gfi1b*$^{fl/fl}$ *MxCre*^{tg} mice were injected 7 times every second day with poly (I:C) to abrogate the *Gfi1b* gene.

Table 21: Characteristics of the Kras mouse model.

AML model	Genotype	*Gfi1b* expression level
***Kras*$^{+/fl}$**	*Gfi1b*$^{wt/wt}$ *MxCre*^{tg}	100%
***Kras*$^{+/fl}$**	*Gfi1b*$^{fl/fl}$ *MxCre*^{tg}	0-10%

Kras mice crossed with *Gfi1b*$^{wt/wt}$ *MxCre*^{tg} (control mice) and *Gfi1b*$^{fl/fl}$ *MxCre*^{tg} were treated every second day with poly (I:C) as described above to excise the *Gfi1b* gene.

Table 22: Characteristics of the MLL-AF9 mouse model.

AML model	Genotype	*Gfi1b* expression level
MLL-AF9	*Gfi1b*$^{fl/fl}$ *MxCre*^{wt}	100%
MLL-AF9	*Gfi1b*$^{fl/fl}$ *MxCre*^{tg}	0-10%

Three weeks after transplantation, mice were treated with poly (I:C), as described above.

2.2.7.3Analysis of leukemic and control mice

Control and leukemic BM cells were extracted from the femur, tibia and humerus of mice. A 5 mL syringe attached to a 25 G needle and approximately 5 mL FACS buffer were used to flush BM cells from the bones. To achieve a single cell suspension, a 20 G needle with the same syringe was used for re-suspending the cell suspension. The cell suspension was kept in approximately 5 mL FACS buffer and was filtered through a 100 µm sterile filter into a new 50 mL falcon tube. Afterwards, cells were centrifuged at 338 x *g* and 4°C for 5min. The supernatant was discarded and the cell pellet was re-suspended in 5 mL FACS buffer. To remove erythrocytes, the cells were taken in 1 mL erythrocyte lysis solution and incubated for 7 min at room temperature. Next, 5 mL FACS buffer was added to stop the lysis and the cells were centrifuged as described above. Spleen was squashed between two microscopy slides and was re-suspended with a 20 G needle to obtain single cell suspension. Afterwards the spleen cells were prepared exactly like the BM cells. The cell number was number was determined by diluting 100 µL of cell suspension in 10 mL Coulter Clenz Cleaning Agent and using the Z2 Coulter Counter Analyzer.

2.2.8 Cell sorting

2.2.8.1MACS sorting of lineage negative cells

Lin^- cell isolation was performed by using the MACS Lineage Cell Depletion Kit. BM cells were isolated as described in section 2.2.7.3. Magnetic labeling was performed according to the cell number. 10^7 cells were resuspended in 40 µL FACS buffer with additional 10 µL α-Lin-Biotin antibody and were incubated for 10 min at 4–8 °C. Then, 30 µL FACS buffer and 20 µL α-Biotin-Microbeads were added to the cell suspension. After 15 min incubation at 4–8 °C, the incubation was stopped by adding 25 mL FACS

buffer to the cell suspension and was centrifuged for 10 min at 300 x *g* in a 50 mL Falcon tube. The supernatant was removed and the cell pellet was resuspended in 500 µL MACS buffer. Magnetic separation was performed with LS columns. The column was rinsed with 3 mL MACS buffer, and the cell suspension was applied to the column. The column was then washed 3 times with 3 mL MACS buffer, and all the effluent was collected in a 15 mL ice-cold Falcon tube. The cell count was determined as described above 2.2.7.3. Isolated Lin^- cells were seeded in Marrow max media with a stem cell factor 20 ng/mL of (SCF), 10ng/mL of interleukin-3 (IL-3), and 10ng/mL of interleukin-6 (IL-6) to prepare them for retroviral transduction (see section 2.2.6.3).

2.2.8.2FACS sorting

BM and spleen cells were stained with appropriate antibodies to identify their lineage origin and retroviral transduced cells were sorted by their green fluorescent protein (GFP) expression, which originates from the MLL-AF9 construct using a BD FACSVantage SE with BD FACSDIVA Option operated by Klaus Lennartz at the University Hospital of Essen.

2.2.9 Flow cytometry

2.2.9.1Immunophenotyping of leukemic BM and SPL cells

Each cell expresses on its surface membrane specific antigens, the so-called cluster of differentiation (CD) (Belov, de la Vega et al. 2001). Based on the CD marker's expression, it is possible to characterize different immunophenotypes of leukemic cells and to identify which kind of leukemia the mice developed. Flow cytometry staining was

also performed with CD117, a leukemic stem cell marker (Wells, Bray et al. 1996). In addition, two single staining were performed with CD45Pe and CD45PerCP for the compensation at the FACScan. For flow cytometry analysis, $1x10^6$ BM and/or SPL cells, respectively, were aliquoted into FACS tubes. First, cells were incubated with the blocking antibody Fc block, which would saturate non-specific binding sites to avoid background fluorescence. The Fc block solution was diluted 1:400 in PBS and 10 µL was added to each FACS tube. Incubation on ice or at 4 °C was performed for at least 10 min. Cells were washed with 1 mL FACS buffer and centrifuged for 5 min at 338 x *g* and 4 °C. The supernatants were discarded. Next, cells were stained with various CD-specific primary antibodies that were conjugated with different fluorescence dyes (see Table 12). T-cells express CD4 (simplified: T helper cells) and CD8 (simplified: T killer cells). Ter119 is a marker for the erythroid lineage (Kina, Ikuta et al. 2000), and B220 is an isoform of CD45 that is expressed on all murine B-cells (Bleesing and Fleisher 2003). Gr1 and Mac-1 are both markers for the myeloid lineage. Granulocytes express Gr1 and macrophages express high amounts of Mac-1. BM and/or SPL cells were stained as listed in Table 23. The cells were incubated with the various antibodies for 10 min at 4–8 °C. Cells were washed again with 1 mL FACS buffer and centrifuged for 5 min at 338 x *g* and 4 °C. Supernatants were removed, and the cells were resuspended in 250 µL FACS buffer. They were now ready to be measured using a BD FACScan or LSRII.

Table 23: Antibody combinations used for flow cytometry staining in BM and SPL-cells.

Staining	Antibody conjugated with PE	Antibody conjugated with PerCP
Single staining	CD117	-
	CD45	-
	-	CD45

Double staining	Ter119	B220
	CD8	CD4
	Gr1	Mac-1

2.2.9.2 Intracellular staining for p38$^{Thr180/Tyr182}$ and pAKT^{Ser473}

BM cells from femur, tibia and humerus were extracted from mice and were stored in ice cold 5 mL PBS. Cells were flushed, and a single cell suspension was prepared as mentioned in section 2.2.7.3. Samples were divided into four different tubes with 4x10^6 BM cells each per 15mL Falcon tube. Tube A was used for cell fixation, tube B was used for cell stimulation and fixation, and the other two tubes were used as controls. The BM cells of all tubes were washed with 2 mL PBS in 15 mL Falcon tubes and centrifuged at 528 x *g* and 4°C for 5 min. Cells were incubated for 15 min one ice with 1 µL fixable viability dye which can pass through the damaged membrane and stain interior and exterior amines of non-living cells. Cells were washed with 2 mL PBS and centrifuged twice at 528 x *g* and 4°C for 5 minutes. Cells were incubated with Fc-Block for 10 min on ice to avoid nonspecific staining by fluorochrome-conjugated antibodies. Next, cells were stained with 4 µL CD117 BV421 antibody for 10 min at 4°C (Table 12). Afterwards cells were washed, and centrifuged and the cell pellet was resuspended in 250 µL PBS. For the stimulation of the BM cells, 250 µL PBS substituted with 20µg/mL anisomycin which facilitates the activation of p38 MAPKs (Cano and Mahadevan 1995) and is used as a positive control was added to tube B and to the respective control tube. Cells were incubated for 20 min at 37 °C in a water bath. For fixation 500 µL BD Phosflow Fix Buffer I prewarmed at 37 °C was added to all four tubes and incubated for 10 min at 37 °C in a water bath. After pelleting the cells, 500 µL ice cold Perm Buffer II was added dropwise while vortexing the samples to avoid cell aggregation. Cells were kept on ice for 30 min, washed with 5 mL FACS buffer and centrifuged at 4 °C for 10 min. As a

negative staining control we used 20 µL of isotype control IgG1 κ and cells were incubated for 15 min at 4 °C. Cells were incubated in the respective tubes with 20 µL of pT180/pY182 (anti-p38 MAPK) or 5 µL pS473 (anti-pAkt) for 30 min at 4 °C (Table 12). Cells were washed with 5 mL FACS buffer and centrifuged. Cell pellet was resuspended in 250 µL FACS buffer and was transferred to a FACS tube. Measurements were taken using the LSRII and the BD FACSDiva Software (version 6.1.3).

2.2.9.3 Reactive oxygen species staining protocol

For the quantitative measurement of cellular reactive oxygen species (ROS) we used the Cellular Reactive Oxygen Species Detection Assay kit from Abcam (Table 4). $1x10^6$ BM cells were washed with 1 mL PBS and centrifuged for 5 min at 300 x *g* at 4 °C. The cells were then incubated with Fc-block at 4–8 °C for 10 min as described above (Section2.2.9.1). After incubation the cells were washed with 1 mL PBS and centrifuged. Cells were stained with CD117 for 10 min at 4–8 °C. Again, cells were washed and centrifuged. Finally, cells were stained with DCDFA (2'.7'–dichlorofluorescin diacetate) for 30 min at 37 °C and measurement was performed immediately afterwards without washing the cells, using a LSRII and the BD FACSDiva Software (version 6.1.3).

2.2.10 *In vivo* experiments

2.2.10.1 Primary transplantation of leukemic BM cells

Mouse leukemia was induced by retroviral transduction of Lin^- BM cells with the *MLL-AF9* oncogene together with green fluorescence protein (*GFP)* as previously described (Botezatu, Michel et al. 2016; Hones, Botezatu et al. 2016). Lin^- cell isolation was

performed as mentioned above in section 2.2.8.1. And retroviral transduction was performed as described in section 2.2.6.3. One day before transplantation, mice 4-8 weeks old were lethally irradiated with 10 Gy using a X-Ray irradiator, applying whole body gamma irradiation to achieve either transient or chronic immunosuppression in mice (Duran-Struuck and Dysko 2009). One day after irradiation 1x10^5 GFP-expressing Lin$^-$ cells of *Gfi1b*$^{fl/fl}$ MxCre^{wt} or *Gfi1b*$^{fl/fl}$ *MxCre*^{tg} mice were transplanted into the tail vein together with 1.5x10^5 competitive BM wildtype cells. Three weeks after transplantation, mice were injected 4 times total with 250 µL poly (I:C) (2 mg/mL) every second day) Figure 6.

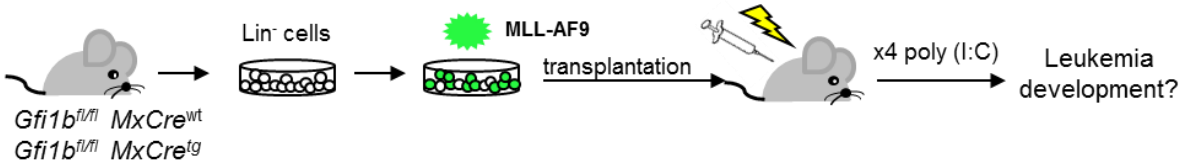

Figure 6: Concept of primary transplantation experiment.
Lin$^-$ cells from *Gfi1b*$^{fl/fl}$ MxCre^{wt} and *Gfi1b*$^{fl/fl}$ *MxCre*^{tg} were isolated and transduced retrovirally with the *MLL-AF9* oncogene fused with *GFP* promoter gene. Successfully transduced *GFP*-positive cells were injected with competitive BM wildtype cells in lethally irradiated *C57BL6/J* mice. After a period of 3 weeks, transplanted mice were treated with 250 µL poly (I:C) 2 mg/mL to abrogate the *Gfi1b* gene locus.

2.2.10.2 Secondary transplantation of leukemic BM cells

Frozen leukemic BM cells from liquid nitrogen were prepared as previously described ((Botezatu, Michel et al. 2016; Hones, Botezatu et al. 2016). One day before transplantation, the mice were sublethally irradiated with 3 Gy. Initially leukemic BM cells were washed with 10 mL PBS and were centrifuged at 338 x *g* for 5min. Cell pellet was re-suspended in 1 mL PBS. A cell count was performed by using the cell counter machine like in Section 2.2.7.3 and 50 µL of cell suspension was taken in 250 µL FACS buffer for the measurement of GFP$^+$ cells or annexin - negative cells. Leukemic BM cells were prepared according to the GFP$^+$ cells or annexin - negative cells and all mice

received a tail vein injection comprising $1x10^5$ MLL-AF9 GFP positive (GFP^+) or *NUP98/HOXD13* leukemic annexin - negative cells.

2.2.10.3 Limiting dilution assay

For limiting dilution assay leukemic cells were prepared as in section 2.2.10.2. One day before transplantation new recipient mice were sublethally irradiated (3Gy). For this approach, a serial gradient of leukemic BM cells were prepared such as $1x10^5$, $5x10^4$, $1x10^4$ and $5x10^3$ from frozen *MLL-AF9* leukemic BM cells (GFP^+) derived from poly (I:C)-treated leukemic *Gfi1b*$^{fl/fl}$*MxCre*^{wt} or *Gfi1b*$^{fl/fl}$*MxCre*^{tg} mice. Leukemic BM cells were re-transplanted in secondary recipient mice (3 - 4 mice/group).

2.2.11 Statistics and software

2.2.11.1 Statstical analyses

Statistical analyses were performed with Graph Pad Prism software (version 6) (La Jolla, CA, USA). All survival curves were generated using the Kaplan-Meier-Curve. Results were described as significant when the p-value was < 0.05. For human data analysis, I used the leukemia gene atlas software version 2.1.0 (Table 14).

3 Results

3.1 Low *GFI1B* expression level resulting in an inferior prognosis of MDS and AML patients

One aim of this thesis was to determine whether different *GFI1B* levels in myeloid blast cells can be used as a marker to better predict prognosis of MDS and AML patients. As a starting point, I used published gene expression data from the blast cells of patients diagnosed with MDS and AML to study the pattern of *GFI1B* expression in healthy and malignant cells (Valk, Verhaak et al. 2004; Wouters, Lowenberg et al. 2009; Rapin, Bagger et al. 2014). In the first study, CD34 was used as a surrogate marker for LSC, and gene expression patterns in CD34 positive AML blast cells of 285 patients were compared to gene expression patterns of CD34 positive BM cells of healthy human BM donors (Valk, Verhaak et al. 2004) (Figure 7: GFI1B expression level in MDS/AML patients *GFI1B* expression was lower in CD34 positive AML blast cells compared to CD34 positive non-malignant BM cells. As introduced, MDS is a pre-leukemic condition where the differentiation of the myeloid cell towards mature cells is severely disturbed. About 30% of MDS patients develop an AML in the course of their disease. Therefore, the *GFI1B* expression patterns in CD34 positive MDS blast cells were compared to *GFI1B* expression in CD34 positive AML blast cells. *GFI1B* expression in AML blasts was lower compared to *GFI1B* expression in CD34 positive cells from the BM of MDS patients (Figure 7B). I also made use of a publicly available webpage (Hebestreit, Grottrup et al. 2012) which allows the comparison of gene expression patterns of a certain gene across different studies (Rapin, Bagger et al. 2014). Using this website, it could be shown, that *GFI1B* expression was lower in human LSCs of different AML subtypes compared to normal HSCs, early HSCs and human myeloid progenitors (CMPs) (Figure 7C). Collectively, these data sets show, that *GFI1B* expression is lower in LSCs compared to healthy HSCs and progenitor cells.

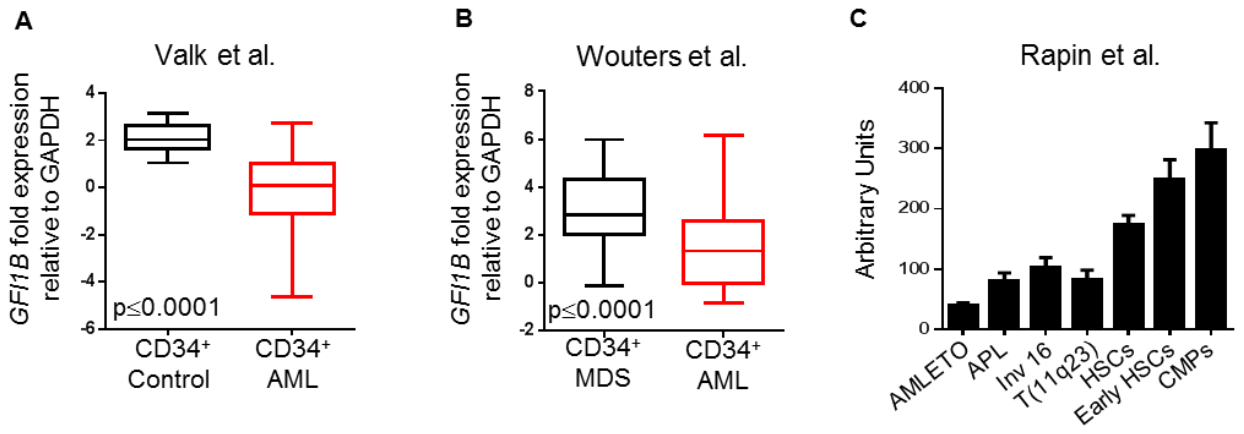

Figure 7: GFI1B expression level in MDS/AML patients.
A. *Comparison of GFI1B expression in CD34+ AML cells (n=269) to CD34+ control cells (n=8) published by (Valk, Verhaak et al. 2004), p<0.0001.*
B. *Comparison of GFI1B expression in CD34+ MDS cells (n=23) to CD34+ AML cells (n=501) published by (Wouters, Lowenberg et al. 2009).*
C. *GFI1B expression in different leukemic stem cell subtypes and early HSCs and CMPs (Rapin, Bagger et al. 2014).*

The next step was to identify whether different levels of *GFI1B* expression could serve as prognostic molecular markers for MDS and AML patients. We used a study for which gene expression patterns of *GFI1B* expression in blast cells were available and in which the disease course was known for every patient (Verhaak, Wouters et al. 2009). In a first step, expression level of *GFI1B* was correlated with survival of AML patients. The boundaries for *GFI1B* expression were chosen for those boundaries, which allowed predicting prognosis of a patient based on the *GFI1B* expression level in the blast cells. Using this approach I could distinguish two different expression level of *GFI1B*: low *GFI1B* expression level (0%–15%) and high *GFI1B* expression level (16%–100%) (Figure 8). These levels correlated with survival (Figure 9), whereby low *GFI1B* expression was associated with inferior overall survival (OS).

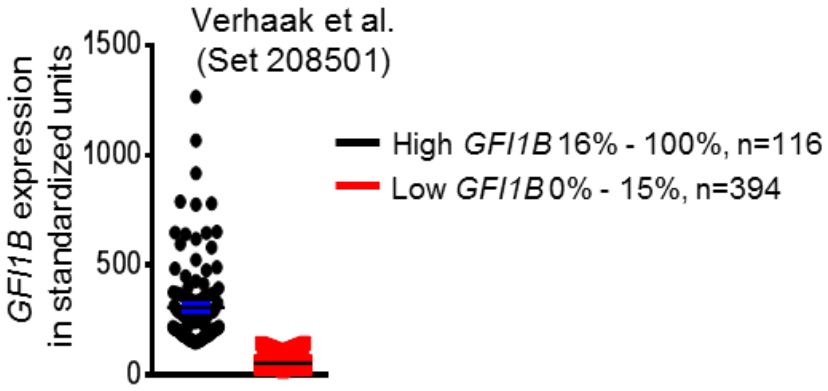

Figure 8: GFI1B expression with two distinct populations.

Based on published data from Verhaak et al. GFI1B expression level was classified into two distinct populations, high GFI1B expression n=116 (black dots) and low GFI1B expression n= 394 (red dots).

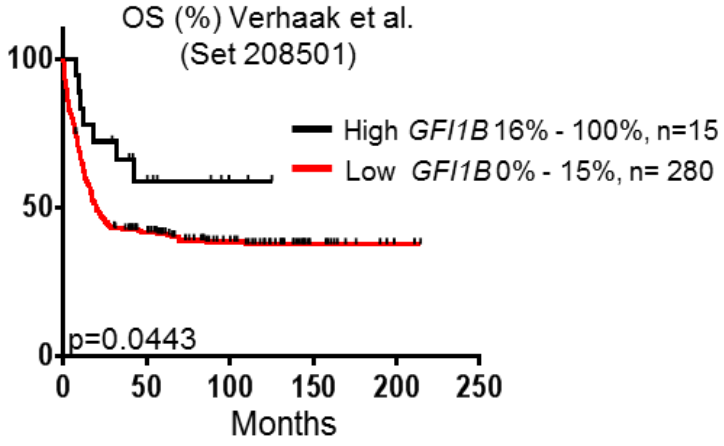

Figure 9: Low GFI1B expression is associated with worse outcomes.

Kaplan-Meier curve of overall survival (OS) from the human AML data set from Verhaak et al. AML patients were split into a group expressing high GFI1B n=15 (indicated in black,) and a group expressing low GFI1B n=280 (indicated in red). The vertical ticks on the curve indicate events.

AML is a heterogeneous disease with variable clinical outcomes. One way to determine a prognosis of AML patients is based on cytogenetic aberrations (Walker and Marcucci 2013). However, for a large group of patients, for whom no cytogenetic aberration can be observed in the leukemic cells, determining prognosis is difficult. Within this cohort of patients with no cytogenetic aberrations, we examined whether the expression level of *GFI1B* could be used as a prognostic marker. Low *GFI1B* expression was associated with poor outcome, regard to overall survival (OS) and event-free survival (EFS) (Figure 10 A and B).

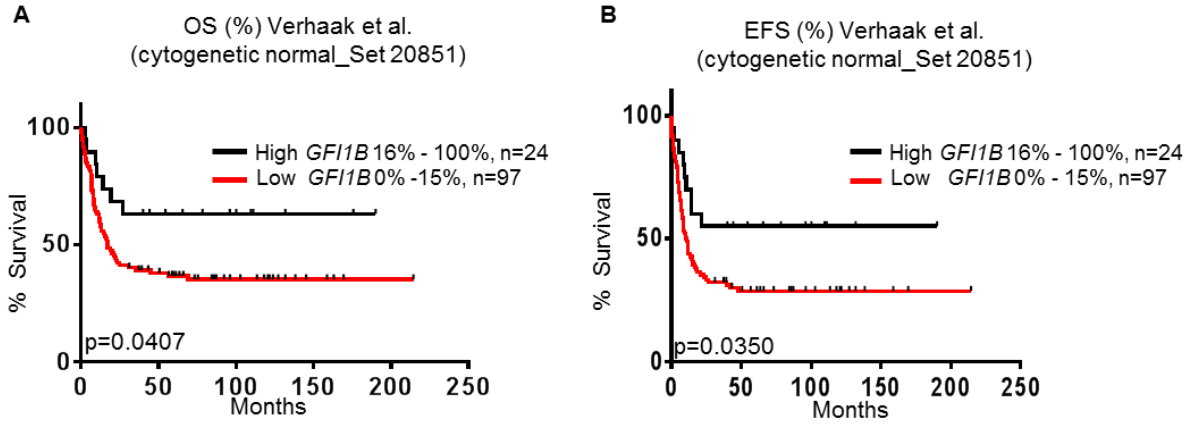

Figure 10: Correlation between GFI1B expression and AML prognosis regarding CN-AML.
A. *Kaplan-Meier curves represent the overall-survival curve of cytogenetically normal AML patients (CN-AML) regarding GFI1B expression level indicated as high, n=24 (black line) and low n= 97 (red line). High GFI1B expression shows a better prognosis compared to low GFI1B expression level.*
B. *Event-free survival (EFS) correlates with GFI1B expression level, high GFI1B expression n=24 (black line) and low GFI1B expression n=97 (red line). AML patients with a low GFI1B expression level showed a poor prognosis. The vertical ticks on the curve indicate events.*

As previously described MDS is a pre-leukemic disease that can progress to AML. MDS patients suffer from anemia (low blood-cell count), neutropenia (low neutrophils) and thrombocytopenia (low platelet-cell count). I was interested in validating the influence of *GFI1B* expression level and disease progression from MDS to AML. To this end, I

analyzed the *GFI1B* expression level in a study for which gene expression pattern and survival data were available (Papaemmanuil, Gerstung et al. 2013). Similarly to the above approach, we identified two distinct populations of *GFI1B* expression level: low *GFI1B* expression level (0%–30%) and high *GFI1B* expression level (31%–100%) with respect to the *GFI1B* expression level Figure 11 and a low level of *GFI1B* expression was associated with an inferior EFS (Figure 12).

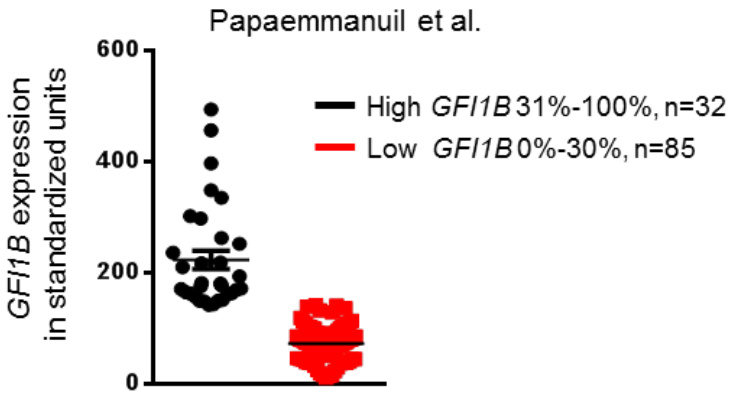

Figure 11: Classification of MDS patients with low and high GFI1B expression.

Based on a published data set, MDS patients were subdivided into two groups based on GFI1B expression level, low GFI1B expression, n=85 (red dots) and high GFI1B expression, n=32 (black dots).

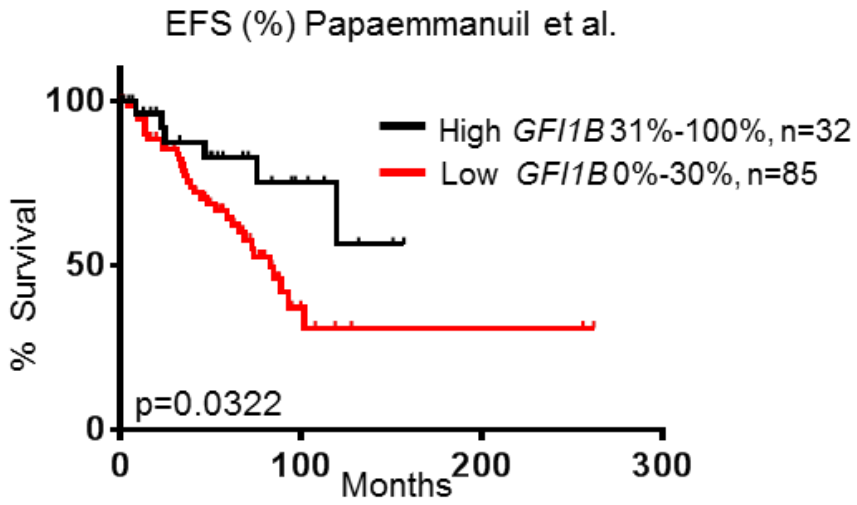

Figure 12: MDS patients with low GFI1B expression level showed a poor prognosis.
A published data set (Papaemmanuil, Gerstung et al. 2013) was analyzed based on the GFI1B expression level, and patients were classified into two subgroups. The Kaplan-Meier curve represents EFS from MDS patients. Patients with a low GFI1B expression level show a worse prognosis compared to patients with a high GFI1B expression level, p (0.0322).

3.2 Low level of *Gfi1b* influence MDS/AML progression in the NUP98/HOXD13 mouse model

3.2.1 AML-free survival curve of *NUP98/HOXD13* transgenic mice according to the *Gfi1b* expression level

The results above show, using different independent studies, that GFI1B plays a dose-dependent role in myeloid malignancies. To assess the role of murine Gfi1b in MDS/AML development, I had different mouse strains available: *Gfi1b*$^{wt/wt}$ mice, in which one allele of *Gfi1b* gene is replaced by a sequence encoding the *GFP* gene and mice in which the expression of *Gfi1b* can be completely abrogated. I first studied the role of different level of *Gfi1b* in MDS. To this end, I used the *NUP98/HOXD13* mouse model. These mice transgenically express the human NUP98/HOXD13 oncofusion protein

which recapitulates the result of the human translocation t(2;11)(q31;p15) (Lin, Slape et al. 2005). *NUP98/HOXD13* transgenic mice develop over their course of their life, features of human MDS such as bone marrow hyperplasia, progressive peripheral blood cytopenia and dysplasia of different myeloid lineages, some of these mice progress to AML. I used two different crossings to examine different expression levels of *Gfi1b*. In a first approach, *NUP98/HOXD13*^{tg} mice were crossed with *Gfi1b*$^{wt/wt}$ mice. These mice express normal level of Gfi1b (control mice). In a second crossing, I crossed *NUP98/HOXD13*^{tg} with *Gfi1b*$^{EGFP/wt}$ mice, in which one allele of *Gfi1b* was replaced by *GFP,* which allows studying the activity of the *Gfi1b* promoter *in vivo* as an indicator for the *Gfi1b* promoter activity (Vassen, Okayama et al. 2007; Khandanpour, Sharif-Askari et al. 2010) (Figure 13).

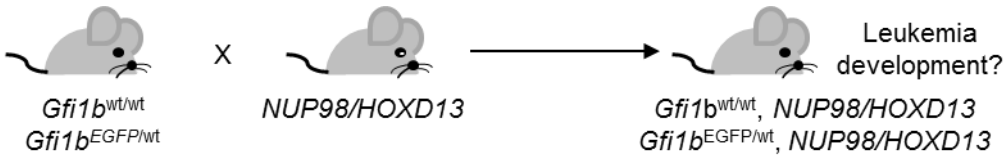

Figure 13: Schematic presentation of the crossing system between Gfi1b$^{wt/wt}$, Gfi1b$^{EGFP/wt}$ transgenic (tg) mice with NUP98/HOXD13^{tg} mice.

Gfi1b$^{wt/wt}$ mice (100% Gfi1b expression level) and Gfi1b$^{EGFP/wt}$ mice (50% Gfi1b expression level) crossed with NUP98/HOXD13^{tg} mice. Leukemia development was observed.

In a separate model we used *Gfi1b* conditional expressing mice. Gfi1b regulates the erythroid and megakaryocytic lineages. Constitutively *Gfi1b*-deficient mice die at day E14.5 due to severe bleeding and anemia, (Saleque, Cameron et al.). To study the role of Gfi1b in adult mice, Vassen, Khandanpour and colleagues developed a *Gfi1b* conditional expressing mouse strain (Khandanpour, Sharif-Askari et al. 2010). To investigate the role of the absence of *Gfi1b* on disease development in *NUP98HOXD13*^{tg} mice, I crossed *NUP98HOXD13*^{tg} mice with *Gfi1b*$^{fl/fl}$ *MxCre*^{tg} mice. To induce deletion of *Gfi1b*, I treated *Gfi1b*$^{fl/fl}$ *MxCre*^{wt} and *Gfi1b*$^{fl/fl}$ *MxCre*^{tg} with polyinosinic:polycytidylic acid poly (I:C). The injection poly (I:C) leads to an interferon

response and that activates the Cre-recombinase which is under the control of the interferon-dependent *Mx1* promoter (Kuhn, Schwenk et al. 1995). The Cre then excises exons 2-4 of the floxed *Gfi1b* allele, leading to deletion of *Gfi1b* expression in the hematopoietic system (Khandanpour, Sharif-Askari et al. 2010). To activate Mx1-Cre in 8- weeks-old mice *in vivo*, 2 mg/mL of poly (I:C) was injected seven times every second day (Figure 14*).*

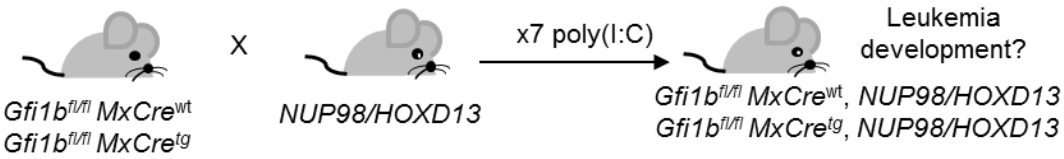

Figure 14: Schematic illustration of the crossing system for conditional expression of Gfi1b and administration of poly (I:C) in Gfi1b$^{fl/fl}$ MxCre^{wt} and Gfi1b$^{fl/fl}$ MxCre^{tg} mice.

Gfi1b$^{fl/fl}$ MxCre^{wt} and Gfi1b$^{fl/fl}$ MxCre^{tg} mice were crossed with NUP98/HOXD13^{tg} mice. 6-8 weeks old mice were injected with poly (I:C) for seven days every second day.

Using the above described different *Gfi1b*-expressing strains, I studied the results of heterozygosity of the *Gfi1b* locus or complete absence of *Gfi1b* expression on AML progression in the *NUP98/HOXD13^{tg}* mouse model.

I observed that the loss of one *Gfi1b* allele (*Gfi1b$^{EGFP/wt}$*, red curve Figure 15*)* shortened the latency period of AML development compared to mice in which both alleles of *Gfi1b* were present *Gfi1b$^{wt/wt}$NUP98HOXD13^{tg}* mice (black curve, Figure 15*).* RT-PCR and Western Blot analyses were performed to examine whether the heterozygosity of *Gfi1b* is associated with different protein level. Indeed, it could be shown that heterozygosity of *Gfi1b* leads to reduced mRNA and protein levels *(*Figure 16 A, B and C).

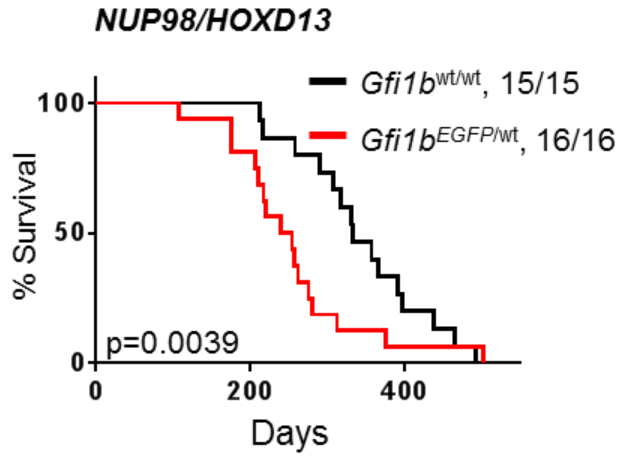

Figure 15: Gfi1b$^{EGFP/wt}$ heterozygotic mice had an accelerated AML progression. *Survival of Gfi1b$^{EGFP/wt}$ and Gfi1b$^{wt/wt}$ NUP98/HOXD13^{tg} mice (p=0.0039). Indicated is the number of mice succumbing to AML. The survival curve representing Gfi1b$^{wt/wt}$ mice is indicated by the black bar, and the curve representing Gfi1b$^{EGFP/wt}$ mice is indicated in red. In Gfi1b$^{wt/wt}$ animals, 15/ 15 mice and in Gfi1b$^{EGFP/wt}$ animals, 16/ 16 mice developed AML.*

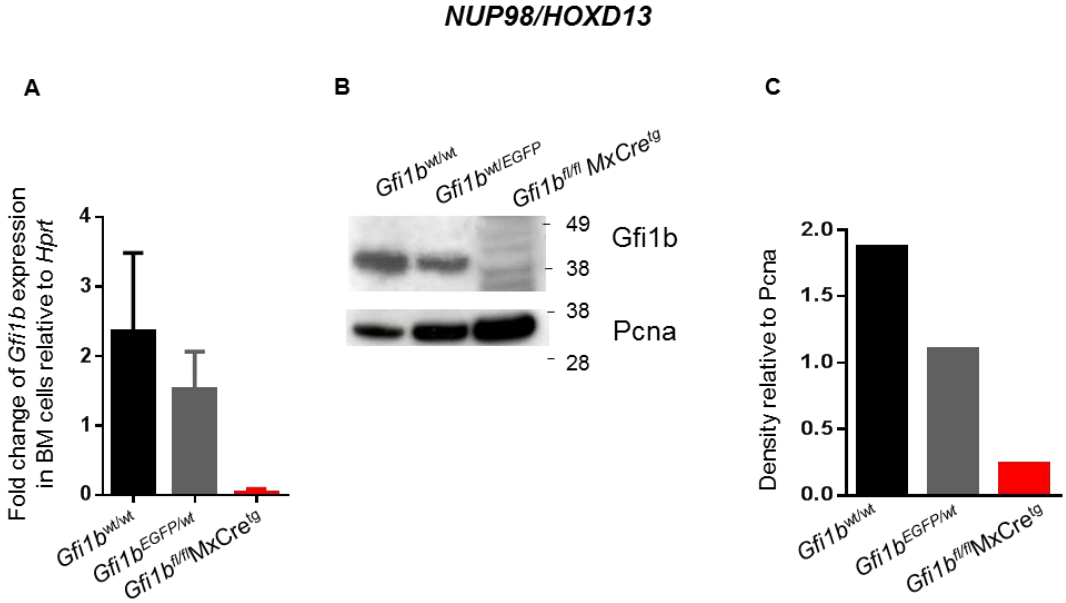

Figure 16: mRNA and protein level in NUP98/HOXD13 leukemic mice.

A. *RT- PCR was performed to verify the complete excision of the Gfi1b alleles upon poly (I:C) injection in both the conditional knock-out model, and in Gfi1b heterozygotic leukemic mice. The plot shows the Gfi1b expression level relative to Hprt expression. The black bars indicate, Gfi1b$^{fl/fl}$ MxCre^{wt} (Gfi1b$^{wt/wt}$) mice, the grey bars indicate, Gfi1b$^{EGFP/wt\ mice,}$ and the red bars indicate, Gfi1b$^{fl/fl}$ Mxcre^{tg} NUP98/HOXD13^{tg} mice.*
B. *Western Blot analysis of leukemic BM cells from Gfi1b$^{wt/wt}$ (Gfi1b$^{fl/fl}$ MxCre^{wt}), Gfi1b$^{wt/EGFP}$ and Gfi1b$^{fl/fl}$ Mxcre^{tg} NUP98/HOXD13^{tg} mice, respectively, was performed. J2E was used as a positive control. Pcna was used as a loading control.*
C. *Density relative to Pcna was measured by using the Image J software.*

After examining the role of reduced expression of *Gfi1b* in the context of the *NUP98/ HOXD13^{tg}* mouse model, we assessed the influence of loss of *Gfi1b*. Complete loss of *Gfi1b* (as demonstrated on the RNA and protein level, Figure 16) even further accelerated the onset of AML compared to the *Gfi1b$^{fl/fl}$ MxCre^{wt}* mice, which were also injected with poly (I:C) to assess for any effects influenced by poly(I:C) injection (Figure 17*)*.

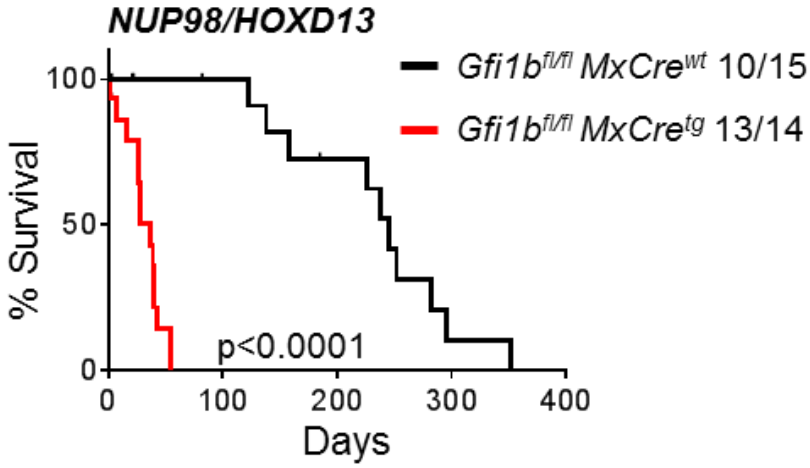

Figure 17: Absence of Gfi1b promotes the leukemia development in NUP98/HOXD13^{tg} mice.
Loss of Gfi1b accelerated leukemia development in NUP98/HOXD13^{tg} mice (p<0.0001). AML-free survival curve represents Gfi1b$^{fl/fl}$ MxCre^{wt} NUP98HOXD13^{tg} mice (black line) and Gfi1b$^{fl/fl}$ MxCre^{tg} NUP98HOXD13^{tg} mice (red line). 10/ 15 Gfi1b$^{fl/fl}$ MxCre^{wt} NUP98HOXD13^{tg} mice and 13/ 14 Gfi1b$^{fl/fl}$ MxCre^{tg} NUP98HOXD13^{tg} mice developed AML.

A complete loss of *Gfi1b* (exons 2- 4) was also further confirmed by PCR genotyping (Figure 18*)*. The expected size of the *Gfi1b*$^{fl/fl}$ *MxCre*^{wt} PCR product was 256 bp. The PCR product size in the *Gfi1b*-deficient leukemic BM cells was 540bp. The faint band in the conditional knock out BM sample characterized the non-excision of the *Gfi1b* gene upon poly (I: C) administration.

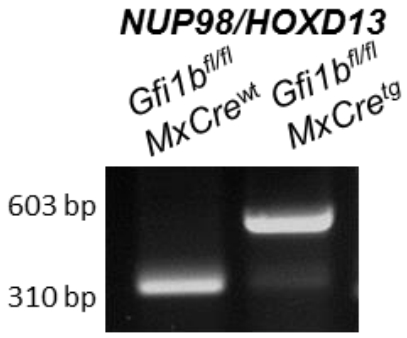

Figure 18: PCR genotyping of Gfi1b-deficient leukemic mice.

For the verification of the conditional knock out of the Gfi1b gene, PCR genotyping was performed with DNA from Gfi1b$^{fl/fl}$ MxCre^{wt} mice (100% Gfi1b expression) and Gfi1b$^{fl/fl}$ Mxcre^{tg} mice (0-10% Gfi1b expression). The expected size of the control PCR product is 256 bp and the PCR product of Gfi1b$^{fl/fl}$ Mxcre^{tg} leukemic mice is 540 bp. A faint band indicates DNA with residual non-excised Gfi1b DNA after poly (I: C) injection

As mentioned above, the GFP protein level is indicative of the *Gfi1b* promoter activity and hence, with all precautions, also of the Gfi1b protein level. Using flow cytometry I analyzed fluorescence intensity of GFP in the blast cells of *Gfi1b*$^{EGFP/wt}$ *NUP98/HOXD13*^{tg} mice that developed AML. The expression level of EGFP was significantly lower in *Gfi1b*$^{EGFP/wt}$ *NUP98/HOXD13*^{tg} mice that developed leukemia within the first 250 days, compared to the GFP level of *Gfi1b*$^{EGFP/wt}$ *NUP98/HOXD13*^{tg} mice that developed AML 250 days after birth (Figure 19). In summary, the loss of one *Gfi1b* allele, and hence a reduced *Gfi1b* expression, accelerates leukemia development.

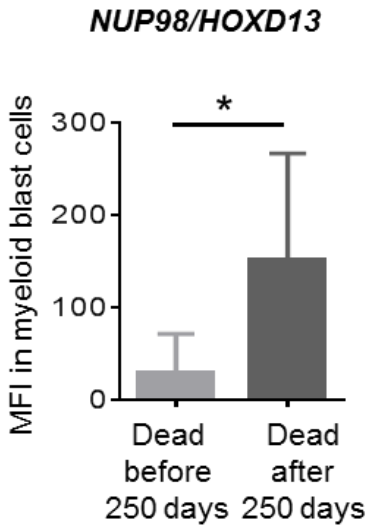

Figure 19: Mice with a low Gfi1b expression level died faster upon AML.

Flow cytometry measurement revealed the mean of GFP fluorescence intensity in the blast cells of Gfi1b$^{EGFP/wt}$ NUP98/HOXD13^{tg} mice. Mice developed leukemia within 250 days, (n=7), and showed a lower GFP intensity (Gfi1b expression) than mice that developed AML after 250 days (n=5) p=0.0272 (left panel).

3.2.2 Analysis of leukemia in *Gfi1b$^{wt/EGFP}$* and *Gfi1b$^{fl/fl}$ MxCre^{tg} NUP98/HOXD13^{tg}* mice

As a next step, I analyzed whether different expression levels of *Gfi1b* might influence the type of leukemia arising in the *NUP98/HOXD13^{tg}* mice. I examined the types of arising leukemia using different approaches such as: immunophenotyping by flow cytometry, microscopic analysis of the cytospins of BM cells, peripheral blood smears and peripheral blood analysis.

3.2.2.1 Classification of leukemic mice based on immunophenotyping

To characterize the arising leukemic cells in the different mouse strains described above, BM and SPL cells were explanted from mice with overt leukemia and flow cytometry analyses were performed with the surface markers described in Table 12. I used different makers such as the myeloid lineage markers Mac-1 and Gr1 in addition to CD117 (c-Kit), in our leukemic mice. The leukemic cells from *Gfi1b*$^{wt/wt}$ or *Gfi1b*$^{EGFP/wt}$ animals showed no significant differences with regard to surface marker expression. However, in contrast, most (13/ 14 *Gfi1b*$^{fl/fl}$ *Mxcre*^{tg} *NUP98/HOXD13*^{tg} leukemic mice*)* did not exhibit expression of the myeloid lineage markers Mac-1 and Gr1 (Figure 20 A and B). But in contrast, most of these cells showed an increased expression of c-Kit in *Gfi1b*-deficient mice (Figure 20 C). Respectively, the FACS plot showed the expression of Gr1 and Mac-1 in *Gfi1b*$^{fl/fl}$ *Mxcre*^{wt} *NUP98/HOXD13*^{tg} and *Gfi1b*$^{fl/fl}$ *Mxcre*^{tg} *NUP98/HOXD13*^{tg} leukemic (Figure 20 D) as well as c-Kit expression (Figure 20 E). However, no difference with regard to expression of the erythroid marker Ter119, the B-Cell marker B220 or the T-cell markers CD4 and CD8 were observed in the different expression levels of *Gfi1b* leukemia mice (Data not shown). Collectively, these data revealed that a loss of *Gfi1b* developed an undifferentiated AML.

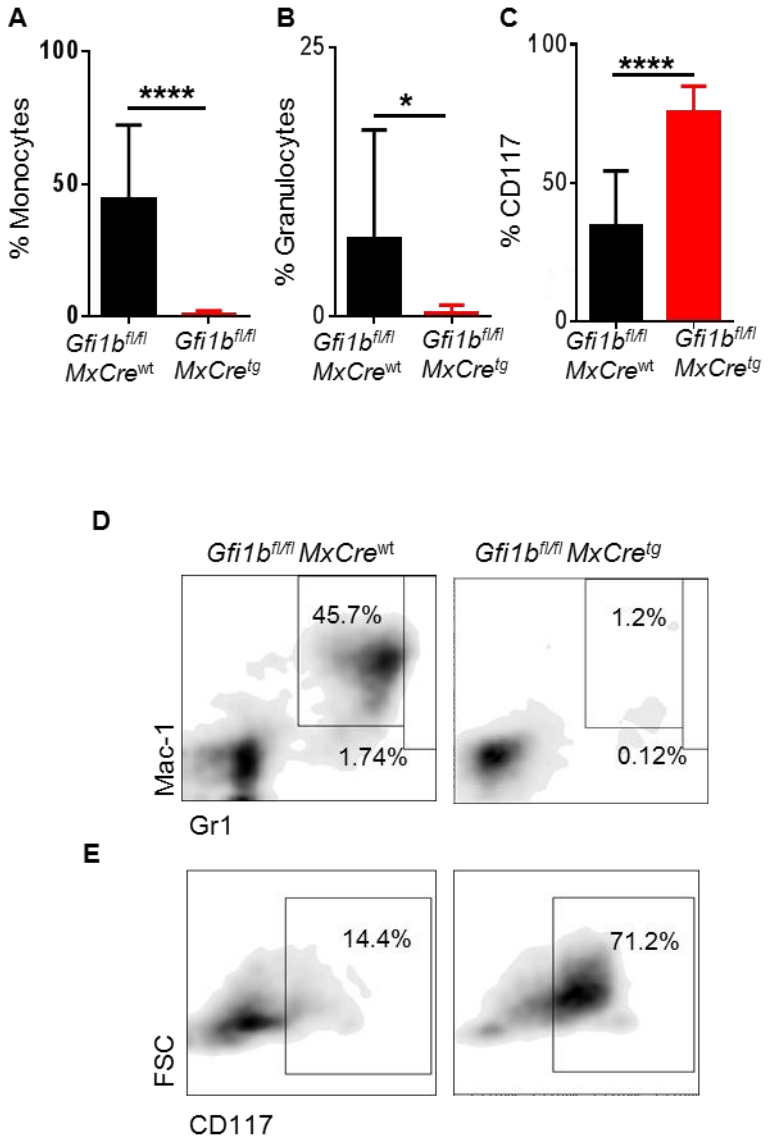

Figure 20: Mice with loss of Gfi1b develop an undifferentiated leukemia.
Leukemic BM cells were stained with antibodies specific to myeloid CD markers and c-kit.
A. *Data presents Mac-1 expression in Gfi1b$^{fl/fl}$ Mxcre^{wt} NUP98/HOXD13^{tg} leukemic mice (black bar) and Gfi1b$^{fl/fl}$ Mxcre^{tg} NUP98/HOXD13^{tg} leukemic mice (red bar).*
B. *Plot shows Gr 1 expression in Gfi1b$^{fl/fl}$ Mxcre^{wt} NUP98/HOXD13^{tg} leukemic mice (black bar) and Gfi1b$^{fl/fl}$ Mxcre^{tg} NUP98/HOXD13^{tg} leukemic mice (red bar).*
C. *Plot shows CD117 (c-kit) expression in Gfi1b$^{fl/fl}$ Mxcre^{wt} NUP98/HOXD13^{tg} leukemic mice (black bar) and Gfi1b$^{fl/fl}$ Mxcre^{tg} NUP98/HOXD13^{tg} leukemic mice (red bar).*

D. *The frequency of macrophages (Mac-1^{hi}Gr1^{int}), granulocytes (Mac-1^{hi}Gr1^{hi}) in Gfi1b$^{fl/fl}$ Mxcre^{wt} NUP98/HOXD13^{tg} leukemic mice (left panel) and Gfi1b$^{fl/fl}$ Mxcre^{tg} NUP98/HOXD13^{tg} leukemic mice (right panel).*
E. *The frequency of c-Kit in Gfi1b$^{fl/fl}$ Mxcre^{wt} NUP98/HOXD13^{tg} leukemic mice (left panel) and Gfi1b$^{fl/fl}$ Mxcre^{tg} NUP98/HOXD13^{tg} leukemic mice (right panel).*

3.2.2.2 Classification of leukemia by peripheral blood analysis in NUP98/HOXD13 mice

Besides BM and SPL cells, the peripheral blood (PB) of the different mice was analyzed. I examined as key parameters white blood counts (WBC), red blood counts (RBC), hemoglobin (HGB), and platelets (PLT). The leukemic cells from *Gfi1b*$^{wt/wt}$ or *Gfi1b*$^{EGFP/wt}$ leukemic animals showed no significant differences with regard to WBC and PLT counts. Yet, a significance difference with regard to HGB and RBC counts (Figure 21 A-D) could be observed between *Gfi1b*$^{wt/wt}$ *NUP98/HOXD13*^{tg} mice and *Gfi1b*$^{EGFP/wt}$ leukemic mice. Leukemic cells from *Gfi1b*$^{fl/fl}$*MxCre*^{wt} and *Gfi1b*$^{fl/fl}$*MxCre*^{tg} animals showed no significant differences with regard to WBC, but significant differences for HGB, RBC, and PLT counts (Figure 21 E-H), which might be due to the fact that Gfi1b regulates erythropoiesis.

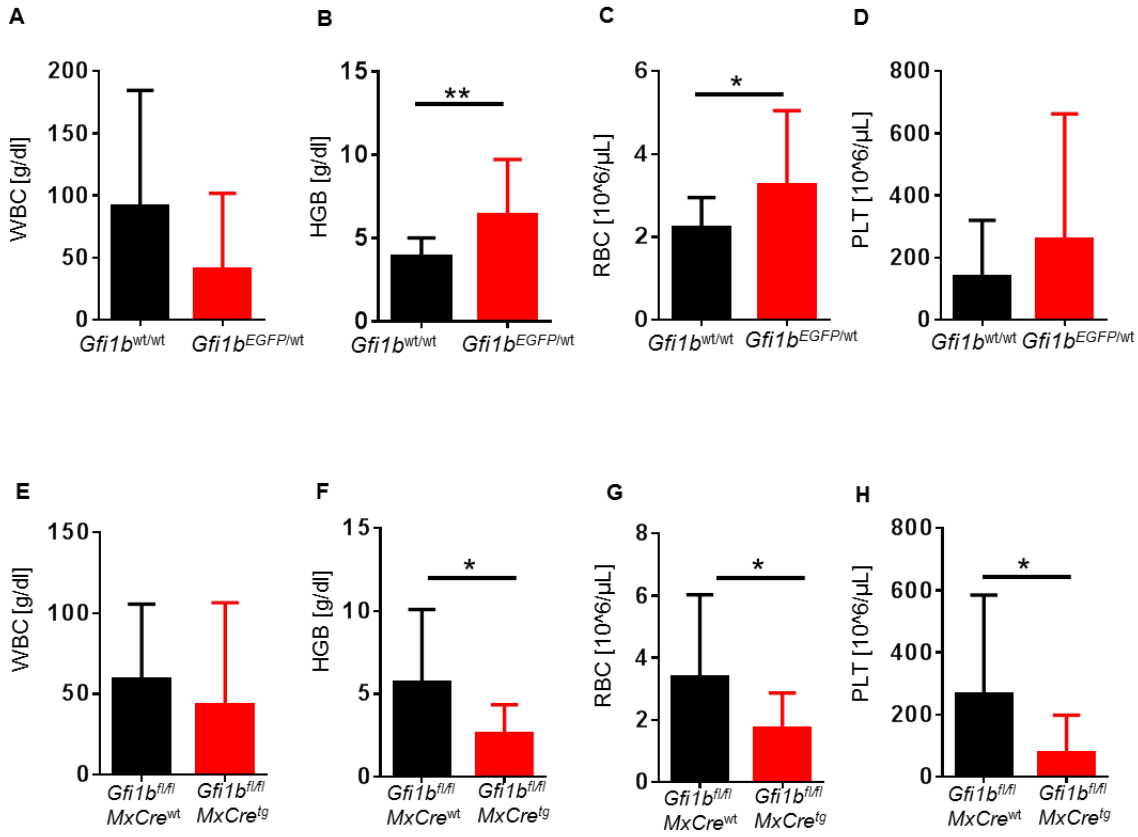

Figure 21: PB analysis of leukemic mice.

A. *WBC in PB of Gfi1b$^{wt/wt}$ (black bar) or Gfi1b$^{EGFP/wt}$ (red bar) leukemic mice.*
B. *Amount of HGB in PB of Gfi1b$^{wt/wt}$ (black bar) or Gfi1b$^{EGFP/wt}$ (red bar) leukemic mice (p=0.0090).*
C. *Amount of RBC in PB of Gfi1b$^{wt/wt}$l (black bar) or Gfi1b$^{EGFP/wt}$ (red bar) leukemic mice (p=0.0473).*
D. *Amount of platelets in PB of Gfi1b$^{wt/wt}$ (black bar) or Gfi1b$^{EGFP/wt}$ (red bar) leukemic mice.*
E. *WBC in PB of Gfi1b$^{fl/fl}$ Mxcre^{wt} (black bar) or Gfi1b$^{fl/fl}$ Mxcre^{tg} (red bar) leukemic mice.*
F. *Amount of HGB in PB of Gfi1b$^{fl/fl}$ Mxcre^{wt} (black bar) or Gfi1b$^{fl/fl}$ Mxcre^{tg} (red bar) leukemic mice (p=0.0224).*
G. *Amount of RBC in PB of Gfi1b$^{fl/fl}$ Mxcre^{wt} (black bar) or Gfi1b$^{fl/fl}$ Mxcre^{tg} (red bar) leukemic mice (p=0.0434).*
H. *Amount of platelets in PB of Gfi1b$^{fl/fl}$ Mxcre^{wt} (black bar) or Gfi1b$^{fl/fl}$ Mxcre^{tg} (red bar) leukemic mice (p=0.0465).*

3.2.2.3 Classification of leukemic mice based on cell morphology in BM and PB

In order to further characterize the type of leukemia developing in the different strains, cytospin of BM leukemic cells and blood smears of PB were generated. Blast cells arising from *Gfi1b$^{wt/EGFP}$ and Gfi1b$^{fl/fl}$MxCre^{tg}* leukemic mice showed no difference of cytological appearance *(*Figure 22*)* and blood smear analysis (data not shown) compared to leukemic Gfi1b wildtype mice.

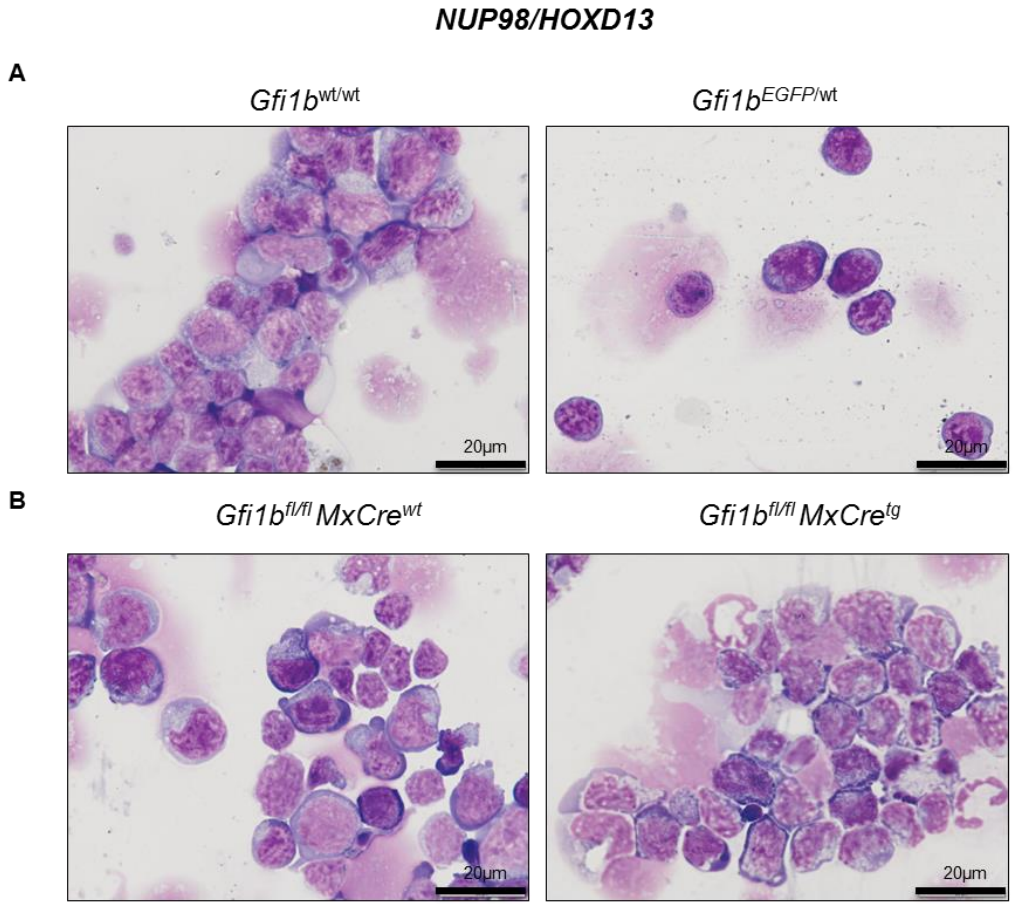

Figure 22 Wright-Giemsa staining of leukemic BM cells.

A. *BM cytospin from representative Gfi1b$^{wt/wt}$ and Gfi1b$^{wt/EGFP}$ NUP98/HOXD13 leukemic cells.*

B. *BM cytospin from representative Gfi1b$^{fl/fl}$ MxCre^{wt} and Gfi1b$^{fl/fl}$ Mxcre^{tg} NUP98/HOXD13^{tg} leukemic cells after poly (I:C) administration of mice in vivo.*

In summary, loss of *Gfi1b* accelerated the AML progression in the *NUP98/HOXD13* mouse model. *Gfi1b*-deficient mice exhibited an immature phenotype with an increased expression of the stem cell marker c-kit.

3.3 *Gfi1b*-deficient mice show a myeloproliferative disease in the oncogenic *Kras* mouse model

3.3.1 *Ras* oncogene activation induces a lethal myeloproliferative disorder

One of the most frequently observed mutations in AML patients affects the *Kras* oncogene. In this study I used the conditional *Kras* mouse model, in which the expression of a mutated form of *Kras* (G12D, exon 1) (Damnernsawad, Kong et al. 2016) can be induced by poly (I:C) injection and subsequent removal of the stop codon in the allele with expression of a mutated form of *Kras* (G12D). After removal of this stop codon, mice develop a lethal myeloproliferative disorder. Figure 23 illustrates the crossing strategy of the conditional *Kras* expression mouse model (Kras$^{+/fl}$) with *Gfi1b*$^{wt/wt}$ *MxCre*^{tg} and *Gfi1b*$^{fl/fl}$ *MxCre*^{tg} mice. Offspring mice were injected with poly (I:C) and observed for the emergence of disease.

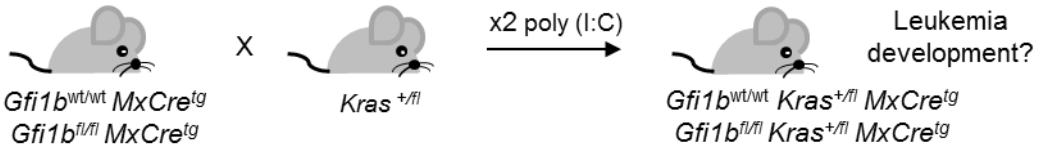

Figure 23: Schematic illustration of transgenic mice crossings and treatment with poly (I:C) for induction of Cre activity.

$Gfi1b^{wt/wt}$ $MxCre^{tg}$ and $Gfi1b^{fl/fl}$ $MxCre^{tg}$ mice were crossed with conditional $Kras^{+/fl}$ expressing mice. Mice 4-8 weeks old were injected with poly (I:C) to induce the activation of the Cre recombinase both to excise Gfi1b gene sequences (only exons 2-4) and to lethally activate the Kras oncogene.

3.3.2 *Gfi1b*-deficient mice develop myeloproliferative disorder by activating the conditional *Kras* expression with poly (I:C)

After treatment between 4 and 8 weeks of age with poly (I:C), the animals were observed for leukemia development. The complete loss of *Gfi1b* promoted the development of a myeloproliferative disorder compared to the $Gfi1b^{fl/fl}$ $MxCre^{wt}$ $Kras^{+/fl}$ mice, which were also injected with poly (I:C) (Figure 24). $Gfi1b^{fl/fl}$ $MxCre^{tg}$ $Kras^{+/fl}$ *mice* had a decreased median survival of 7 days compared to $Gfi1b^{wt/wt}$ $MxCre^{tg}$ $Kras^{+/fl}$ mice, which had a median survival of 25 days.

.

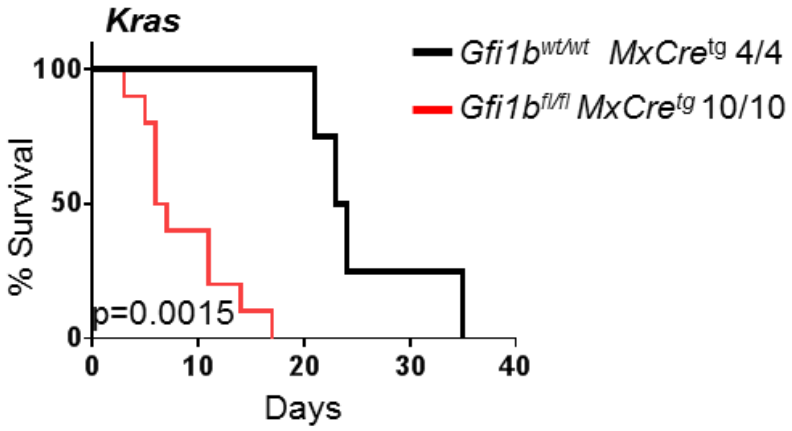

Figure 24: Loss of Gfi1b shortened the latency and promoted lethal myeloproliferative disorder.

The Kaplan–Meier curve shows the survival rate of Gfi1b$^{wt/wt}$ MxCre^{tg} Kras$^{+/fl}$ (black bar) and Gfi1b$^{fl/fl}$ MxCre^{tg} Kras$^{+/fl}$ (red bar) mice. Gfi1b-deficient mice developed myeloproliferative disease even faster compared to Gfi1b$^{wt/wt}$ MxCre^{tg} Kras$^{+/fl}$ mice, (p=0.0015). In both groups all mice developed disease.

3.3.2.1 Flow cytometry analysis of *Kras* oncogene mice with presence and absent functional *Gfi1b*

To further characterize the disease arising in these mice, I analyzed the immunophenotype of the hematopoietic cells of the mice with overt disease as defined by enlarged spleen and pale bones using antibodies described in Table 12. The myeloproliferative disorder phenotype in *Gfi1b*$^{wt/wt}$ *MxCre*^{tg} *Kras*$^{+/fl}$ *and Gfi1b*$^{fl/fl}$ *MxCre*^{tg} *Kras*$^{+/fl}$ mice showed no differences by flow cytometry. In both strains we observed an increased percentage of macrophages (defined here as Mac1^{hi}Gr1^{int}) and a reduced number of granulocytes (Mac1^{hi}Gr1^{hi} expression) (Figure 25).

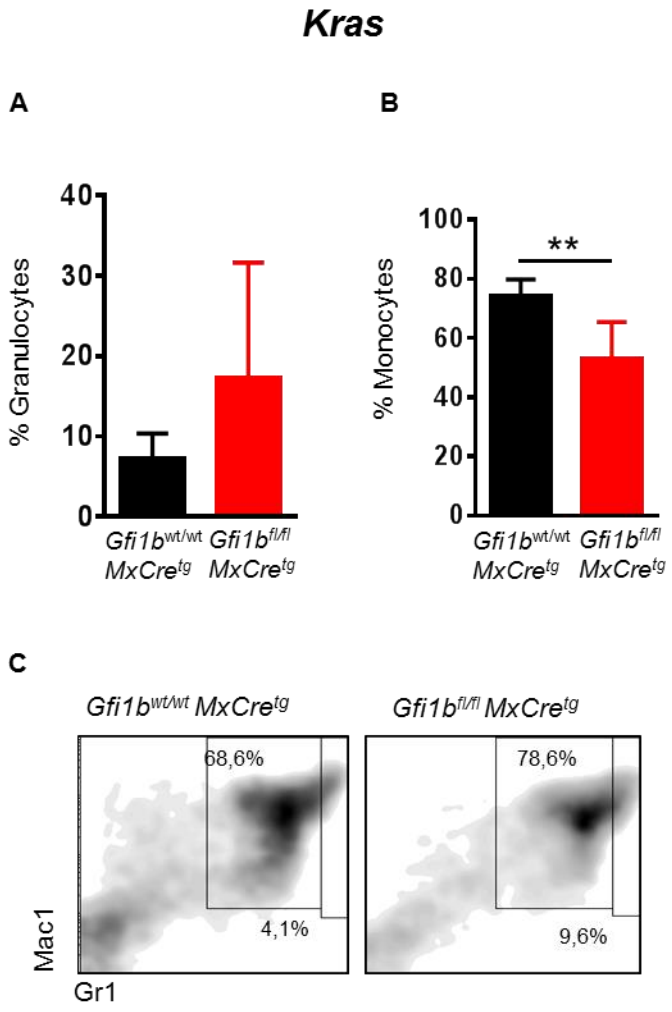

Figure 25: Identification of the immunophenotype in Kras oncogene mice with different Gfi1b expression levels.

A. *Plot shows Gr1 expression in Gfi1b$^{wt/wt}$ MxCre^{tg} Kras$^{+/fl}$ leukemic mice (black bar) and Gfi1b$^{fl/fl}$ MxCre^{tg} Kras$^{+/fl}$ mice (red bar).*

B. *Data presents monocytes (Mac1) expression in Gfi1b$^{fl/fl}$ Mxcre^{wt} NUP98/HOXD13^{tg} leukemic mice (black bar) and Gfi1b$^{fl/fl}$ MxCre^{tg} Kras$^{+/fl}$ mice (red bar).*

C*. FACS plot (left) shows the frequency of monocytes (Mac1^{hi}Gr1^{int}) and granulocytes (Mac1^{hi}Gr1^{hi}) in Gfi1b$^{wt/wt}$ MxCre^{tg} Kras$^{+/fl}$ BM cells. FACS plot (right) shows the frequency of monocytes (Mac1^{hi}Gr1^{int}) and granulocytes (Mac1^{hi}Gr1^{hi}) in Gfi1b$^{fl/fl}$ MxCre^{tg} Kras$^{+/fl}$ BM cells.*

3.3.2.2 PB analysis of *Kras* oncogenic mice

Finally, key PB parameters were analyzed in the PB of mice with an overt myeloproliferative disease. With respect to WBC and PLT counts mice showed no significant differences. Significant differences were, however, observed for HGB and RBC between *Gfi1b*$^{wt/wt}$ *MxCre*^{tg} *Kras*$^{+/fl}$ and *Gfi1b*$^{fl/fl}$ *MxCre*^{tg} *Kras*$^{+/fl}$ mice (Figure 26 A-D).

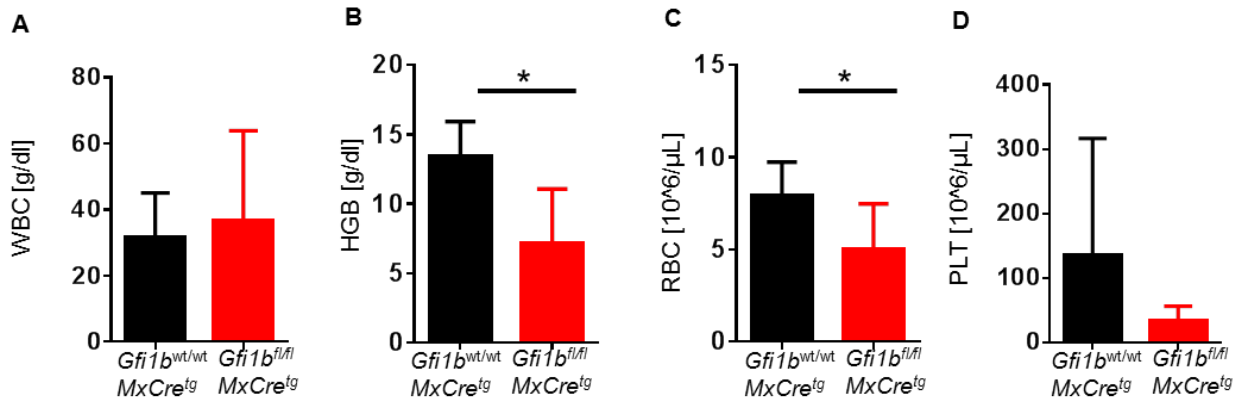

Figure 26: PB values between Gfi1b$^{wt/wt}$ MxCre^{tg} Kras$^{+/fl}$ and Gfi1b$^{fl/fl}$ MxCre^{tg} Kras$^{+/fl}$ mice.

A. *Data shows the amount of WBC in PB of Gfi1b$^{wt/wt}$ MxCre^{tg} Kras$^{+/fl}$ (black bar) or Gfi1b$^{fl/fl}$ MxCre^{tg} Kras$^{+/fl}$ (red bar) leukemic mice.*
B. *Amount of HGB in PB of Gfi1b$^{wt/wt}$ MxCre^{tg} Kras$^{+/fl}$ (black bar) or Gfi1b$^{fl/fl}$ MxCre^{tg} Kras$^{+/fl}$ (red bar) leukemic mice (p=0.0128).*
C. *RBC in PB of Gfi1b$^{wt/wt}$ MxCre^{tg} Kras$^{+/fl}$ (black bar) or Gfi1b$^{fl/fl}$ MxCre^{tg} Kras$^{+/fl}$ (red bar) leukemic mice (p=0.0186).*
D. *Amount of platelets in PB of Gfi1b$^{wt/wt}$ MxCre^{tg} Kras$^{+/fl}$ (black bar) or Gfi1b$^{fl/fl}$ MxCre^{tg} Kras$^{+/fl}$ (red bar) leukemic mice.*

3.3.2.3 Classification of leukemic mice based on cell morphology in BM and PB

Similar to the approach to the *NUP98/HOXD13*^{tg} mice, I also performed cytological analysis for *Kras* oncogenic mice. BM cytospins as well as PB blood smears of *Gfi1b*$^{wt/wt}$ *MxCre*^{tg} *Kras*$^{+/fl}$ and *Gfi1b*$^{fl/fl}$ *MxCre*^{tg} *Kras*$^{+/fl}$ mice showed no differences in cytological appearance (Figure 27) (Data not shown).

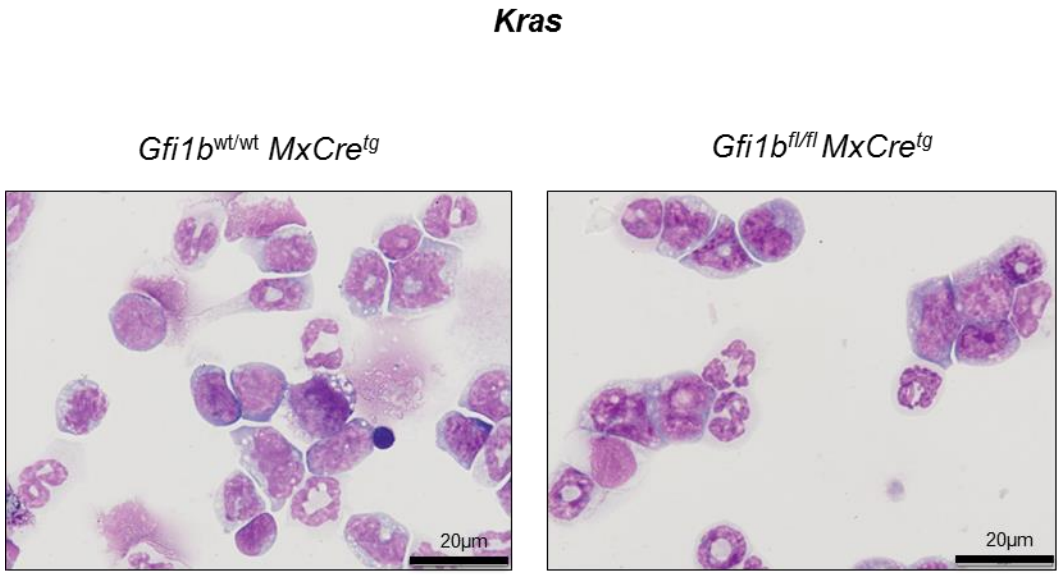

Figure 27: Cytological features of Kras oncogenic mice.
BM cytospin from representative Gfi1b$^{wt/wt}$ *MxCre*^{tg} *Kras*$^{+/fl}$ *(left) and BM cytospin from Gfi1b*$^{fl/fl}$ *MxCre*^{tg} *Kras*$^{+/fl}$ *(right) mice.*

3.4 Loss of *Gfi1b* in mice accelerated the onset of leukemia development

3.4.1 Primary transplantation of leukemic BM cells expressing the *MLL-AF9* fusion-oncogene

To confirm in a third leukemia mouse model that loss of *Gfi1b* influences leukemia development, I used a model in which the *MLL-AF9* oncofusion protein can be retrovirally expressed in murine hematopoietic cells. MLL-AF9 is the product of the t (9;11)(q22;p23) (Krivtsov and Armstrong 2007) and is frequently found in AML patients. Lin$^-$ BM cells of *Gfi1b$^{fl/fl}$ MxCre^{wt} and Gfi1b$^{fl/fl}$ MxCre^{tg}* were isolated and transduced with pMSCV- *MLL-AF9* -IRES-*GFP*. GFP-positive cells, expressing the *MLL-AF9* fusion oncogene were transplanted into lethally irradiated primary recipient mice (Figure 28). After 3 weeks, the mice were treated with poly (I:C) to activate the *Cre*-mediated excision of *Gfi1b* sequences to prevent expression of a functional Gfi1b protein.

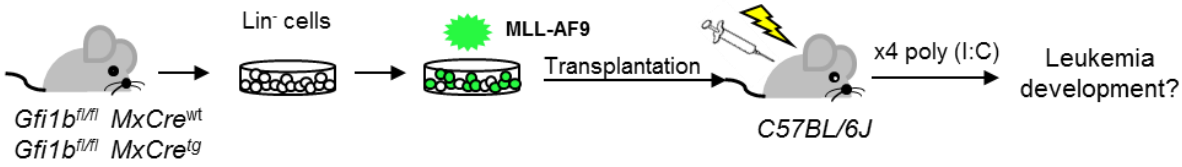

Figure 28: Experimental design of primary transplantation with MLL-AF9.

Lin$^-$ BM cells derived from Gfi1b$^{fl/fl}$ MxCre^{wt} and Gfi1b$^{fl/fl}$ MxCre^{tg} mice were isolated, transduced with a retroviral plasmid expressing the MLL-AF9-IRES-GFP genes, and transplanted intravenously in lethally irradiated mice. Mice were injected with poly (I:C). Mice were monitored for signs of leukemia as described.

3.4.2 Absence of *Gfi1b* promoted AML development

Mice that received *Gfi1b*$^{fl/fl}$*MxCre*^{wt} BM cells transduced with *MLL-AF9* and treated with poly (I:C) developed leukemia with a median survival of 27 days. In contrast, mice transplanted with *Gfi1b*$^{fl/fl}$*MxCre*^{tg} cells transduced with *MLL-AF9* and subsequently injected with poly (I:C) developed overt leukemia with a median survival of 7 days (Figure 29).

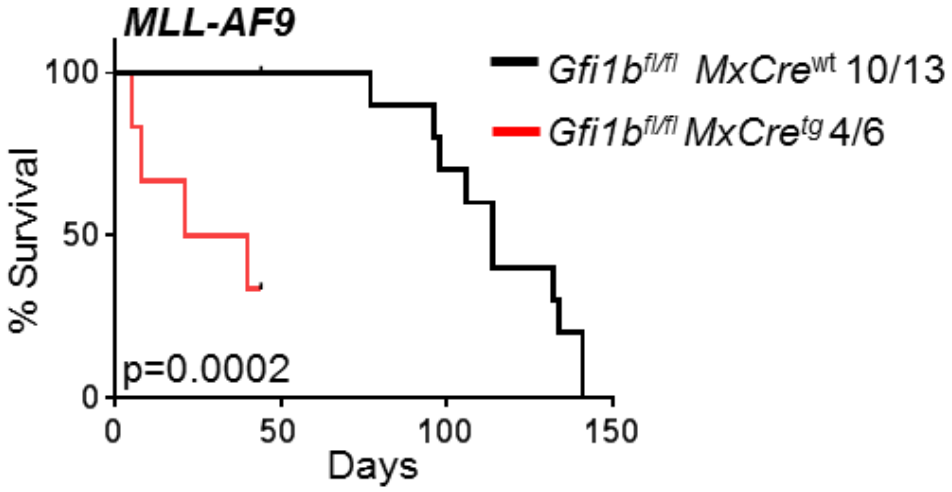

Figure 29: Loss of Gfi1b fastened the onset of AML development in MLL-AF9 oncogenic mice.

Kaplan-Meier curve represents the survival rate of retrovirally transduced MLL-AF9 leukemic cells in Gfi1b$^{fl/fl}$ *MxCre*^{wt} *(black bar) and Gfi1b*$^{fl/fl}$ *MxCre*^{tg} *(red bar). Indicated is the number of mice succumbing to AML (p=0.0002).*

3.4.2.1 Immunophenotypic characterization of leukemic cells expressing the *MLL-AF9* oncogene and with different *Gfi1b* expression level

Similar to the procedures described above, the immunophenotypic analysis of BM cells derived from *Gfi1b*$^{fl/fl}$ *MxCre*^{wt} *and Gfi1b*$^{fl/fl}$ *Mxcre*^{tg} leukemic mice expressing *MLL-AF9* were performed (Figure 30A). Both, *Gfi1b*$^{fl/fl}$ *MxCre*^{wt} and *Gfi1b*$^{fl/fl}$ *MxCre*^{tg} *MLL-AF9*-expressing BM cells showed no significant differences according to myeloid markers such as Gr1, Mac1(Figure 30B + 30C), and c-kit (Figure 30D).

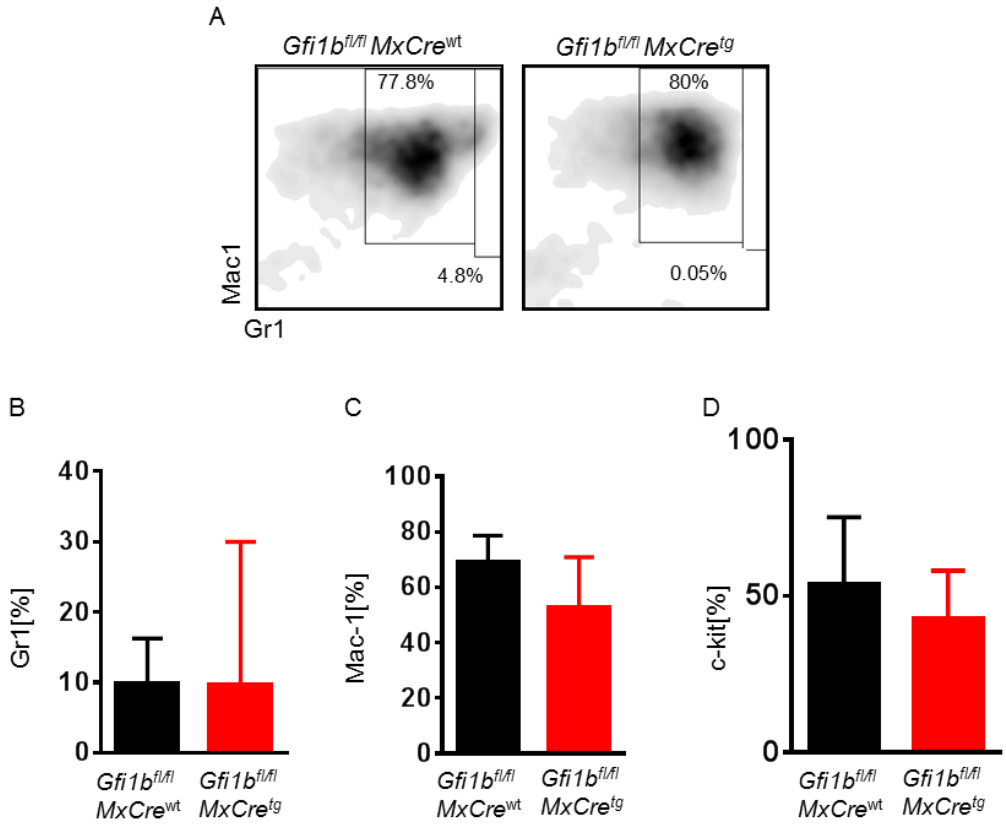

Figure 30: Immunophenotype of MLL-AF9-expressing cells in Gfi1b$^{fl/fl}$ MxCre^{wt} and Gfi1b$^{fl/fl}$ MxCre^{tg} cells.

A. *FACS plot (left) shows the frequency of monocytes (Mac1^{hi}Gr1^{int}) and granulocytes (Mac1^{hi}Gr1^{hi}) in Gfi1b$^{fl/fl}$ MxCre^{wt} MLL-AF9 BM cells. FACS plot (right) shows the frequency of monocytes (Mac1^{hi}Gr1^{int}) and granulocytes (Mac1^{hi}Gr1^{hi}) in Gfi1b$^{fl/fl}$ MxCre^{tg} MLL-AF9 BM cells.*
B. *Data presents the percentage of granulocytes in Gfi1b$^{fl/fl}$ MxCre^{wt} MLL-AF9 BM cells (n=6) and Gfi1b$^{fl/fl}$ MxCre^{tg} MLL-AF9 BM cells (n=4).*
C. *Data presents the percentage of monocytes in Gfi1b$^{fl/fl}$ MxCre^{wt} MLL-AF9 BM cells (n=6) and Gfi1b$^{fl/fl}$ MxCre^{tg} MLL-AF9 BM cells (n=4).*
D. *Data presents the percentage of c-kit in Gfi1b$^{fl/fl}$ MxCre^{wt} MLL-AF9 BM cells (black bar) (n=6) and Gfi1b$^{fl/fl}$ MxCre^{tg} MLL-AF9 BM cells (red bar) (n=4).*

3.4.2.2 Blood analysis of *MLL-AF9* oncogenic mice with different expression levels of *Gfi1b*

Similar to the approaches above, PB cells of *MLL-AF9* leukemic mice were analyzed with regard to key parameters. There were no major differences detected in WBC, HGB, and RBC, but significant difference in PLT between *Gfi1b$^{fl/fl}$ MxCre^{wt} MLL-AF9 and Gfi1b$^{fl/fl}$ MxCre^{tg} MLL-AF9* mice were found (Figure 31).

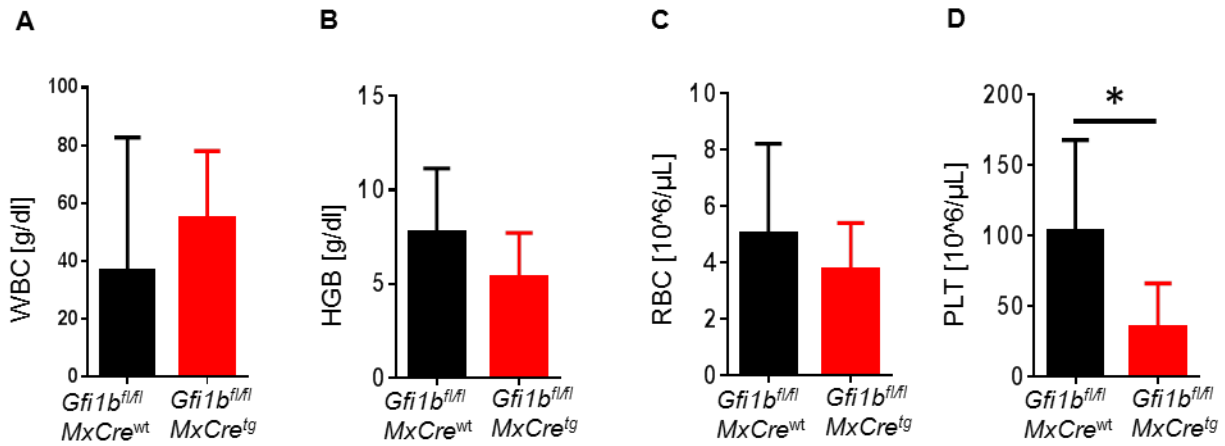

Figure 31: PB analysis of MLL-AF9 leukemic cells.

A. *WBC in PB of Gfi1b$^{fl/fl}$ MxCre^{wt} MLL-AF9 (black bar) (n=6) or Gfi1b$^{fl/fl}$ MxCre^{tg} MLL-AF9 (red bar) (n=4) leukemic mice.*
B. *Amount of HGB in PB of Gfi1b$^{fl/fl}$ MxCre^{wt} MLL-AF9 (black bar) (n=6) or Gfi1b$^{fl/fl}$ MxCre^{tg} MLL-AF9 (red bar) (n=4) leukemic mice.*
C. *RBC in PB of Gfi1b$^{fl/fl}$ MxCre^{wt} MLL-AF9 (black bar) (n=6) or Gfi1b$^{fl/fl}$ MxCre^{tg} MLL-AF9 (red bar) (n=4) leukemic mice.*
D. *Amount of platelets in PB of Gfi1b$^{fl/fl}$ MxCre^{wt} MLL-AF9 (black bar) (n=6) or Gfi1b$^{fl/fl}$ MxCre^{tg} MLL-AF9 (red bar) (n=4) leukemic mice(p=0.0128).*

3.4.2.3Classification of leukemic mice based on cell morphology in BM and PB

Cytospins of leukemic BM cells and PB smears were morphologically examined. *MLL-AF9*-expressing blast cells in *Gfi1b$^{fl/fl}$ MxCre*^{wt} and *Gfi1b$^{fl/fl}$ MxCre^{tg}* mice showed no major differences with regard to cytological appearance in BM cells (Figure 32) and PB (Data not shown).

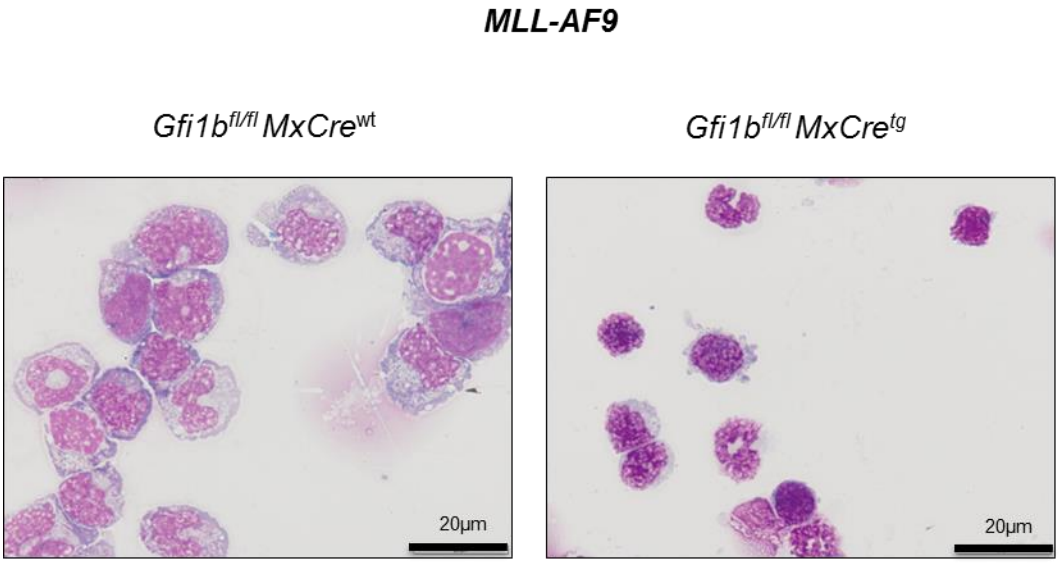

Figure 32: Cytological features of MLL-AF9 oncogene BM cells.

BM cytospin from representative Gfi1b$^{fl/fl}$ MxCre^{wt} MLL-AF9 (left) and BM cytospin from Gfi1b$^{fl/fl}$ MxCre^{tg} MLL-AF9 (right).

In summary, these data indicate that loss of *Gfi1b* increased the incidence and shortened the latency of AML development in three various mouse models; thus pointing to an important role of this TF in AML leukemogenesis.

3.4.3 Loss of *Gfi1b* leads to expansion of functional leukemic stem cells

After examining the role of Gfi1b with regard to the onset and progression of malignant hematopoiesis, I examined the possible mechanism behind this. It has been shown before, that loss of *Gfi1b* increases the functional stem cells (Khandanpour, Sharif-Askari et al. 2010). Therefore, I assumed that loss of *Gfi1b* might also increase the number of LSCs. To estimate the frequency of LSCs in *Gfi1b*-deficient cells, an *in vivo* limiting dilution transplantation assay was performed.

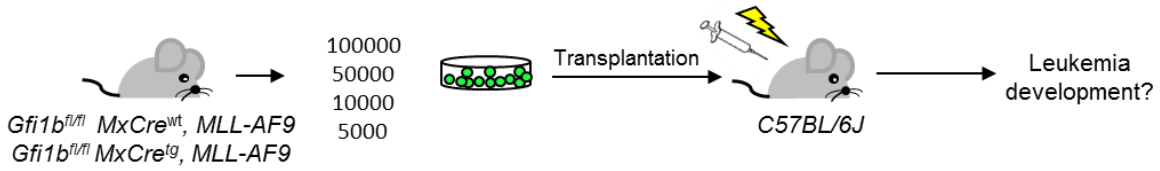

Figure 33: Experimental design for an in vivo limiting dilution transplantation assay.
MLL-AF9 BM leukemic cells, both Gfi1b$^{fl/fl}$ MxCre^{wt} and Gfi1b$^{fl/fl}$ MxCre^{tg} cells were retransplanted into new recipient sublethally irradiated mice. Serial dilutions were performed with 1x10^5, 5x10^4, 1x10^4 and 5x10^3 cells and injected intravenously in sublethally irradiated mice. Leukemia development was monitored.

Gfi1b$^{fl/fl}$ MxCre^{wt}, MLL-AF9 and Gfi1b$^{fl/fl}$ MxCre^{tg}, MLL-AF9 (with already induced deletion of the *Gfi1b* alleles) leukemic cells were injected intravenously into new sublethally irradiated recipient animals (Figure33). In summary, cohorts of 4 groups of mice were assembled. One day before transplantation mice were sublethally irradiated with 3Gy.

$1x10^5$ GFP^+ (4 mice / group), $5x10^4$ GFP^+ (3mice / group), $1x10^4$ GFP^+ (3 mice / group) and $5x10^3$ GFP^+ (3 mice / group) leukemic BM cells were intravenously transplanted, respectively, into each cohort. Mice transplanted with *Gfi1b*$^{fl/fl}$ *MxCre*^{tg} *MLL-AF9* with a total amount of $1x10^5$ GFP^+ or $5x10^4$ GFP^+ leukemic BM cells had a shorter survival rate compared to those mice which were transplanted with $1x10^4$ GFP^+ and $5x10^3$ GFP^+ cells. When comparing mice transplanted with *Gfi1b*-deficient leukemic BM cells, (*Gfi1b*$^{fl/fl}$ *MxCre*^{tg}, *MLL-AF9* leukemic cells), which expresses functional Cre, developed faster leukemia than mice transplanted with *Gfi1b*$^{wt/wt}$, *MLL-AF9* (*Gfi1b*$^{fl/fl}$ MxCre^{wt}, *MLL-AF9*) leukemic cells, confirming the results reported above (Figure 34 A+B).

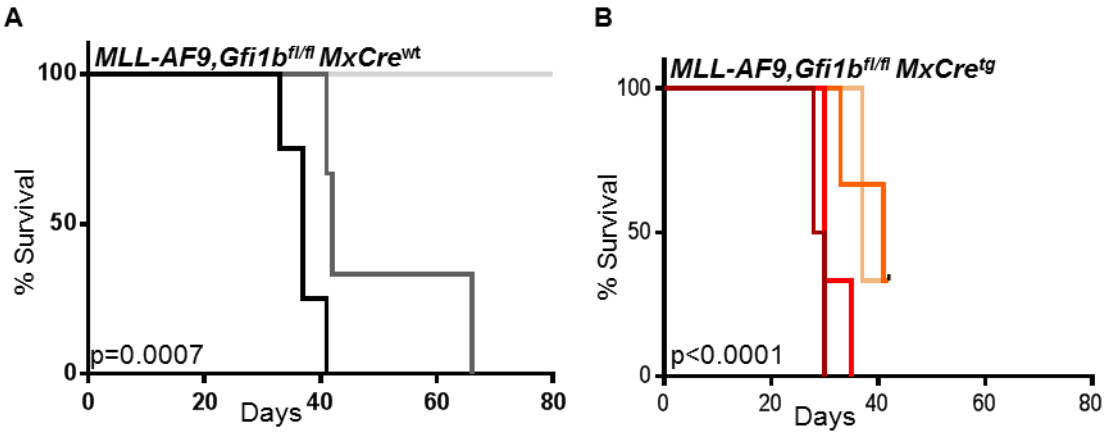

C

Genotype, no. of transplanted cells	Positive recipients	One functional stem cell within	Upper and lower limit
MLL-AF9, Gfi1b$^{fl/fl}$ MxCre^{wt}			
100000	4/4	1:63000	1:30000 - 1:200000
50000	3/3		
10000	0/3		
5000	0/3		
MLL-AF9, Gfi1b$^{fl/fl}$ MxCre^{tg}			
100000	4/4	1:3500	1:2000 - 1:20000
50000	3/3		
10000	3/3		
5000	2/3		

Figure 34: Loss of Gfi1b increased the number of LSCs in mice.

A. *The Kaplan-Meier curves present the survival rates of the Gfi1b$^{fl/fl}$ MxCre^{wt}, MLL-AF9 expressing mice (p=0.0007).*
B. *The Kaplan-Meier curves show the survival rates of Gfi1b$^{fl/fl}$ MxCre^{tg}, MLL-AF9 mice (p<0.0001).*
C. *Leukemic cells were transplanted with serial dilution numbers of GFP^{+} cells; 1x10^{5}, 5x10^{4}, 1x10^{4} and 5x10^{3} each per animal. The calculation of the number of functional leukemic stem cells in both groups was performed by using the website http://bioinf.wehi.edu.au/software/elda.*

Using this approach, the frequency of LSCs was determined. Loss of *Gfi1b* increased the LSC frequency to 1:3.500 (Figure 34C) compared to a LSC frequency in *Gfi1b*$^{wt/wt}$, *MLL-AF9* (*Gfi1b$^{fl/fl}$ MxCre^{wt}, MLL-AF9)* leukemic cells of 1:63.000. Conclusively, loss of *Gfi1b* increased the number of LSCs by a factor of 18.

3.5 Molecular function of loss of *Gfi1b* in progress of AML development

Loss of *Gfi1b* influenced the AML progression, but the molecular function of Gfi1b in AML progression and how it increased the number of LSC remains unclear. In a first approach, I wanted to identify differentially expressed signal cascades in *Gfi1b*$^{wt/wt}$ leukemic mice *(Gfi1b$^{fl/fl}$ MxCre^{wt}, NUP98/HOXD13^{tg})* and *Gfi1b*-deficient leukemic mice *(Gfi1b$^{fl/fl}$ MxCre^{tg}, NUP98/HOXD13^{tg})*. As a model, I chose *NUP98/HOXD13^{tg}* mice, both because this mouse model recapitulates the human features of MDS/AML progression (Lin, Slape et al. 2005) and because there was a striking difference in the survival of *Gfi1b*$^{wt/wt}$ *leukemic cells* and *Gfi1b*-deficient leukemic cells. BM leukemic blast cells of these two mouse strains from *Gfi1b$^{fl/fl}$ MxCre^{wt}, NUP98/HOXD13^{tg}* and *Gfi1b$^{fl/fl}$ MxCre^{tg}, NUP98/HOXD13^{tg}* were analyzed using microarrays (Figure 35). The analysis of the

arrays was performed in the genomic core facility of the UK Essen led by **PD Ludger Klein-Hitpass**.

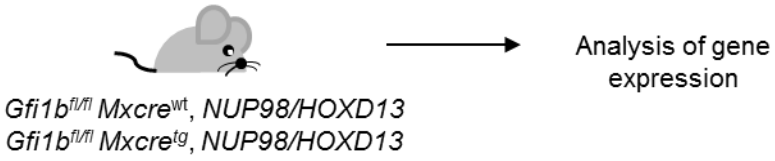

Figure 35: Illustration of experimental design.

$Gfi1b^{fl/fl}$ $MxCre^{wt}$, $NUP98/HOXD13^{tg}$ and $Gfi1b^{fl/fl}$ $MxCre^{tg}$, $NUP98/HOXD13^{tg}$ leukemic BM cells were chosen for genome wide expression analyses.

For microarray analyses, the Affymetrix GeneChip platform using the Express Kit protocol for sample preparation and microarray hybridization were used. Finally, data analysis by ANOVA was performed with PartekGS by **PD Ludger Klein-Hitpass and Dr. Lothar Vassen** (who is the responsible bioinfomatician in our group).

Gene set enrichment analysis (GSEA) is a tool to identify which pathways are deregulated in a set of expression data (Subramanian, Tamayo et al. 2005). The gene expression data were analyzed using the GSEA approach (http://software.broadinstitute.org/gsea/index.jsp) (Mootha, Lindgren et al. 2003; Subramanian, Tamayo et al. 2005) to identify gene expression pathways, which are significantly enriched or depleted in *$Gfi1b^{wt/wt}$* and *Gfi1b*-deficient leukemic BM cells. Loss of *Gfi1b* was associated with the enrichment of gene signatures governing AML development and stem cell regulation. GSEA results showed a positive enrichment score for Valk AML cluster 8 (Valk, Verhaak et al. 2004) and Ramalho stemness up (Ramalho-Santos, Yoon et al. 2002) (Figure 36). *Gfi1b*-deficient leukemic BM cells showed a negative enrichment score and hence a depletion of gene sets involved in myelo-monocytic differentiation, which in turn recapitulated the flow cytometry data of Mac1 and Gr1 in *$NUP98/HOXD13^{tg}$* leukemic mice (see Section 3.2.2.1). Basically, enrichment score (ES) reflect the overrepresented gene set at the top and bottom of our

uploaded ranked gene list. As shown in Figure 36, a distinct peak at the start point or at the end of the GSEA plot are the most interesting gene sets (Subramanian, Tamayo et al. 2005). Finally, genes regulating hematopoietic cell lineage development were depleted in the gene expression profile of *Gfi1b*-deficient leukemic BM cells (Kluger, Tuck et al. 2004) (Figure 36). Collectively, these data indicate that loss of *Gfi1b* leads to a gene expression signature resembling that of very early progenitors/stem cells and LSC.

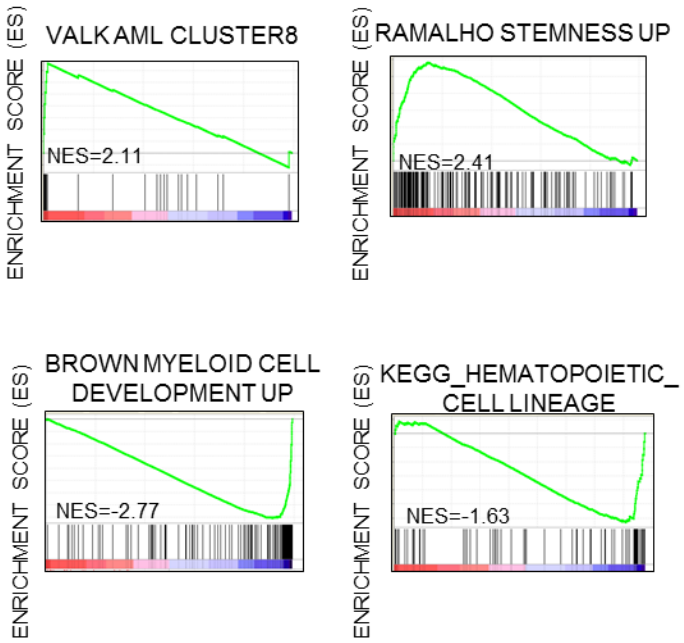

Figure 36: Results of GSEA in Gfi1b$^{fl/fl}$ MxCre^{tg} NUP98/HOXD13^{tg} BM cells.

Leukemic Gfi1b$^{fl/fl}$ MxCre^{tg}, NUP98/HOXD13^{tg} mice show a significant enrichment score for the GSEA for Valk AML Cluster 8 (NES=2.11and p (<0.000)) and Ramalho stemness up (NES=2.41and p (<0.000)). Leukemic Gfi1b$^{fl/fl}$ MxCre^{tg}, NUP98/HOXD13^{tg} mice show a significant enrichment score for the GSEA for Brown myeloid cell development up (NES=-2,77 and p(<0.000)) and KEGG hematopoietic cell lineage (NES=-1.63 and p(<0.000)). NES= normalized enrichment score.

Gfi1b is a transcriptional repressor that recruits histone modifying enzymes, such as histonedeacetylase (HDACs), to its target gene promoters (Saleque, Kim et al. 2007). Therefore, I next investigated which epigenetic differences can be observed between *Gfi1b*- deficient and *Gfi1b*-expressing *NUP98/HOXD13*^{tg} leukemic mice.

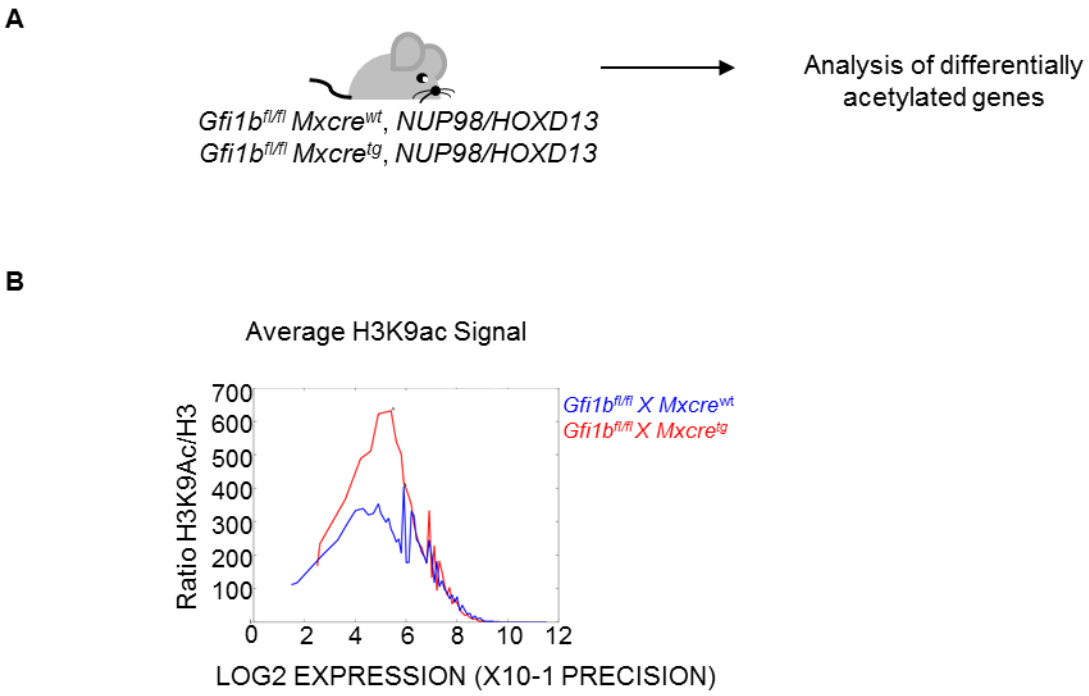

Figure 37: Gfi1b-deficient mice showed a high H3K9 acetylation in leukemic BM cells.

A*. Chromatin immunoprecipitation (ChIP) analysis was performed with Gfi1b*$^{fl/fl}$ *MxCre*^{wt} *NUP98/HOXD13*^{tg} *and Gfi1b*$^{fl/fl}$ *MxCre*^{tg} *NUP98/HOXD13*^{tg} *leukemic BM cells.*
B*. The histogram profile shows the average distribution of H3K9 acetylation level in Gfi1b-deficinet leukemic BM cells (red line) and Gfi1b-expressing leukemic BM cells (blue line).*

We analyzed genome-wide H3K9 acetylation levels in *Gfi1b*$^{wt/wt}$ and *Gfi1b*-deficient leukemic cells. We chose this marker, because Gfi1b recruits HDACs to its target genes, which in turn induce deacetylation of Lysin 9 of Histon 3 (H3K9acetyl). H3K9 is an epigenetic marker for active transcription (Wilson, Foster et al. 2010). All analysis shown here were performed by **Dr. Lothar Vassen**. ChIP preparation was performed with the

help of Dr. Judith Schütte. Basically protein-DNA interaction will be fixed using formaldehyde as a cross linker. Next, the chromatin was sonicated into small pieces of 200-250 bp. Finally immnuoprecipitation was perfomed with Gfi1b antibody and the sample was prepared for library preparation (Liu, Pott et al. 2010). Chromatin immunoprecipitation sequencing (ChIP-Seq) is a method to analyse genome-wide protein-DNA interactions, such as histone modifications. The ChIP-Seq analysis was performed using leukemic cells originating from *Gfi1b*$^{fl/fl}$ *MxCre*^{wt} *NUP98/HOXD13*^{tg} and *Gfi1b*$^{fl/fl}$ *MxCre*^{tg} *NUP98/HOXD13*^{tg} ChIP-Seq analysis indicated that loss of *Gfi1b* was associated mice injected with poly (I:C) with genome-wide higher levels of H3K9 acetylation around the transcription start site (TSS) of Gfi1b target genes compared to the acetylation level in *Gfi1b*-expressing leukemic cells (Figure 37 B). Kyoto encyclopaedia of genes and genomes (KEGG) is an online tool for studying the biological system in different organism. Using this tool, we compared which genes are more highly acetylated in *Gfi1b*-deficient leukemic cells compared to *Gfi1b*-expressing leukemic cells. We found that genes regulating erythroid development showed higher levels of H3K9 acetylation of their respective promoter areas, which reflects the known function of Gfi1b in erythroid development (Vassen, Beauchemin et al. 2014). I also observed differential acetylation of promoter areas of genes involved in myeloid development (Figure 38 A and B), which mirrors my results using flow cytometry analysis, in which I observed significantly lower expression of myeloid surface markers.

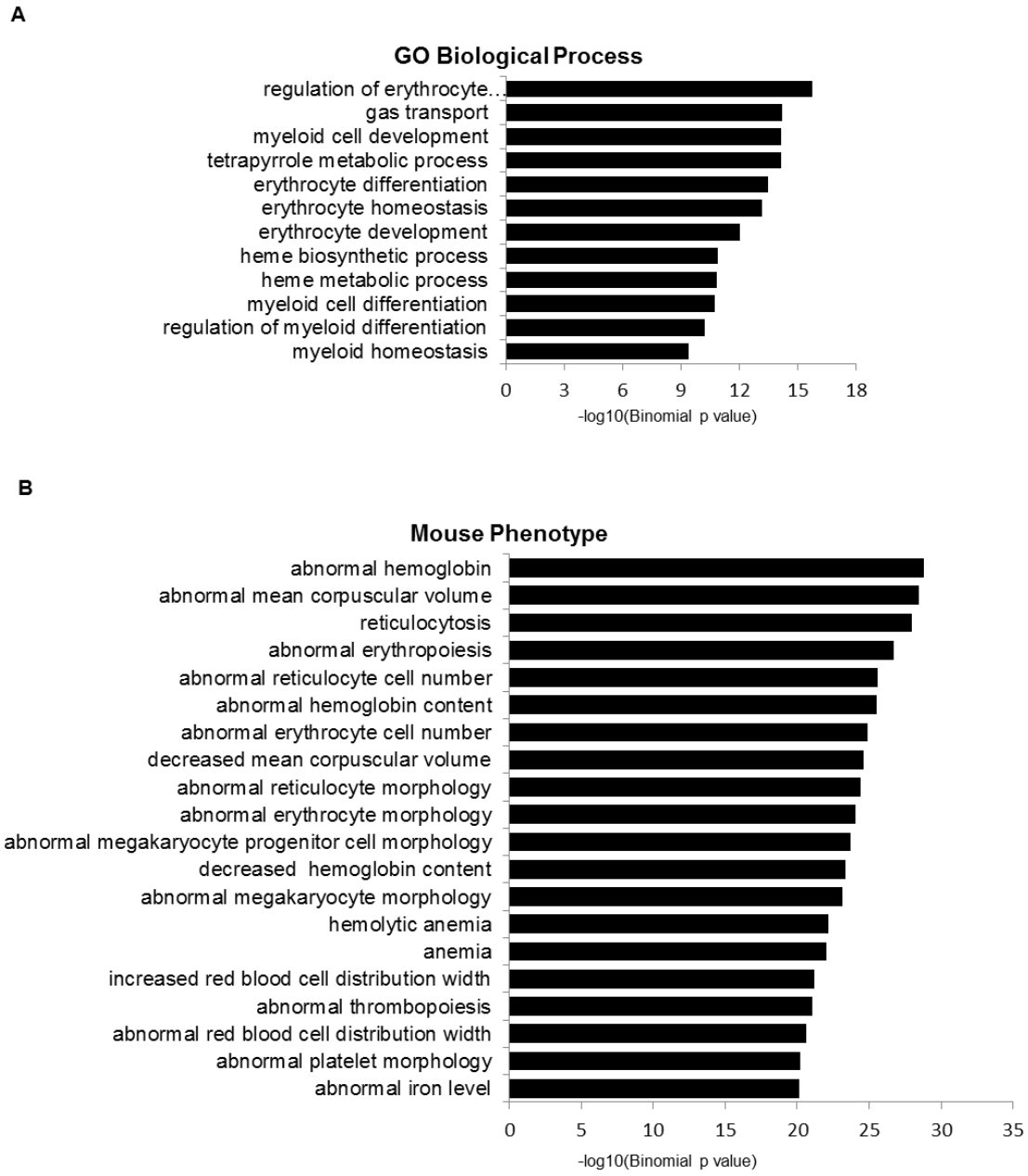

Figure 38: KEGG pathway analysis in Gfi1b-deficient leukemic BM cells.

A. *Gene Ontology (GO) biological process showed that both erythroid and myeloid functions were enriched in Gfi1b-deficient leukemic mice.*
B. *Mouse phenotype showed that in Gfi1b-deficient mice erythroid regulation came up, respectively. Analysis was performed by using a binominal test.*

As a third bioinformatics analysis, GSEA analysis was performed by comparing differentially acetylated genes in *Gfi1b*-expressing and *Gfi1b*-deficient leukemic BM cells. GSEA analysis showed that gene sets associated with the regulation of cell growth (cell proliferation) and GNF2_MAP2K3 (Figure 39, left and right) were enriched in *Gfi1b*-deficient leukemic BM cells. Finally, functional Molecular Signatures Databases (MSigDB), a tool for gene sets for performing GSEA analysis (Liberzon, Birger et al. 2015) was used. Basically gene collection analysis revealed that pathways such as the regulation of p38-alpha and p38-beta, IL-2 signaling events mediated by PI3K and p38 signaling pathway were significantly enriched in *Gfi1b*-deficient leukemic BM cells (Figure 40).

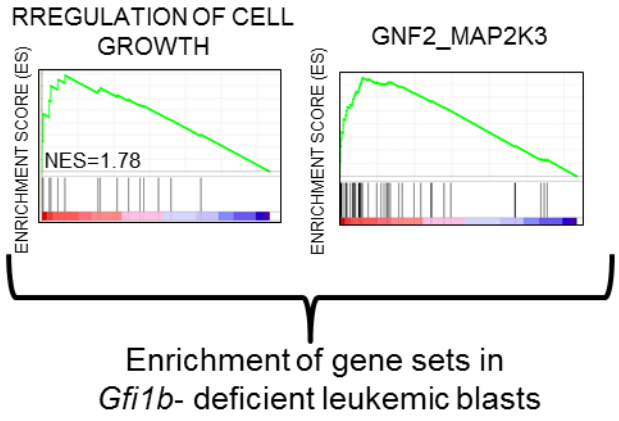

Figure 39: Results of GSEA in Gfi1b-deficient leukemic BM cells.

Leukemic Gfi1b$^{fl/fl}$ MxCre^{tg} NUP98/HOXD13^{tg} mice showed a significant enrichment score for the GSEA for regulation of cell growth (NES=1.78 and p (<0.0047)) and GNF2_MAPK3 (NES=2.02 and p(<0.000)). NES= normalized enrichment score.

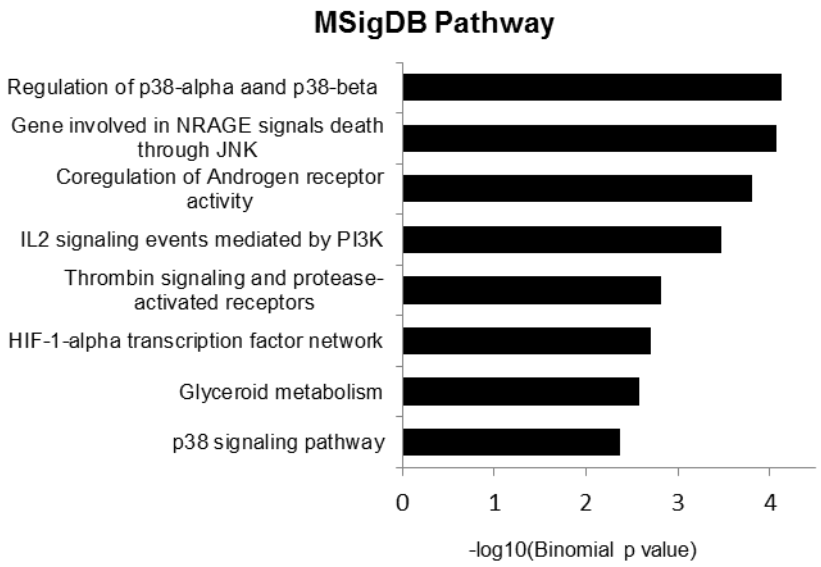

Figure 40: MAPK signaling pathway came up in Gfi1b-deficient leukemic BM cells.

Chip-Seq data revealed MAPK signaling pathway were enriched in Gfi1b-deficient leukemic BM cells by using the MSigDB (molecular signatures databases) pathway approach.

To confirm the data from the gene expression array and ChIP-Seq analysis, I performed RT^2 profiler PCR array analysis with a set of genes involved in cancer stem cells to validate the results obtained in the gene expression arrays. Genes which are involved in regulating stem cells/ leukemic stem cells like *Abcg2, Gata3, Itga2, Thy1, Cd24a, Pecam1, Prom1, Plaur, Klf4, Mycn, Ptch1, Pecam1, Sav1, and Notch1* were deregulated more than 2-fold between in *Gfi1b*-deficient *NUP98/HOXD13*^{tg} leukemic cells and *Gfi1b*$^{wt/wt}$ *NUP98/HOXD13*^{tg} cells. These results were in accordance with regard to up or downregulation of the results in the gene expression arrays (Figure 41).

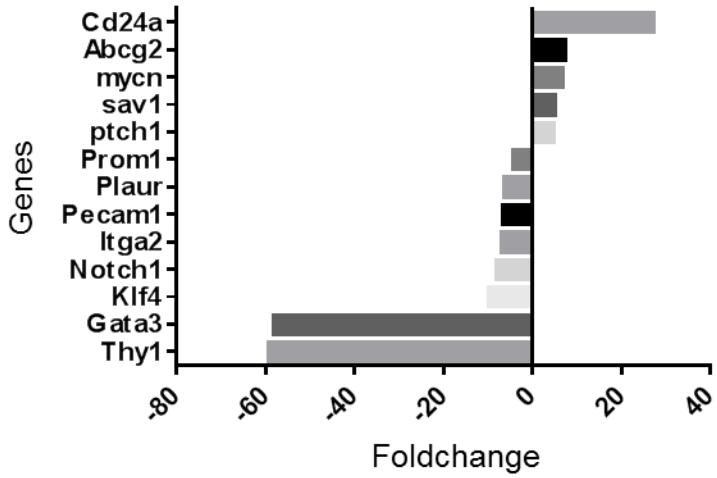

Figure 41 RT^2 Profiler^{TM} PCR array results in NUP98/HOXD13^{tg} leukemic mice.

Gene expression results revealed, genes which are involved in stem cell regulation are deregulated in Gfi1b$^{fl/fl}$ MxCre^{tg} NUP98/HOXD13^{tg} mice. Down-regulated genes are like Thy1, Gata3, Klf4, Notch1, Itga2, Pecam1, Plaur and Prom1 and up-regulated genes are Cd24a, Abcg2, Mycn, Sav1, Ptch1. Genes were selected by more than 2-fold change between Gfi1b$^{wt/wt}$ and Gfi1b-deficient leukemic BM cells.

Initially I used published gene expression data from blast cells of patients diagnosed with MDS and AML to study patterns of *GFI1B* expression in healthy and malignant cells. To test whether a similar signaling pattern can be found in murine AML cells, **Dr. Lothar Vassen** correlated published gene expression array of *GFI1B* low and *GFI1B* high expression human leukemic cells with the gene expression pattern in *Gfi1b*$^{wt/wt}$ and *Gfi1b*-deficient leukemic BM cells based on an AltAnalyze approach. I observed that in both, murine and human, low level of *GFI1B* or loss of *Gfi1b* was associated with an AML signaling pathway involving JAK-STAT, MAPK, and ROS signaling (Figure 42).

human GFI1B			
Pathway	Genes in List	p-value	FDR
JAK-STAT	11	0	0
MAPK_PI3K	9	0.007	0.006
ROS related	8	0.000	0.000

mouse Gfi1b			
Pathway	Genes in List	p-value	FDR
JAK-STAT	14	4.55E-06	6.72E-06
MAPK_PI3K	11	0.000558	0.00047
ROS related	8	0.003	0.002

Figure 42: Signaling pathways in human GFI1B and mouse Gfi1b cells.

Tables show which pathways are similar deregulated in Gfi1b low expressing human AML cells and Gfi1b-deficient murine AML cells. The first table presents human low GFI1B- expressing leukemic cells: JAK-STAT pathway with 11 genes in list with a p=0 and FDR=0, MAPK_PI3K with 9 genes in list with a p=0.007 and FDR=0.006, ROS-signaling with 8 genes in list with a p=0.000 and FDR=0.000.The second table presents mouse Gfi1b-deficient leukemic cells: JAK-STAT pathway with 14 genes in list with a p=0.000000455 and FDR=0.000000672, MAPL_PI3K with 11 genes in list with a p=0.000558 and FDR=0.00047, ROS-signaling with 8 genes in list with a p=0.003 and FDR=0.002. (FDR=false discovery rate).

3.6 *Gfi1b*-deficient leukemic cells show elevated ROS levels

As shown above, pathways involved in ROS regulation were similarly regulated in *Gfi1b*-deficient murine leukemic cells and *GFI1B* low expressing human leukemic cells. Therefore I next investigated the ROS levels in murine leukemic blast cells. As shown above, low levels of *GFI1B* in human blast cells as well as absent expression of *Gfi1b* in murine leukemic cells led to similar patterns of deregulation of genes involved in ROS signaling. In a previous study, it was shown that *Gfi1b*-deficient HSCs had elevated ROS levels compared to the *Gfi1b*$^{wt/wt}$ HSC (Khandanpour, Sharif-Askari et al. 2010). ROS is also involved in the pathogenesis of AML development (Zhou, Shen et al. 2013),

thus, I measured the intracellular ROS levels in *c-kit* positive leukemic blast cells. I focused the analysis on *c-kit*-expressing blast cells, as it has been shown before that *c-kit* is a marker for LSCs (Wang, Krivtsov et al. 2010) as well as a dye (2',7' – dichlorofluorescin diacetate (DCFDA)) which specifically marks ROS (Wang, Wu et al. 2017). Upon reaction with ROS elements, this dye gives a signal in the FITC channel. Hence the x-.axis is the logarithmic representation of the signal strength of the DCFDA dye and the y-axis is the frequency of the different measurements (Figure 43 A). *Gfi1b*$^{fl/fl}$ *MxCre*^{wt} *NUP98/HOXD13*^{tg} *and Gfi1b*$^{fl/fl}$ *MxCre*^{tg} *NUP98/HOXD13*^{tg} *cells* showed two ROS-containing cell-populations in the *c-kit* positive fraction, which also contains the LSC fraction, ROS low and ROS high. Two differentially ROS-expressing populations in leukemic cells were previously described (Jang and Sharkis 2007; Ludin, Gur-Cohen et al. 2014). The ROS low population was characterized as quiescent long-term repopulating HSCs and ROS high as short-term repopulating HSCs, respectively (Ludin, Gur-Cohen et al. 2014). Another study also showed that ROS low cells are characterized as human LSC and over-express *BCL-2* (Lagadinou, Sach et al. 2013). Loss of *Gfi1b* showed an increased level of ROS, in both populations, the ROS low and the ROS high expressing *c-kit* positive leukemic blast cells as defined by mean fluorescence intensity (MFI) (Figure 43 B). Overall, these results showed that loss of *Gfi1b* was associated with higher ROS level in leukemic cells, recapitulating the findings for ROS in "healthy" murine HSCs (Khandanpour, Sharif-Askari et al. 2010).

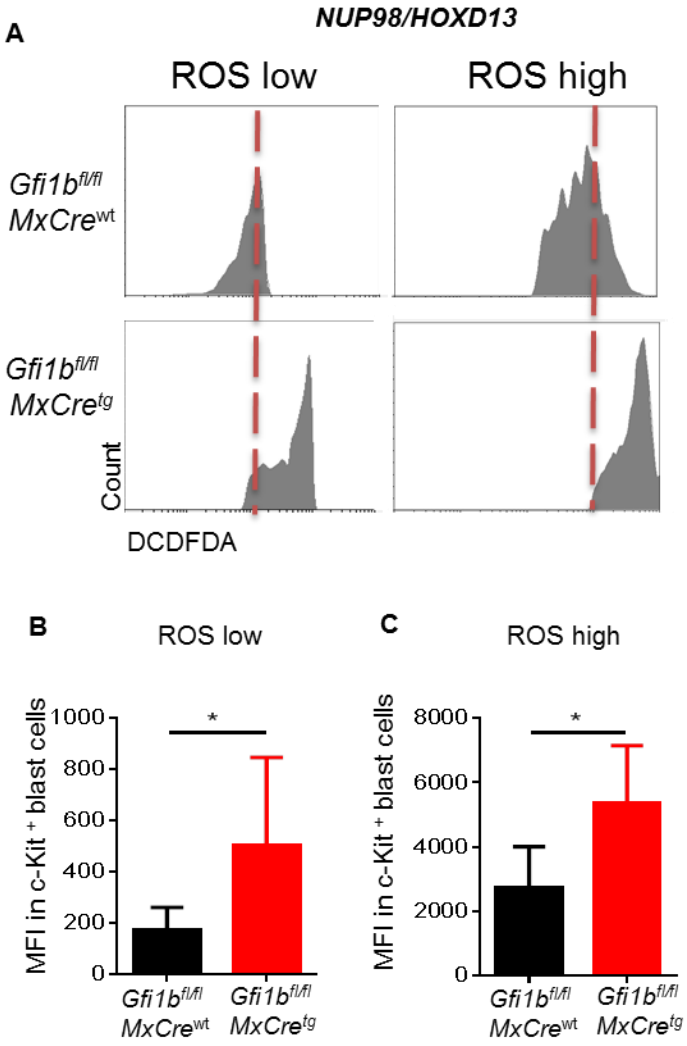

Figure 43: Loss of Gfi1b showed an increased ROS level in LSC populations.

$Gfi1b^{fl/fl}$ $MxCre^{wt}$ $NUP98/HOXD13^{tg}$ and $Gfi1b^{fl/fl}$ $MxCre^{tg}$ $NUP98/HOXD13^{tg}$ leukemic BM cells were stained with an anti c-Kit antibody (CD117) and DCFDA-FITC.
A. *Gating strategy of two different ROS populations by mean fluorescence intensity (MFI) in Gfi1b-expressing leukemic BM cells and Gfi1b-deficient leukemic BM cells.*
B and C. *Comparison of ROS low (p=0.0488) and ROS high (p=0.0191) populations defined as MFI in LSC populations in Gfi1b-expressing leukemic BM cells (n=6, black bar) and Gfi1b-deficient leukemic BM cells (n=5, red bar).*

3.7 Correlation between *Gfi1b* level and p38 signaling

As shown before, ROS levels were found to be higher in *Gfi1b*-deficient leukemic blasts. One of the pathways induced by ROS is the p38 signaling cascade. In addition, an analysis of gene expression data from human and murine leukemic cells as well as ChipSeq data of murine leukemic cells showed that Gfi1b might regulate the p38/MAPK signal cascade (Sengupta, Upadhyay et al. 2016). Many studies examined the role of p38 in cancer development, which seems be context-dependent. p38-MAPK was characterized as both a tumor suppressor (Xu, Li et al. 2014) and an oncogene (del Barco Barrantes and Nebreda 2012). In HSCs p38-MAPK was shown to limit stemness by promoting apoptosis via oxidative stress response (Ito, Hirao et al. 2006). Therefore, I analyzed the intracellular p38 MAPK-phospho phosphorylation pattern of threonine (T) 180 and tyrosine (Y) 182 in *Gfi1b*$^{wt/wt}$ and *Gfi1b*-deficient leukemic cells. Intracellular staining in *Gfi1b*-deficient *NUP98/HOXD13*^{tg} leukemic cells revealed that the level of p38 phosphorylated leukemic cells was decreased compared to the level of phosphorylated p38 in *Gfi1b*-expressing cells (Figure 44).

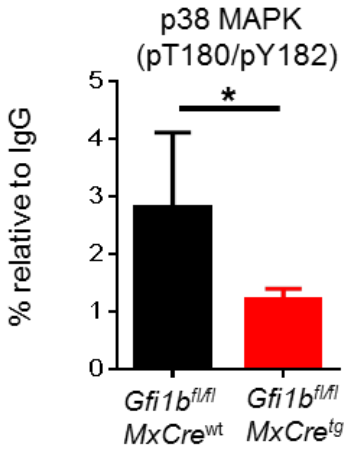

Figure 44: Intracellular staining of p38 MAPK.

Comparison of p38 (T180/Y182) levels between Gfi1b$^{fl/fl}$ MxCre^{wt} NUP98/HOXD13^{tg} (black bar, n=5) and Gfi1b$^{fl/fl}$ MxCre^{tg} NUP98/HOXD13^{tg} (red bar, n=6) in leukemic BM cells.

3.8 Downregulation of Akt signaling in absence of *Gfi1b*

We next analyzed the effect of Akt activation, a downstream target of p38 signaling, in *Gfi1b*-deficient leukemic cells. Akt is activated by phosphorylation at either Thr^{308} or Ser^{473} (Alessi, Deak et al. 1997). AKT phosphorylation at Ser473 was observed in leukemic cells of 50-80% of AML patients (Xu, Simpson et al. 2003). However, ROS also triggers the activation of PI3K/Akt signaling pathway in leukemia (Silva, Girio et al. 2011) and expression of phosphorylated Akt decreased the number of LSC (Sykes, Lane et al. 2011). Cells with loss of *Gfi1b* showed a decreased level of phosphorylated Akt^{Ser473} in LSC (Figure 45), which would correspond with the enhanced number of LSC in *Gfi1b*-deficient leukemia.

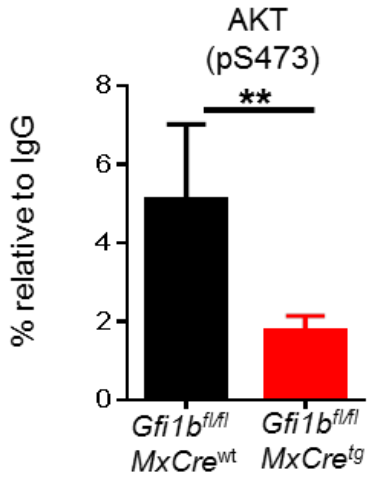

Figure 45: Loss of Gfi1b showed low levels of phosphorylation of Akt^{Ser473}.

Comparison of Akt^{Ser473} levels between $Gfi1b^{fl/fl}$ $MxCre^{wt}$ $NUP98/HOXD13^{tg}$ (black bar, n=5) and $Gfi1b^{fl/fl}$ $MxCre^{tg}$ $NUP98/HOXD13^{tg}$ (red bar, n=6) in leukemic BM cells.

Collectively, I observed that loss of *Gfi1b* was associated with an AML signature, which had previously been found to be associated with poor prognosis and with a role for

signaling pathways of p38/AKT/ROS in maintaining the increased level of LSC in *Gfi1b*-deficient leukemia.

3.9 Target genes of FoXO3 are altered in *Gfi1b*-deficient leukemic cells

As mentioned above, I examined the connection between loss of *Gfi1b* and pAkt^{Ser473} and found that the level of phosphorylated Akt^{Ser473} is reduced in *Gfi1b*-deficient leukemia. Downstream effectors of Akt are different FoXO proteins (Guertin, Stevens et al. 2006). Recently it was shown that FoXO3 expression is activated in 40% of AML patients and acts as an oncogene (Sykes, Lane et al. 2011). Based on the available gene sets from FoXO target genes, GSEA analysis was performed by Dr.Lothar Vassen. FoXO3 binding sites were identified as second most enriched in *Gfi1b* –deficient leukemic cells (Figure 46). To get an idea how FoXO targets behave in the *Gfi1b*-deficient cells compared to normal *Gfi1b* level contexts Dr. Lothar Vassen defined the FoXO 1,3,4 knock -out target genes from (Tothova and Gilliland 2007) as a geneset named “FOXO SPECIFIC GENE SIGNATURE“, combined them with other FoXO target genesets from the GSEA database and ran an GSEA analysis (Figure 47). Indeed, he found that a number of deregulated genes observed in the *Gfi1b*-deficient leukemic cells are influenced by FoXO.

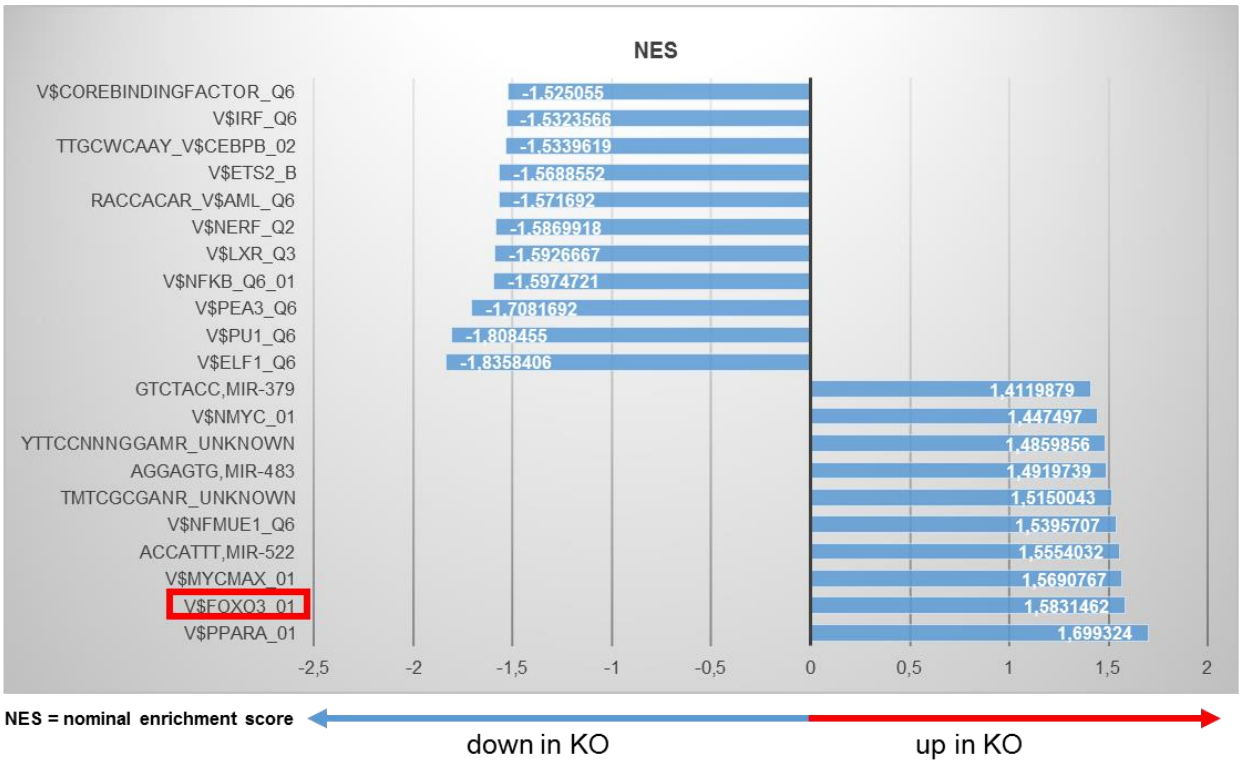

Figure 46: Gfi1b-deficient leukemia showed an enrichment of the FoXO3 binding site.

Leukemic Gfi1b$^{fl/fl}$ MxCre^{tg} NUP98/HOXD13^{tg} mice showed a significant enrichment of binding sites for V$PPARA_01, V$FOXO3_01, V$MYCMAX_01, ACCATTT, MIR-522, V$NFMUE1_Q6, TMTCGCGANR_UNKNOWN; AGGAGTG; and MIR-379 (right). Gfi1b-deficient leukemia mice also have negative nominal enrichment score for several genes such as V$COREBINDINGFACTOR_Q6, V$IRF_Q6,TTGCWCAAY_V$CEPBP_02, V$ETS2_B, RACCACAR_V$AML_Q6; V$NERF_Q2, VLXR_Q3, VNFKB_Q6_01, V$PEA3_Q6, V$PU1_Q6, V$ELF1_Q6.

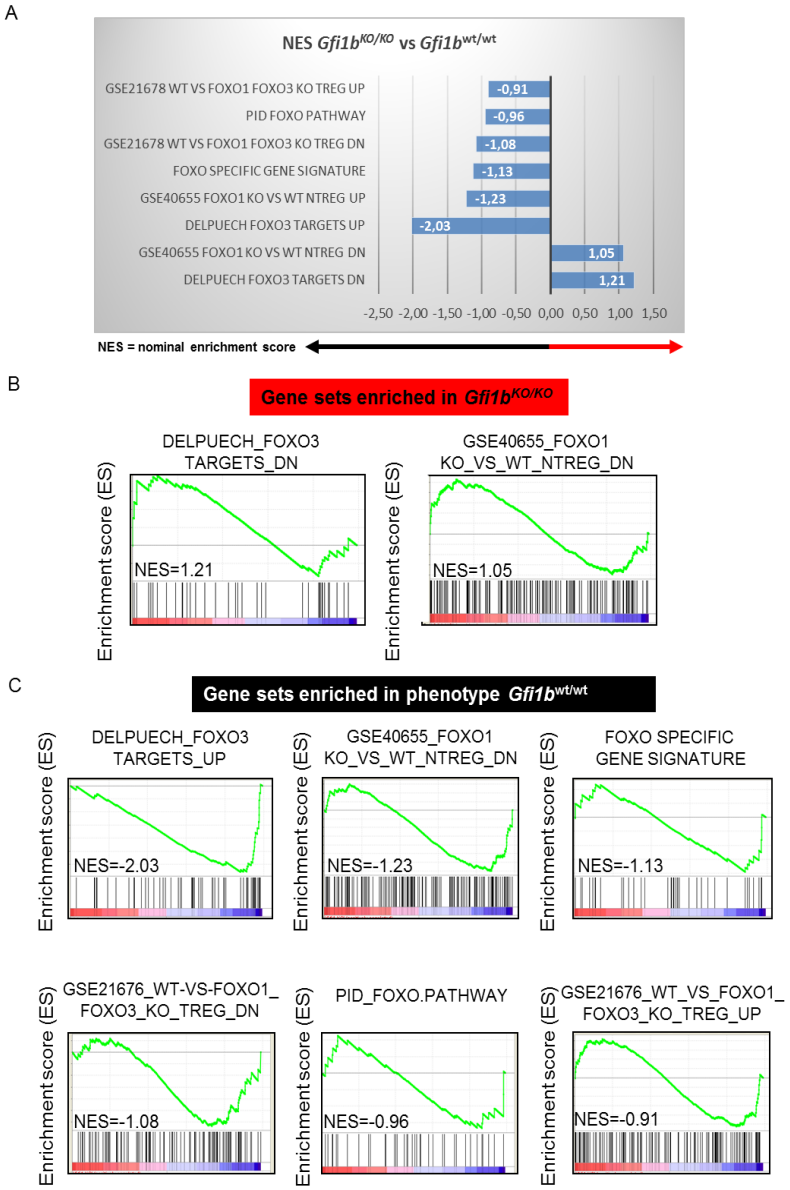

Figure 47: Gfi1b-deficient leukemia showed enrichment score of FoXO related pathway and gene signatures.

A. *GSEA analysis was performed for FoXO family in Gfi1b-deficient leukemic cells (Gfi1bKO/KO) and normal level of Gfi1b (Gfi1bwt/wt).*
B. *Up-regulation of DELPUECH_FOXO3_TARGETS_DN (NES=1.21) and GSE40655_FOXO1_KO_VS_WT_NTREG_DN (NES=1.05) in Gfi1b-deficient leukemia.*
C. *Gene sets are negatively enriched in gene signature sets such Delpuch_FoXO3_Targets_Up (NES=-2.03), GSE40655_FoXO1_KO_V_WT_Ntreg_Dn (NES= -1.08), FoXO specific gene signature (NES=-1.13), GSE1676_WT-VS-*

FoXO1_FoXO3_KO_TREG_DN (NES=1.08), PID_FoXO Pathway (NES=-0.96), Gse21676_Wt-Vs-Foxo1_Foxo3_Ko_Treg_Up (NES=-0.91). Nes= Nominal Enrichment Score.

It has been described that FoXO can deregulate different genes (Sykes, Lane et al. 2011). It has been shown that FoXO3 downregulates *Atm* and upregulates both *Meis1* and *Cdknb1.* As a first approach to confirm the results of the gene expression arrays, I analyzed the expression of the above genes in the Gfi1b-deficient leukemic cells using RT-PCR. While *Atm* in my experiments was downregulated upon loss of *Gfi1b*, *Meis1* expression was highly upregulated and no difference was observed for *Cdknb1* (Figure 48). It could be that the gene regulation of FoXO3 protein is enhanced by Gfi1b or other proteins which in turn leads to increased stemness of LSC.

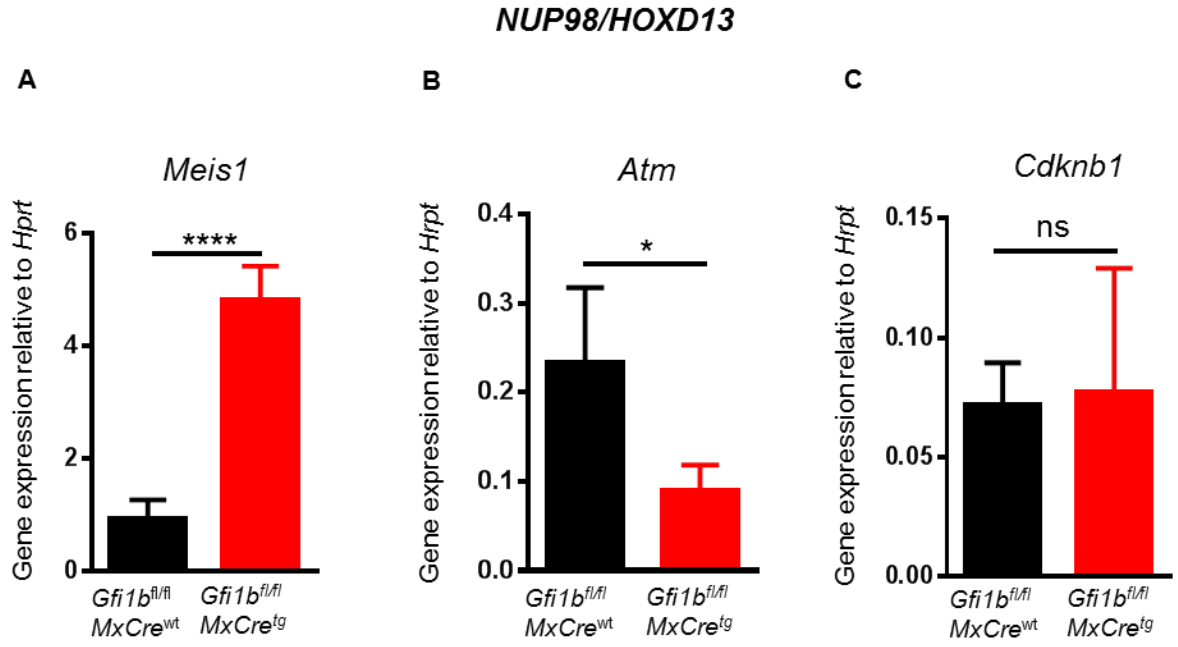

Figure 48: FoxO3 target genes in NUP98/HOXD13^{tg} mice at different Gfi1b expression levels.

A. *Meis1 expression relative to Hrpt in Gfi1b$^{fl/fl}$ MxCre^{wt} NUP98/HOXD13^{tg} (black bar, n=3) and Gfi1b$^{fl/fl}$ MxCre^{tg} NUP98/HOXD13^{tg} (red bar, n=3) BM cells, p=0.0006.*

B. *Atm expression relative to Hrpt in Gfi1b$^{fl/fl}$ MxCre^{wt} NUP98/HOXD13^{tg} (black bar, n=3) and Gfi1b$^{fl/fl}$ MxCre^{tg} NUP98/HOXD13^{tg} (red bar, n=3) BM cells, p=0.0481.*

C. *Cdknb1 expression relative to Hprt in Gfi1b$^{fl/fl}$ Mxcre^{wt} NUP98/HOXD13^{tg} (black bar, n=3) and Gfi1b$^{fl/fl}$ MxCre^{tg} NUP98/HOXD13 ^{tg} (red bar, n=3) BM cells, ns.*

Overall, different level of *Gfi1b* influence the AML development in various AML mouse models, and deregulation of the p38/Akt/ROS/FoXO signaling pathway might be one explanation.

4 Discussion

Lineage-specific transcription factors (TFs) are important for the proper differentiation of HSC. Dysregulation or mutation TFs can contribute to leukemogenesis. Gfi1b is a transcriptional repressor protein which regulates the numbers of HSCs as well as the development of erythrocytes and megakaryocytes. In a previous study, it was shown that the loss of *Gfi1b* leads to the expansion of functional HSCs (Khandanpour, Sharif-Askari et al. 2010). In the present work, I investigated the influence of different levels of *Gfi1b* expression and its molecular signaling in MDS/AML.

4.1 Low *GFI1B* expression levels result in an inferior prognosis of MDS and AML patients

The prognostic influence of different levels of *GFI1B* expression was analyzed in human MDS/AML patients. Based on published human data sets, the *GFI1B* expression level was determined in MDS/AML blast cells compared to *GFI1B* expression in CD34-positive cells from healthy donors. Results showed that the *GFI1B* expression was lower in CD34-positive AML blast cells compared to normal CD34 cells. MDS is a pre-leukemic condition of AML, therefore I analyzed the *GFI1B* expression level in CD34-positive MDS cells compared to CD34-positive AML blast cells. Here again, the *GFI1B* expression level was lower in CD34-positive AML blast cells compared to CD34-positive MDS cells. In addition, I used the available online tool leukemia gene atlas (Hebestreit, Grottrup et al. 2012), which allows studying *GFI1B* expression level across different studies. In this study, I focused on the measure of the expression level of GFI1B in different human progenitor sets such as GMPs, CMP and HSCS and compared it to the expression pattern of isolated leukemic stem cells of different entities such as

AML1/ETO, APL, t(11q23) or *Inv16* associated AML. *GFI1B* expression was lower in human LSCs of different AML subtypes compared to normal HSCs and other primitive cell subtypes. These data indicate that *GFI1B* might be down-regulated in the process of human MDS/AML development. Not only low *GFI1B* was generally lower in AML and MDS blasts compared to normal HSCs, but lower levels of *GFI1B* were indicative of an inferior prognosis. The fact that different level of TFs might be indicative of prognosis has been shown before for the paralogue of GFI1B/Gfi1b called GFI1/Gfi1 (Hones, Botezatu et al. 2016). Here, lower levels of Gfi1 lead to the epigenetic dysregulation of genes involved in leukemogenesis. In addition, a similar role has been described for the transcription factor erythroid Krüppel-like factor (EKLF) (Ayala, Martínez-López et al. 2012). In that case, a high level of *EKLF* was associated with longer overall survival and event-free survival compared to AML patients with low *EKLF* level (Ayala, Martínez-López et al. 2012). Overexpression of *AML1a*, an isoform of the TF AML1/RUNX1, was oncogenic in AML development (Liu, Zhang et al. 2009). Finally, a paper by *(see* Florentien E.M. in 't Hout, 2014, Haematologica) showed that low expression of the transcription factor 4 (TCF4) is indicative of an inferior prognosis *(in 't Hout, van der Reijden et al. 2014)* in AML patients*.* On the other hand, our predictions with regard to prognosis of GFI1B/Gfi1b rely on one AML study and one MDS study. In addition, these studies were all retrospective. To confirm these data, additional studies need to be analyzed retrospectively, and ideally a prospective study would examine the role of lower *GFI1B* expression as a therapeutic indication marker.

For these reasons, it is well conceivable that the different levels of a TF influence prognosis. Therefore, I made use of different mouse models of leukemia and found that low level or absence of *Gfi1b* accelerates AML development and increases the number of functional leukemic stem cells. It remains to be elucidated for Gfi1b which mechanisms are responsible for this.

4.2 Molecular function of Gfi1b in leukemic stem cells

Gfi1b was previously described as restricting histone-modifying enzymes, which in turn induce deacetylation of Lysin 9 of Histon 3 (H3K9acetyl) which is an epigenetic marker for active transcription (Wilson, Foster et al. 2010). Using ChIP-Seq and microarray approaches (in cooperation with Dr.Schütte and Dr.Vassen), I found out that indeed a number of genes were dysregulated on an epigenetic level and that loss of *Gfi1b* led to epigenetic changes (notably, an increased level of H3K9 acetylation of genes, which is involved in stem cell, myeloid, and cell growth regulation). One pathway, the p38/Akt/ROS, came up as a hint both in the ChIP-Seq analysis of the murine leukemic cells and in the gene expression analysis of human and murine leukemia. In one human study, it was shown that the PI3K/AKT and mTOR signaling pathways are highly activated in AML (Park, Chapuis et al. 2010). ROS signaling has already been reported to regulate leukemogenesis (Zhang, Fang et al. 2014). In the context of this thesis, I could identify, using FACS, two distinct ROS populations: ROS low and ROS high. In primitive mouse HSCs, the ROS low population has been defined as quiescent. The ROS high population has been shown to have a higher level of proliferation and differentiation capacity (Jang and Sharkis 2007). Another study examined in primary AML samples the role of ROS in LSC. It showed that LSCs mainly belong to the ROS low expressing cell population; however, some LSCs were also identified to be in the ROS high population (Lagadinou, Sach et al. 2013). In our case, loss of *Gfi1b* led to a higher ROS level in both the Ros low and the ROS high populations. *Gfi1b*-deficient leukemic cells showed an increased population of c-Kit-positive cells, which could mean that the number of LSCs is metabolically more active. Another possibility is that the ROS high population possesses high proliferating precursor cells and thus produces more ROS.

One of the downstream pathways of ROS signaling is p38. It has been shown before that a high level of ROS leads to the activation of stress-response signaling pathways such as the p38 MAPK pathway, which in turn blocks proliferation or promotes apoptosis and thus functions as a tumor suppressor (Dolado, Swat et al. 2007). In HSCs, an elevated level of p38 was found to limit stemness by promoting apoptosis induced by activated ROS signaling (Ito, Hirao et al. 2006). In the present study, p38 signaling was down-regulated in murine *Gfi1b*-deficient leukemic cells. This means that Gfi1b may influence the stress response and tumor suppressor function of p38 in a way, and that an increased level of ROS does not lead to an increase in the level of p38. The reason for this is yet unknown. Konopleva and colleagues showed in primary AML samples and in myeloid leukemia cell lines, treated with C-28 methyl ester of 2-cyano-3,12-dioxoolen-1,9-dien-28-oic acid (CDDO-ME) which induces apoptosis of leukemic cells by activation of p38 phosphorylation (Konopleva, Contractor et al. 2005) which induce apoptosis of AML blast cells.

One possibility might be to treat *GFI1B* low/ and *Gfi1b*-deficient leukemic cells with this therapeutic approach in order to increase the p38 signaling in *Gfi1b*-deficient leukemic cells and to decrease the stemness of LSCs. A recent publication demonstrated that the activation of Toll-like receptor 8 (TLR8) promotes AML differentiation and cell growth inhibition in a TLR8/MyD88/p38-dependent manner by using the TLR7/8 agonist R848 (Ignatz-Hoover, Wang et al. 2015) in AML patients. In addition, all-trans retinoic acid (ATRA) is also an AML differentiation reagent, only it shows a therapeutic effect for acute promyelocytic leukemia (APL) patients (Tallmann 2004). TLR signaling is a well-characterized pathway for the differentiation of hematopoietic cells and undergoes myeloid differentiation in a MyD88-dependent manner (Nagai, Garrett et al. 2006). Interestingly, a previous study suggests that TLR ligands stimulate the activation of the MAPK (Akira and Takeda 2004). Additional studies show that the activation of p38 promotes differentiation in other tumors (Puri, Wu et al. 2000; Sato, Okada et al. 2014). As a next step, it would be interesting to analyze the expression of TLR8 and MyD88 in

Gfi1b-deficient leukemic cells and to treat with the R484 agonist in order to rescue the activation of p38 in a TLR8/MyD88-dependent manner and to promote the differentiation of leukemic blast cells.

Given that p38 activates pAkt signaling, I studied the phosphorylated pAkt^{Ser473} in *Gfi1b*-deficient leukemic cells. The result revealed a significant down-regulation of activated Akt, as previously seen for p38. Recent studies revealed an association between high ROS levels and the subsequent activation of the AKT/ASK1/p38 pathway that leads to apoptosis in human bronchial epithelial cells (BEAS-2B) (Pan, Chang et al. 2010; Ahn, Won et al. 2013). This finding not only connects the Akt signaling pathway to elevated ROS levels, but also links AKT (see above) to p38 signaling. Furthermore, AKT signaling was found to be upregulated in many cases of AML (Park, Chapuis et al. 2010). However, other studies revealed that the downregulation of *AKT* expression is involved in the maintenance of an immature state of LSCs and thus in enhanced stemness (Sykes, Lane et al. 2011). Hence, it remains to be elucidated in additional studies whether and how alteration of the AKT pathway alters the leukemic stem cell properties of AML cells.

Interestingly, the higher ROS levels in *Gfi1b*-deficient cells did not seem to activate Akt or the signaling cascade involving p38, as mentioned above, but rather to reduce its activation. This would be in congruency with the mentioned connection between a diminished activity of Akt and an enhanced stemness, where not only Akt seems to be involved but also the direct downstream target FoxO3 (Sykes, Lane et al. 2011).

FoXO3 belongs to the forkhead family of proteins and acts as a transcriptional regulator (Kaestner, Knochel et al. 2000). Initial studies showed that FoXO3 is a direct target of Akt signaling. Phosphorylation of FoXO3 leads to change of its nuclear localization to ctyoplasmatic localization and is located in the cytoplasma (Datta, Dudek et al. 1997). The *FoXO3* gene was detected in an AML patient as affected by the translocation

t(6;11)(q21;q23) (Barr 2001). The protein possesses a dual function in AML; first of all, it has been described as a tumor suppressor (Downing 2011), but a recent study showed that it functions as a tumor oncogene (Sykes, Lane et al. 2011). Published Gfi1b ChIP-Seq data in different cell lines J2E (Smith, Calero-Nieto et al. 2012), HPC7 (Wilson, Foster et al. 2010) and 416B (Schutte, Wang et al. 2016) revealed by using UCSC Genome Browser an enhanced binding site at the promoter for the *FoXO3* gene. Hence, it would be conceivable that Gfi1b binds to the *FoXO3* promoter and represses its expression. A similar role has already been described with regard to a different member of the FoXO family: Schulz and colleagues reported a binding of Gfi1b to the *FoXO1* promoter and its role in B-cell maturation (Schulz, Vassen et al. 2012). Furthermore, FoXO3 is involved in erythropoiesis (Bakker, van Dijk et al. 2007) and, like Gfi1b, is also important for megakaryopoesis and erythropoiesis (Vassen, Beauchemin et al. 2014). Based on the GSEA results performed by Dr. Lothar Vassen, loss of *Gfi1b* was associated with an enrichment of genes regulated by FoXO3. To study the role of FoXO3 in leukemic stem cells, three target genes were chosen for further analysis. *Meis1, Atm (ataxia-telangiectasia mutated) and Cdknb1* are FoXO3 target genes (Sykes, Lane et al. 2011) that play an important role in normal hematopoiesis (Unnisa, Clark et al. 2012), DNA damage response (Kitagawa and Kastan 2005) and cell cycle control (Moller 2000).

Meis1 plays an important role in erythropoesis, megakaryopoesis, and hematopetic stem cell expansion, and evidence has shown that Meis1 is involved in ROS signaling (Miller, Rosten et al. 2016), MAP Kinase signaling, and PI3K/Akt signaling (Gibbs, Jager et al. 2012). Meis1 plays a role in adult mouse HSCs by regulating ROS levels and maintaining the quiescent state (Kocabas, Zheng et al. 2012). It was also shown that Meis1 interacts with the NUP98/HOXD13 oncofusion protein and HOX proteins and thus accelerates the development of leukemia ((Thorsteinsdottir, Kroon et al. 2001). Recently, it was shown that *Meis1* is activated by FoXO3 (Sykes, Lane et al. 2011). Loss of *Gfi1b* showed a significant increased expression of *Meis1* in LSC. This result

validates one study in which Meis1 directly regulated *Gfi1b* repression (Chowdhury, Ramroop et al. 2013). Interestingly, since Meis1 seems to be involved in inducing AML by collaborating with NUP98/HOXD13 oncofusion proteins, the increased expression of *Meis1* due to a loss of *Gfi1b* could be one reason for an even more accelerated onset of AML or the progression from MDS to AML in *NUP98/HOXD13* tg mice. Collectively, Meis1 plays a major role in AML development, independent of both the activity of FoXO3 and the absence of *Gfi1b* and interaction with other oncofusion proteins.

Atm is involved in the DNA damage response and is primarily activated by double-strand DNA breaks (DSBs) (Maréchal and Zou 2013). Furthermore, it enhances the stemness of HSCs by regulating oxidative stress and thus ROS levels (Ito, Hirao et al. 2004). Ito and colleagues showed that an increased ROS level and absence of *Atm* lead to an activation of the p38 MAPK, thus triggering apoptosis in HSCs (Ito, Hirao et al. 2006) however, a lower *Atm* level of would possibly pave the way for increased rate of mutations and hence malignant development. Loss of *Gfi1b* showed a decreased expression of the *Atm* gene at the mRNA Sykes and colleagues showed that FoXO3 represses the expression of *Atm* (Sykes, Lane et al. 2011). Therefore, FoxO3 and Atm are involved in the DNA damage response (Tsai, Chung et al. 2008). This seems to indicate that the loss of *Gfi1b* could activate other proteins that repress *Atm* expression and thus counteract FoXO3. Additionally, the obtained results reveal an important relationship between ROS, Atm, and p38. Stem cells have multiple mechanisms to deal with elevated ROS levels, two of which are the activation of Atm or p38. If the cell cycle arrest initiated by Atm cannot be induced and other mechanisms to rescue the quiescent state are failing, p38 induces apoptosis. In *Gfi1b*- deficient leukemic cells, both of these mechanisms are down-regulated, which explains the measured elevation of ROS levels.

CDKN1B (p27) is a G1-checkpoint CDK inhibitor, regulates the cell cycle progression (Abukhdeir and Park 2008), and is involved in maintaining the quiescence of HSCs (Zou, Yoshihara et al. 2011). FoXO3 regulates the maintenance of the HSC pool

(Miyamoto, Araki et al. 2007), and since FoXO3 repressed the activation of p27 (Sykes, Lane et al. 2011), loss of *Gfi1b* could enhance the expression of p27 in LSC and thus maintain the quiescence of LSC populations. In the present study, no significant differences were observed in *Gfi1b* wt and *Gfi1b*-deficient leukemic cells according to *p27* gene expression.

The summarized evidence presented in this study shows that loss of *Gfi1b* increased the number of functional LSC by deregulating the ROS/p38/Akt/FoXO signaling pathway (Figure 49).

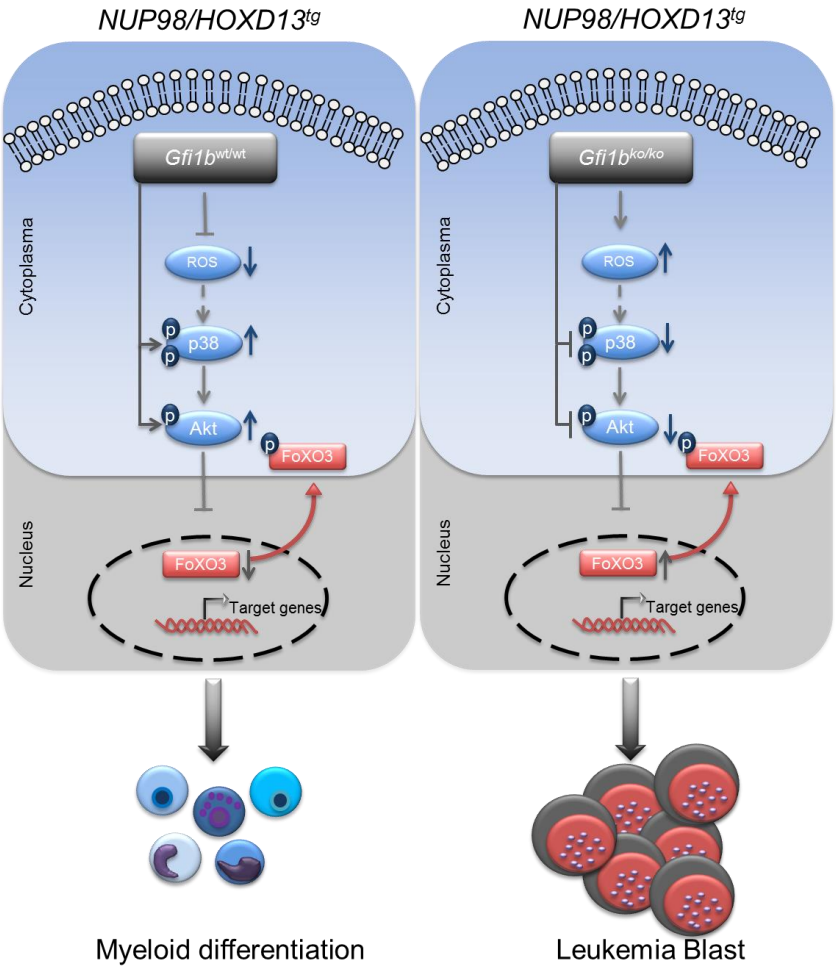

Figure 49: Overview of my doctoral thesis.

Loss of Gfi1b leads to a deregulation of key AML-signaling pathways. Gfi1b-deficient leukemic cells showed elevated ROS levels and high expression of FoXO3 oncogene. In addition to the p38-signaling and Akt-signaling are downregulated. The increased epxression of FoXO3 and ROS as well as reduced level of activated p38 and Akt drive the expansion of leukemia blast.

5 Outlook

In this doctoral thesis, I studied how different expression levels of *GFI1B/Gfi1b* influence the prognosis of MDS/AML patients, how different Gfi1b level affect the initiation and progression of leukemia in murine models of leukemia, and which molecular pathways could explain our observation. With regard to the human data, it is important to note that the current study presents only the human data sets from the full length of GFI1B. Recent studies have highlighted the role of different GFI1B isoforms in human hematopoiesis (Polfus, Khajuria et al. 2016; Schulze, Schlagenhauf et al. 2017). Therefore, it would be interesting to study the role of different isoforms of GFI1B and their functional role in AML development. I studied the role of low level of *Gfi1b* in AML development. Therefore, it would also be interesting to study the functional role of a higher level of *GFI1B/Gfi1b* in the prognosis of AML and the pathogenesis of MDS/AML, since it has been shown that different levels of *Gfi1* have a different impact on AML pathogenesis (Hönes 2016, Hönes 2017); the same could also apply for *Gfi1b*.

On a molecular level, loss of *Gfi1b* increased the number of functional LSCs by deregulating the ROS/p38/Akt/FoXO signaling pathways. In future studies, it would be interesting to examine how this could be exploited for leukemia therapy; for example, one approach would be reducing ROS by using N-Acetyl L-Cystein (NAC) (Halasi, Wang et al. 2013), since ROS levels were elevated in *Gfi1b*-deficient LSCs and proteins such as p38, AKT, and ATM, which regulate ROS-mediated cell cycle arrest or apoptosis, were down-regulated. This approach would be a novel treatment strategy for AML patients.

6 Summary

Myelodysplastic syndrome (MDS) is a clonal hematopoietic blood disorder and is a preleukemic state of leukemia. In some cases, MDS can transform into acute myeloid leukemia (AML). Both diseases affect the myeloid lineage of hematopoiesis and are characterized by an accumulation of blast cells. Lineage-specific transcription factors (TFs) are required for a proper differentiation of mature cells. Dysfunctions of these TFs cause diseases such as MDS/AML. Gfi1b plays an important role in the hematopoiesis; it is important for the maintenance of HSC and for erythropoiesis and megakrayopoiesis. The aim of my thesis is to characterize the functional role of GFI1B/Gfi1b in the context of AML development. I show that a low *GFI1B* expression level in human blast cells is associated with an inferior outcome with regard to overall survival and event-free survival. Using three different AML mouse models (*NUP98/HOXD13, Kras and MLL-AF9*), I showed that loss of *Gfi1b* accelerated AML. In addition, loss of *Gfi1b* showed an enhanced frequency of functional leukemic stem cells (LSCs) in the BM of *Gfi1b*-deficient leukemic mice compared to mice with normal Gfi1b levels. Previous studies have shown that loss of *Gfi1b* in mice leads to an expansion of HSCs accompanied with elevated levels of reactive oxygen species (ROS). Different groups have shown that ROS can promote AML development. Yet,increased level of ROS lead in normal cells to elevated level of activated p38 and Akt, which in turn limit oncogenic potential of cells, However in case of loss of *Gfi1b*, despite increased level of ROS, level of activated p38 and Akt are downregulated. In addition, FoXO3, a known oncogenic element in AML, was upregulated in *Gfi1b*-deficient LSCs, which in turn led to a repression of *Atm* gene expression and an activation of *Meis1*. Collectively, these data represent, that loss of *GFI1B/Gfi1b* plays a key role in generating AML and this could open new therapeutic possibilities in the future.

6.1 Summary in german

Die akute myeloische Leukämie (AML) ist eine maligne Erkrankung des blutbildenden Systems, die durch eine Ansammlung unreifer, in der Entwicklung arretierter myeloischer Blasten gekennzeichnet ist. Myelodysplastisches Syndrom (MDS) und AML beeinflussen die myeloische Linie der Hämatopoese und sind durch eine Anreicherung von Blasten im Knochenmark gekennzeichnet. Transkriptionsfaktoren (TF) spielen eine fundamentale Rolle in der Hämatopoese. Eine Funktionsstörung dieser Faktoren kann zur Entstehung einer AML führen und eine Bedeutung für die Prognose darstellen. Gfi1b ist ein TF, der eine tragende Rolle in der Regulation der Hämatopoese für die Differenzierung der verschiedenen hämatopoetischen Linien spielt. In der vorliegenden Arbeit konnte gezeigt werden, dass GFI1B in CD34-positiven AML-Blastzellen von Patienten im Vergleich zu gesunden Probanden niedriger exprimiert wird. Ebenso konnte in drei verschiedenen AML-Mausmodellen gezeigt werden, dass der Verlust von *Gfi1b* die AML-Entwicklung im Vergleich mit Tieren mit normalen *Gfi1b*-Expressionslevel beschleunigte. Ein niedriger Expressionslevel des *Gfi1b*-Gens erhöhte die Anzahl der funktionellen leukämischen Stammzellen im Knochenmark. In früheren Publikationen konnte gezeigt werden, dass der Verlust von *Gfi1b* bei Mäusen zu einer Expansion von hämatopoetischen Stammzellen führte und von erhöhten Mengen an reaktiven Sauerstoffspezies (ROS) begleitet wurde. Es wurde von verschiedenen Arbeitsgruppen beschrieben, dass ROS zur Entstehung und Progression der AML beitragen. Jedoch führen erhöhte ROS Level auch zu erhöhten Mengen an aktivierten p38 and Akt, was wiederum, die onkogene Potenzial der Zellen beschränkt. Im Falle von *Gfi1b*-defizienten leukämischen Zellen sind p38 and Akt Level reduziert. FoXO3 fungiert als ein onkogenes Element in AML Zellen und ich konnte zeigen, dass die Aktivität von FoXO3 in *Gfi1b*-defizienten leukämischen Stammzellen hochreguliert ist, was zu einer Repression von Atm und einer Aktivierung von Meis1 führte. Zusammenfassend lässt sich erschließen, dass der TF GFI1B/Gfi1b eine dosisabhängige Rolle in der

Progression der AML spielt. Er kann daher als ein tendenzieller Marker für die AML-Heilung angewendet werde.

7 References

Abukhdeir, A. M. and B. H. Park (2008). "p21 and p27: roles in carcinogenesis and drug resistance."

*Ahn, J., M. Won, et al. (2013). "Reactive oxygen species-mediated activation of the Akt/ASK1/p38 signaling cascade and p21(Cip1) downregulation are required for shikonin-induced apoptosis." Apoptosis **18**(7): 870-881.*

*Akira, S. and K. Takeda (2004). "Toll-like receptor signalling." Nat Rev Immunol **4**(7): 499-511.*

*Alessi, D. R., M. Deak, et al. (1997). "3-Phosphoinositide-dependent protein kinase-1 (PDK1): structural and functional homology with the Drosophila DSTPK61 kinase." Curr Biol **7**(10): 776-789.*

*Anguita, E., F. J. Candel, et al. (2017). "Transcription Factor GFI1B in Health and Disease." Front Oncol **7**: 54.*

*Anguita, E., A. Villegas, et al. (2010). "GFI1B controls its own expression binding to multiple sites." Haematologica **95**(1): 36-46.*

*Ayala, R., J. Martínez-López, et al. (2012). "Acute myeloid leukemia and transcription factors: role of erythroid Krüppel-like factor (EKLF)." Cancer Cell Int **12**: 25.*

*Bakker, W. J., T. B. van Dijk, et al. (2007). "Differential regulation of Foxo3a target genes in erythropoiesis." Mol Cell Biol **27**(10): 3839-3854.*

*Barr, F. G. (2001). "Gene fusions involving PAX and FOX family members in alveolar rhabdomyosarcoma." Oncogene **20**(40): 5736-5746.*

*Barzi, A. and M. A. Sekeres (2010). "Myelodysplastic syndromes: a practical approach to diagnosis and treatment." Cleve Clin J Med **77**(1): 37-44.*

*Bayliss, R., T. Littlewood, et al. (2002). "GLFG and FxFG nucleoporins bind to overlapping sites on importin-beta." J Biol Chem **277**(52): 50597-50606.*

*Belov, L., O. de la Vega, et al. (2001). "Immunophenotyping of leukemias using a cluster of differentiation antibody microarray." Cancer Res **61**(11): 4483-4489.*

*Bennett, J. M., D. Catovsky, et al. (1976). "Proposals for the classification of the acute leukaemias. French-American-British (FAB) co-operative group." Br J Haematol **33**(4): 451-458.*

*Bleesing, J. J. and T. A. Fleisher (2003). "Human B cells express a CD45 isoform that is similar to murine B220 and is downregulated with acquisition of the memory B-cell marker CD27." Cytometry B Clin Cytom **51**(1): 1-8.*

*Bonnet, D. and J. E. Dick (1997). "Human acute myeloid leukemia is organized as a hierarchy that originates from a primitive hematopoietic cell." Nat Med **3**(7): 730-737.*

*Botezatu, L., L. C. Michel, et al. (2016). "Epigenetic therapy as a novel approach for GFI136N-associated murine/human AML." Exp Hematol **44**(8): 713-726 e714.*

*Botezatu, L., L. C. Michel, et al. (2016). "GFI1(36N) as a therapeutic and prognostic marker for myelodysplastic syndrome." Exp Hematol **44**(7): 590-595.e591.*

*Brewster, J. L., T. de Valoir, et al. (1993). "An osmosensing signal transduction pathway in yeast." Science **259**(5102): 1760-1763.*

*Cano, E. and L. C. Mahadevan (1995). "Parallel signal processing among mammalian MAPKs." Trends Biochem Sci **20**(3): 117-122.*

*Chowdhury, A. H., J. R. Ramroop, et al. (2013). "Differential transcriptional regulation of meis1 by Gfi1b and its co-factors LSD1 and CoREST." PLoS One **8**(1): e53666.*

Cook, G. J. and T. S. Pardee (2013). Animal Models of Leukemia: Any closer to the real thing?, Cancer Metastasis Rev. 2013 Jun;32(0):63-76. doi:10.1007/s10555-012-9405-5.

Cox, A. D. and C. J. Der (2010). "Ras history: The saga continues."

*Cross, C. E., B. Halliwell, et al. (1987). "Oxygen radicals and human disease." Ann Intern Med **107**(4): 526-545.*

*Cuenda, A. and S. Rousseau (2007). "p38 MAP-kinases pathway regulation, function and role in human diseases." Biochim Biophys Acta **8**(75): 24.*

Damnernsawad, A., G. Kong, et al. (2016). Kras is required for adult hematopoiesis, Stem Cells. 2016 Jul;34(7):1859-71. Epub 2016 Mar 28 doi:10.1002/stem.2355.

*Datta, S. R., H. Dudek, et al. (1997). "Akt phosphorylation of BAD couples survival signals to the cell-intrinsic death machinery." Cell **91**(2): 231-241.*

*de Figueiredo-Pontes, L. L., M. C. Pintao, et al. (2008). "Determination of P-glycoprotein, MDR-related protein 1, breast cancer resistance protein, and lung-resistance protein expression in leukemic stem cells of acute myeloid leukemia." Cytometry B Clin Cytom **74**(3): 163-168.*

*del Barco Barrantes, I. and A. R. Nebreda (2012). "Roles of p38 MAPKs in invasion and metastasis." Biochem Soc Trans **40**(1): 79-84.*

*Dohner, H., E. Estey, et al. (2017). "Diagnosis and management of AML in adults: 2017 ELN recommendations from an international expert panel." Blood **129**(4): 424-447.*

*Dolado, I., A. Swat, et al. (2007). "p38alpha MAP kinase as a sensor of reactive oxygen species in tumorigenesis." Cancer Cell **11**(2): 191-205.*

*Downing, J. R. (2011). "A new FOXO pathway required for leukemogenesis." Cell **146**(5): 669-670.*

*Duran-Struuck, R. and R. C. Dysko (2009). "Principles of Bone Marrow Transplantation (BMT): Providing Optimal Veterinary and Husbandry Care to Irradiated Mice in BMT Studies." J Am Assoc Lab Anim Sci **48**(1): 11-22.*

*Fenaux, P. and L. Ades (2013). "How we treat lower-risk myelodysplastic syndromes." Blood **121**(21): 4280-4286.*

*Finkel, T. (2003). "Oxidant signals and oxidative stress." Curr Opin Cell Biol **15**(2): 247-254.*

*Finkel, T. (2011). "Signal transduction by reactive oxygen species." J Cell Biol **194**(1): 7-15.*

*Freshney, N. W., L. Rawlinson, et al. (1994). "Interleukin-1 activates a novel protein kinase cascade that results in the phosphorylation of Hsp27." Cell **78**(6): 1039-1049.*

*Gibbs, K. D., Jr., A. Jager, et al. (2012). "Decoupling of tumor-initiating activity from stable immunophenotype in HoxA9-Meis1-driven AML." Cell Stem Cell **10**(2): 210-217.*

Görgens, A., A. K. Ludwig, et al. (2014). "Multipotent Hematopoietic Progenitors Divide Asymmetrically to Create Progenitors of the Lymphomyeloid and Erythromyeloid Lineages."

*Gorrini, C., I. S. Harris, et al. (2013). "Modulation of oxidative stress as an anticancer strategy." Nat Rev Drug Discov **12**(12): 931-947.*

*Grimes, H. L., T. O. Chan, et al. (1996). "The Gfi-1 proto-oncoprotein contains a novel transcriptional repressor domain, SNAG, and inhibits G1 arrest induced by interleukin-2 withdrawal." Mol Cell Biol **16**(11): 6263-6272.*

*Guertin, D. A., D. M. Stevens, et al. (2006). "Ablation in mice of the mTORC components raptor, rictor, or mLST8 reveals that mTORC2 is required for signaling to Akt-FOXO and PKCalpha, but not S6K1." Dev Cell **11**(6): 859-871.*

*Halasi, M., M. Wang, et al. (2013). "ROS inhibitor N-acetyl-L-cysteine antagonizes the activity of proteasome inhibitors." Biochem J **454**(2): 201-208.*

*Hamblin, T. (1992). "Clinical features of MDS." Leuk Res **16**(1): 89-93.*

*Han, J., J. D. Lee, et al. (1994). "A MAP kinase targeted by endotoxin and hyperosmolarity in mammalian cells." Science **265**(5173): 808-811.*

Han, L., Y. M. Shang, et al. Biological Character of RetroNectin Activated Cytokine-Induced Killer Cells, J Immunol Res. 2016;2016:5706814. Epub 2016 Jun 28 doi:10.1155/2016/5706814.

*Hebestreit, K., S. Grottrup, et al. (2012). "Leukemia gene atlas--a public platform for integrative exploration of genome-wide molecular data." PLoS One **7**(6): e39148.*

*Hemavathy, K., S. C. Guru, et al. (2000). "Human Slug is a repressor that localizes to sites of active transcription." Mol Cell Biol **20**(14): 5087-5095.*

*Hole, P. S., L. Pearn, et al. (2010). "Ras-induced reactive oxygen species promote growth factor-independent proliferation in human CD34+ hematopoietic progenitor cells." Blood **115**(6): 1238-1246.*

*Hole, P. S., J. Zabkiewicz, et al. (2013). "Overproduction of NOX-derived ROS in AML promotes proliferation and is associated with defective oxidative stress signaling." Blood **122**(19): 3322-3330.*

*Hones, J. M., L. Botezatu, et al. (2016). "GFI1 as a novel prognostic and therapeutic factor for AML/MDS." Leukemia **30**(6): 1237-1245.*

Hones, J. M., L. Botezatu, et al. (2016). "GFI1 as a novel prognostic and therapeutic factor for AML/MDS." Leukemia.

*Huang, D. Y., Y. Y. Kuo, et al. (2005). "GATA-1 mediates auto-regulation of Gfi-1B transcription in K562 cells." Nucleic Acids Res **33**(16): 5331-5342.*

*Huggett, J., K. Dheda, et al. (2005). "Real-time RT-PCR normalisation; strategies and considerations." Genes Immun **6**(4): 279-284.*

*Ignatz-Hoover, J. J., H. Wang, et al. (2015). "The role of TLR8 signaling in Acute Myeloid Leukemia Differentiation." Leukemia **29**(4): 918-926.*

in 't Hout, F. E. M., B. A. van der Reijden, et al. (2014). "High expression of transcription factor 4 (TCF4) is an independent adverse prognostic factor in acute myeloid leukemia that could guide treatment decisions."

*Insinga, A., A. Cicalese, et al. (2014). "DNA damage response in adult stem cells." Blood Cells Mol Dis **52**(4): 147-151.*

*Irwin, M. E., N. Rivera-Del Valle, et al. (2013). "Redox Control of Leukemia: From Molecular Mechanisms to Therapeutic Opportunities." Antioxidants & Redox Signaling **18**(11): 1349-1383.*

*Ito, K., A. Hirao, et al. (2004). "Regulation of oxidative stress by ATM is required for self-renewal of haematopoietic stem cells." Nature **431**(7011): 997-1002.*

*Ito, K., A. Hirao, et al. (2006). "Reactive oxygen species act through p38 MAPK to limit the lifespan of hematopoietic stem cells." Nat Med **12**(4): 446-451.*

*Jang, Y. Y. and S. J. Sharkis (2007). "A low level of reactive oxygen species selects for primitive hematopoietic stem cells that may reside in the low-oxygenic niche." Blood **110**(8): 3056-3063.*

*Janssen, J. W., A. C. Steenvoorden, et al. (1987). "RAS gene mutations in acute and chronic myelocytic leukemias, chronic myeloproliferative disorders, and myelodysplastic syndromes." Proc Natl Acad Sci U S A **84**(24): 9228-9232.*

*Jude, C. D., L. Climer, et al. (2007). "Unique and independent roles for MLL in adult hematopoietic stem cells and progenitors." Cell Stem Cell **1**(3): 324-337.*

*Kaestner, K. H., W. Knochel, et al. (2000). "Unified nomenclature for the winged helix/forkhead transcription factors." Genes Dev **14**(2): 142-146.*

*Karihtala, P. and Y. Soini (2007). "Reactive oxygen species and antioxidant mechanisms in human tissues and their relation to malignancies." Apmis **115**(2): 81-103.*

*Khandanpour, C., E. Sharif-Askari, et al. (2010). "Evidence that growth factor independence 1b regulates dormancy and peripheral blood mobilization of hematopoietic stem cells." Blood **116**(24): 5149-5161.*

*Kharas, M. G., R. Okabe, et al. (2010). "Constitutively active AKT depletes hematopoietic stem cells and induces leukemia in mice." Blood **115**(7): 1406-1415.*

*Kina, T., K. Ikuta, et al. (2000). "The monoclonal antibody TER-119 recognizes a molecule associated with glycophorin A and specifically marks the late stages of murine erythroid lineage." Br J Haematol **109**(2): 280-287.*

*Kitagawa, R. and M. B. Kastan (2005). "The ATM-dependent DNA damage signaling pathway." Cold Spring Harb Symp Quant Biol **70**: 99-109.*

*Kluger, Y., D. P. Tuck, et al. (2004). "Lineage specificity of gene expression patterns." Proc Natl Acad Sci U S A **101**(17): 6508-6513.*

Kocabas, F., J. Zheng, et al. (2012). "Meis1 regulates the metabolic phenotype and oxidant defense of hematopoietic stem cells."

*Konopleva, M., R. Contractor, et al. (2005). "The novel triterpenoid CDDO-Me suppresses MAPK pathways and promotes p38 activation in acute myeloid leukemia cells." Leukemia **19**(8): 1350-1354.*

*Krivtsov, A. V. and S. A. Armstrong (2007). "MLL translocations, histone modifications and leukaemia stem-cell development." Nat Rev Cancer **7**(11): 823-833.*

*Krivtsov, A. V., Z. Feng, et al. (2008). "H3K79 methylation profiles define murine and human MLL-AF4 leukemias." Cancer Cell **14**(5): 355-368.*

*Kuhn, R., F. Schwenk, et al. (1995). "Inducible gene targeting in mice." Science **269**(5229): 1427-1429.*

*Lagadinou, E. D., A. Sach, et al. (2013). "BCL-2 inhibition targets oxidative phosphorylation and selectively eradicates quiescent human leukemia stem cells." Cell Stem Cell **12**(3): 329-341.*

*Laity, J. H., B. M. Lee, et al. (2001). "Zinc finger proteins: new insights into structural and functional diversity." Curr Opin Struct Biol **11**(1): 39-46.*

*Lee, H. J., Y. S. Lee, et al. (2009). "Retronectin enhances lentivirus-mediated gene delivery into hematopoietic progenitor cells." Biologicals **37**(4): 203-209.*

Lelli, K. M., M. Slattery, et al. (2012). "Disentangling the Many Layers of Eukaryotic Transcriptional Regulation."

*Liberzon, A., C. Birger, et al. (2015). "The Molecular Signatures Database (MSigDB) hallmark gene set collection." Cell Syst **1**(6): 417-425.*

Lin, Y. W., C. Slape, et al. (2005). "NUP98-HOXD13 transgenic mice develop a highly penetrant, severe myelodysplastic syndrome that progresses to acute leukemia."

*Liu, E. T., S. Pott, et al. (2010). "Q&A: ChIP-seq technologies and the study of gene regulation." BMC Biol **8**(56): 1741-7007.*

*Liu, X., Q. Zhang, et al. (2009). "Overexpression of an isoform of AML1 in acute leukemia and its potential role in leukemogenesis." Leukemia **23**(4): 739-745.*

Ludin, A., S. Gur-Cohen, et al. (2014). "Reactive Oxygen Species Regulate Hematopoietic Stem Cell Self-Renewal, Migration and Development, As Well As Their Bone Marrow Microenvironment."

Maréchal, A. and L. Zou (2013). "DNA Damage Sensing by the ATM and ATR Kinases."

*Matharu, N. K., T. Hussain, et al. (2010). "Vertebrate homologue of Drosophila GAGA factor." J Mol Biol **400**(3): 434-447.*

Miller, M. E., P. Rosten, et al. (2016). "Meis1 Is Required for Adult Mouse Erythropoiesis, Megakaryopoiesis and Hematopoietic Stem Cell Expansion."

*Miyamoto, K., K. Y. Araki, et al. (2007). "Foxo3a is essential for maintenance of the hematopoietic stem cell pool." Cell Stem Cell **1**(1): 101-112.*

*Moller, M. B. (2000). "P27 in cell cycle control and cancer." Leuk Lymphoma **39**(1-2): 19-27.*

*Mootha, V. K., C. M. Lindgren, et al. (2003). "PGC-1alpha-responsive genes involved in oxidative phosphorylation are coordinately downregulated in human diabetes." Nat Genet **34**(3): 267-273.*

*Moroy, T., L. Vassen, et al. (2015). "From cytopenia to leukemia: the role of Gfi1 and Gfi1b in blood formation." Blood **126**(24): 2561-2569.*

*Nagai, Y., K. P. Garrett, et al. (2006). "Toll-like receptors on hematopoietic progenitor cells stimulate innate immune system replenishment." Immunity **24**(6): 801-812.*

*Nakamura, T., T. Mori, et al. (2002). "ALL-1 is a histone methyltransferase that assembles a supercomplex of proteins involved in transcriptional regulation." Mol Cell **10**(5): 1119-1128.*

Neubauer, A., K. Maharry, et al. (2008). Patients With Acute Myeloid Leukemia and RAS Mutations Benefit Most From Postremission High-Dose Cytarabine: A Cancer and Leukemia Group B Study, J Clin Oncol. 2008 Oct 1;26(28):4603-9. Epub 2008 Jun 16 doi:10.1200/JCO.2007.14.0418.

*Nicholson, K. M. and N. G. Anderson (2002). "The protein kinase B/Akt signalling pathway in human malignancy." Cell Signal **14**(5): 381-395.*

*Pan, J., Q. Chang, et al. (2010). "Reactive oxygen species-activated Akt/ASK1/p38 signaling pathway in nickel compound-induced apoptosis in BEAS 2B cells." Chem Res Toxicol **23**(3): 568-577.*

Papaemmanuil, E., M. Gerstung, et al. (2013). Clinical and biological implications of driver mutations in myelodysplastic syndromes, Blood. 2013 Nov 21;122(22):3616-27. doi:10.1182/blood-2013-08-518886.

*Park, S., N. Chapuis, et al. (2010). "Role of the PI3K/AKT and mTOR signaling pathways in acute myeloid leukemia." Haematologica **95**(5): 819-828.*

*Polfus, L. M., R. K. Khajuria, et al. (2016). "Whole-Exome Sequencing Identifies Loci Associated with Blood Cell Traits and Reveals a Role for Alternative GFI1B Splice Variants in Human Hematopoiesis." Am J Hum Genet **99**(2): 481-488.*

*Puri, P. L., Z. Wu, et al. (2000). "Induction of terminal differentiation by constitutive activation of p38 MAP kinase in human rhabdomyosarcoma cells." Genes Dev **14**(5): 574-584.*

*Quentmeier, H., J. Reinhardt, et al. (2003). "MLL partial tandem duplications in acute leukemia cell lines." Leukemia **17**(5): 980-981.*

*Ramalho-Santos, M., S. Yoon, et al. (2002). ""Stemness": transcriptional profiling of embryonic and adult stem cells." Science **298**(5593): 597-600.*

Rao, X., X. Huang, et al. (2013). "An improvement of the 2ˆ(–delta delta CT) method for quantitative real-time polymerase chain reaction data analysis."

*Rapin, N., F. O. Bagger, et al. (2014). "Comparing cancer vs normal gene expression profiles identifies new disease entities and common transcriptional programs in AML patients." Blood **123**(6): 894-904.*

*Rodel, B., T. Wagner, et al. (1998). "The human homologue (GFI1B) of the chicken GFI gene maps to chromosome 9q34.13-A locus frequently altered in hematopoietic diseases." Genomics **54**(3): 580-582.*

*Rosenblum, J. S. and G. Blobel (1999). "Autoproteolysis in nucleoporin biogenesis." Proc Natl Acad Sci U S A **96**(20): 11370-11375.*

*Rouse, J., P. Cohen, et al. (1994). "A novel kinase cascade triggered by stress and heat shock that stimulates MAPKAP kinase-2 and phosphorylation of the small heat shock proteins." Cell **78**(6): 1027-1037.*

Saleque, S., S. Cameron, et al. The zinc-finger proto-oncogene Gfi-1b is essential for development of the erythroid and megakaryocytic lineages, Genes Dev. 2002 Feb 1;16(3):301-6. doi:10.1101/gad.959102.

*Saleque, S., J. Kim, et al. (2007). "Epigenetic regulation of hematopoietic differentiation by Gfi-1 and Gfi-1b is mediated by the cofactors CoREST and LSD1." Mol Cell **27**(4): 562-572.*

*Sato, A., M. Okada, et al. (2014). "Pivotal role for ROS activation of p38 MAPK in the control of differentiation and tumor-initiating capacity of glioma-initiating cells." Stem Cell Res **12**(1): 119-131.*

Saultz, J. N. and R. Garzon (2016). "Acute Myeloid Leukemia: A Concise Review."

*Schulz, D., L. Vassen, et al. (2012). "Gfi1b negatively regulates Rag expression directly and via the repression of FoxO1." J Exp Med **209**(1): 187-199.*

*Schulze, H., A. Schlagenhauf, et al. (2017). "Recessive grey platelet-like syndrome with unaffected erythropoiesis in the absence of the splice isoform GFI1B-p37." Haematologica **102**(9): e375-e378.*

*Schutte, J., H. Wang, et al. (2016). "An experimentally validated network of nine haematopoietic transcription factors reveals mechanisms of cell state stability." Elife **22**(5): 11469.*

*Seita, J. and I. L. Weissman (2010). "Hematopoietic stem cell: self-renewal versus differentiation." Wiley Interdiscip Rev Syst Biol Med **2**(6): 640-653.*

*Sengupta, A., G. Upadhyay, et al. (2016). "Reciprocal regulation of alternative lineages by Rgs18 and its transcriptional repressor Gfi1b." J Cell Sci **129**(1): 145-154.*

*Silva, A., A. Girio, et al. (2011). "Intracellular reactive oxygen species are essential for PI3K/Akt/mTOR-dependent IL-7-mediated viability of T-cell acute lymphoblastic leukemia cells." Leukemia **25**(6): 960-967.*

*Slape, C. and P. D. Aplan (2004). "The role of NUP98 gene fusions in hematologic malignancy." Leuk Lymphoma **45**(7): 1341-1350.*

*Smith, A. M., F. J. Calero-Nieto, et al. (2012). "Integration of Elf-4 into stem/progenitor and erythroid regulatory networks through locus-wide chromatin studies coupled with in vivo functional validation." Mol Cell Biol **32**(4): 763-773.*

*Smith, B. D., C. L. Beach, et al. (2014). "Survival and hospitalization among patients with acute myeloid leukemia treated with azacitidine or decitabine in a large managed care population: a real-world, retrospective, claims-based, comparative analysis." Experimental Hematology & Oncology **3**: 10-10.*

*Song, G., G. Ouyang, et al. (2005). "The activation of Akt/PKB signaling pathway and cell survival." J Cell Mol Med **9**(1): 59-71.*

*Subramanian, A., P. Tamayo, et al. (2005). "Gene set enrichment analysis: a knowledge-based approach for interpreting genome-wide expression profiles." Proc Natl Acad Sci U S A **102**(43): 15545-15550.*

*Sykes, S. M., S. W. Lane, et al. (2011). "AKT/FOXO signaling enforces reversible differentiation blockade in myeloid leukemias." Cell **146**(5): 697-708.*

*Tallmann, M. S. (2004). "Curative therapeutic approaches to APL." Ann Hematol **83**(1): S81-82.*

*Tan, Y., R. Yu, et al. (2003). "Betulinic acid-induced programmed cell death in human melanoma cells involves mitogen-activated protein kinase activation." Clin Cancer Res **9**(7): 2866-2875.*

*Testa, J. R. and P. N. Tsichlis (2005). "AKT signaling in normal and malignant cells." Oncogene **24**(50): 7391-7393.*

Thorsteinsdottir, U., E. Kroon, et al. (2001). Defining Roles for HOX and MEIS1 Genes in Induction of Acute Myeloid Leukemia, Mol Cell Biol. 2001 Jan;21(1):224-34. doi:10.1128/MCB.21.1.224-234.2001.

*Tong, B., H. L. Grimes, et al. (1998). "The Gfi-1B proto-oncoprotein represses p21WAF1 and inhibits myeloid cell differentiation." Mol Cell Biol **18**(5): 2462-2473.*

*Tothova, Z. and D. G. Gilliland (2007). "FoxO transcription factors and stem cell homeostasis: insights from the hematopoietic system." Cell Stem Cell **1**(2): 140-152.*

*Trachootham, D., J. Alexandre, et al. (2009). "Targeting cancer cells by ROS-mediated mechanisms: a radical therapeutic approach?" Nat Rev Drug Discov **8**(7): 579-591.*

*Trachootham, D., W. Lu, et al. (2008). "Redox regulation of cell survival." Antioxid Redox Signal **10**(8): 1343-1374.*

*Tsai, W. B., Y. M. Chung, et al. (2008). "Functional interaction between FOXO3a and ATM regulates DNA damage response." Nat Cell Biol **10**(4): 460-467.*

*Tsukada, M., Y. Ota, et al. (2017). "In Vivo Generation of Engraftable Murine Hematopoietic Stem Cells by Gfi1b, c-Fos, and Gata2 Overexpression within Teratoma." Stem Cell Reports **9**(4): 1024-1033.*

Unnisa, Z., J. P. Clark, et al. (2012). Meis1 preserves hematopoietic stem cells in mice by limiting oxidative stress, Blood. 2012 Dec 13;120(25):4973-81. doi:10.1182/blood-2012-06-435800.

*Valk, P. J., R. G. Verhaak, et al. (2004). "Prognostically useful gene-expression profiles in acute myeloid leukemia." N Engl J Med **350**(16): 1617-1628.*

*Vardiman, J. W., J. Thiele, et al. (2009). "The 2008 revision of the World Health Organization (WHO) classification of myeloid neoplasms and acute leukemia: rationale and important changes." Blood **114**(5): 937-951.*

*Vassen, L., H. Beauchemin, et al. (2014). "Growth factor independence 1b (gfi1b) is important for the maturation of erythroid cells and the regulation of embryonic globin expression." PLoS One **9**(5): e96636.*

*Vassen, L., T. Okayama, et al. (2007). "Gfi1b:green fluorescent protein knock-in mice reveal a dynamic expression pattern of Gfi1b during hematopoiesis that is largely complementary to Gfi1." Blood **109**(6): 2356-2364.*

Verhaak, R. G. W., B. J. Wouters, et al. (2009). Prediction of molecular subtypes in acute myeloid leukemia based on gene expression profiling, Haematologica. 2009 Jan;94(1):131-4. Epub 2008 Oct 6 doi:10.3324/haematol.13299.

Walker, A. and G. Marcucci (2013). Molecular prognostic factors in cytogenetically normal acute myeloid leukemia, Expert Rev Hematol. 2012 Oct;5(5):547-58. doi:10.1586/ehm.12.45.

*Wang, F., P. Jiao, et al. (2010). "Turning Tumor-Promoting Copper into an Anti-Cancer Weapon via High-Throughput Chemistry." Current medicinal chemistry **17**(25): 2685-2698.*

*Wang, L. J., Z. H. Wu, et al. (2017). "Zinc Finger E-Box Binding Protein 2 (ZEB2) Suppress Apoptosis of Vascular Endothelial Cells Induced by High Glucose Through Mitogen-Activated Protein Kinases (MAPK) Pathway Activation." Med Sci Monit **23**: 2590-2598.*

*Wang, Y., A. V. Krivtsov, et al. (2010). "The Wnt/β-catenin Pathway Is Required for the Development of Leukemia Stem Cells in AML." Science **327**(5973): 1650-1653.*

*Warlick, E. D., A. Cioc, et al. (2009). "Allogeneic stem cell transplantation for adults with myelodysplastic syndromes: importance of pretransplant disease burden." Biol Blood Marrow Transplant **15**(1): 30-38.*

*Wells, S. J., R. A. Bray, et al. (1996). "CD117/CD34 expression in leukemic blasts." Am J Clin Pathol **106**(2): 192-195.*

*Wilson, N. K., S. D. Foster, et al. (2010). "Combinatorial transcriptional control in blood stem/progenitor cells: genome-wide analysis of ten major transcriptional regulators." Cell Stem Cell **7**(4): 532-544.*

*Winterbourn, C. C. and M. B. Hampton (2008). "Thiol chemistry and specificity in redox signaling." Free Radical Biology and Medicine **45**(5): 549-561.*

*Wouters, B. J., B. Lowenberg, et al. (2009). "Double CEBPA mutations, but not single CEBPA mutations, define a subgroup of acute myeloid leukemia with a distinctive gene expression profile that is uniquely associated with a favorable outcome." Blood **113**(13): 3088-3091.*

*Xu, Q., S. E. Simpson, et al. (2003). "Survival of acute myeloid leukemia cells requires PI3 kinase activation." Blood **102**(3): 972-980.*

*Xu, W. and B. L. Kee (2007). "Growth factor independent 1B (Gfi1b) is an E2A target gene that modulates Gata3 in T-cell lymphomas." Blood **109**(10): 4406-4414.*

*Xu, Y., N. Li, et al. (2014). "Emerging roles of the p38 MAPK and PI3K/AKT/mTOR pathways in oncogene-induced senescence." Trends Biochem Sci **39**(6): 268-276.*

*Yahata, T., Y. Muguruma, et al. (2008). "Quiescent human hematopoietic stem cells in the bone marrow niches organize the hierarchical structure of hematopoiesis." Stem Cells **26**(12): 3228-3236.*

*Yahata, T., T. Takanashi, et al. (2011). "Accumulation of oxidative DNA damage restricts the self-renewal capacity of human hematopoietic stem cells." Blood **118**(11): 2941-2950.*

*Zhang, H., H. Fang, et al. (2014). "Reactive oxygen species in eradicating acute myeloid leukemic stem cells." Stem Cell Investig **1**.*

*Zhang, H., H. Fang, et al. (2014). "Reactive oxygen species in eradicating acute myeloid leukemic stem cells." Stem Cell Investigation **1**: 13.*

*Zhou, F., Q. Shen, et al. (2013). "Novel roles of reactive oxygen species in the pathogenesis of acute myeloid leukemia." J Leukoc Biol **94**(3): 423-429.*

*Zou, P., H. Yoshihara, et al. (2011). "p57(Kip2) and p27(Kip1) cooperate to maintain hematopoietic stem cell quiescence through interactions with Hsc70." Cell Stem Cell **9**(3): 247-261.*

8 Publications

8.1 Publication arising from this thesis

"Growth factor independence 1b – A key player in genesis and maintenance of acute myeloid leukaemia and myelodysplastic syndrome"

Aniththa Thivakaran, Lacramioara Botezatu, Judith M. Hönes, Judith Schütte, Lothar Vassen, Yahya S. Al-Matary, Michael Heuser, Felicitas Thol, Razif Gabdoulline, Nadine Olberding, Renata Köster, Klaus Lennartz, Andre Görgens, Bernd Giebel, Bertram Opalka, Ulrich Dührsen and Cyrus Khandanpour

Haematologica, 2018, has been accepted for publication

8.2 Published publications

"Enforced GFI1 expression impedes human and murine leukemic cell growth"

Aniththa Thivakaran†, Judith M. Hönes†, Lacramioara Botezatu†, Symone Vitoriano da Conceição Castro, Judith Schütte, Karen B. I. Fischer, Yahya S. Al-Matary, Lothar Vassen, André Görgens, Ulrich Dührsen, Bernd Giebel, and Cyrus Khandanpour

Scientific Reports-Nature, 2017

† shared authorship

“GFI1 as a novel prognostic and therapeutic factor for AML/MDS”

J.M. Hönes†, L. Botezatu†, A. Helness, C. Vadnais, L.Vassen, F. Robert, S.M. Hergenhan, **A.Thivakaran**, J. Schütte, Y. S. Al-Matary, R. F. Lams, J. Fraszczak, H. Makishima, T. Radivoyevitch, B. Przychodzen, S. Vitoriano da Conceição Castro,A. Görgens B.Giebel, L. Klein-Hitpass, K.Lennartz, M. Heuser, C.Thiede, G.Ehringer, U.Dührsen, JP. Maciejewski, T. Möröy, C.Khandanpour

Leukemia-Nature, 2016

† shared authorship

“Epigenetic therapy as a novel approach for GFI136N-associated murine/human AML”

L. Botezatu†, Michel LC†, Helness A, Vadnais C, Makishima H, Hönes JM, Robert F, Vassen L, **Thivakaran A**, Al-Matary Y, Lams RF, Schütte J, Giebel B, Görgens B, Heuser M, Medyouf H, Maciejewski J, Dührsen U, Möröy T, Khandanpour C

Exp Hematol, 2016

† shared authorship

"**Acute myeloid leukemia cells polarize macrophages towards a leukemia supporting state in a Growth factor independence 1 dependent manner."**

Al-Matary, Y. S. †, L. Botezatu †, B. Opalka, J. M. Hones, R. F. Lams, **A. Thivakaran**, J. Schütte, R. Koster, K. Lennartz, T. Schroeder, R. Haas, U. Duhrsen and C. Khandanpour

Haematologica, 2016

† shared authorship

9 Acknowledgments

First, I would like to express my deep gratitude and respect to my supervisor, PD Dr. Cyrus Khandanpour. He was a brilliant and kind supervisor during my PhD journey, advising and supporting me throughout.

I also thank my group members in my lab. Dr. Lacra Botezatue, the postdoc in our lab, provided tips and tricks about *in vivo* study. My friend Dr. Judith Hönes is a great person, and both of us had a lot of fun in the lab. It was really a good time with her. One more important person is my colleague Yahya Al-Matary, who is a very helpful person. In many cases he was ready to help me. I would like also thank Pradeep, our new PhD student from India. We were a good team; we managed a lot of trouble in some projects, ultimately with positive results. He always helped me, like my friend Yahya Al-Matary. I would also like to thank Dr. Judith Schütte, who gave me lot of advice about writing my paper/thesis. She also advised me on planning experiments, and I gained some new knowledge from her about bioinformatics study. My thanks go also to Renata Köster, Marina Suslo, Daria Frank.

Last, I would like to thank my friends and family, especially my mother and father for always believing in me, for their continuous love and their support of my decisions. My greatest appreciation goes to my husband, Thivakaran Aritharan, who has always been a great support in all my struggles and frustrations in my life and studies. Without my parents and my husband, I could not have made it here.

My life will change completely by the start of the year 2018—I will have a baby boy. So I will face a new challenge in my life, and it is never boring.

.

10 Awards

58th ASH Annual Meeting, San Diego, USA, 2016

22nd Congress of EHA, Madrid, 2017

11 Congress Contributions

2015 Oral presentation in DGHO, Basel, Switzerland

2016 Poster in Heidelberg, Germany

2016 Poster show in 58th ASH Annual Meeting in San Diego, USA

2017 Poster and 2-Minute-Talk, Mildreed Sheel, Bonn, Germany

2017 Poster show in EHA, Madrid, Spain

12 Curriculum Vitae

Der Lebenslauf ist in der Online-Version aus Gründen des Datenschutzes nicht enthalten.

Der Lebenslauf ist in der Online-Version aus Gründen des Datenschutzes nicht enthalten.

Der Lebenslauf ist in der Online-Version aus Gründen des Datenschutzes nicht enthalten.

13 Eidesstaatliche Erklärung

Erklärung

Hiermit erkläre ich, gem. § 6 Abs. (2) g) der Promotionsordnung der Fakultät für Biologie zur Erlangung der Dr. rer. nat., dass ich das Arbeitsgebiet, dem das Thema ***„Die Rolle von Gfi1b in der akuten myeloischen Leukämie (AML)“*** zuzuordnen ist, in Forschung und Lehre vertrete und den Antrag von ***Aniththa Thivakaran*** befürworte und die Betreuung auch im Falle eines Weggangs, wenn nicht wichtige Gründe dem entgegenstehen, weiterführen werde.

Essen, den _____

_____
PD. Dr. Cyrus Khandanpour

Erklärung

Hiermit erkläre ich, gem. § 7 Abs. (2) d) + f) der Promotionsordnung der Fakultät für Biologie zur Erlangung des Dr. rer. nat., dass ich die vorliegende Dissertation selbständig verfasst und mich keiner anderen als der angegebenen Hilfsmittel bedient, bei der Abfassung der Dissertation nur die angegeben Hilfsmittel benutzt und alle wörtlich oder inhaltlich übernommenen Stellen als solche gekennzeichnet habe.

Essen, den _____

_____
Aniththa Thivakaran

Erklärung

Hiermit erkläre ich, gem. § 7 Abs. (2) e) + g) der Promotionsordnung der Fakultät für Biologie zur Erlangung des Dr. rer. nat., dass ich keine anderen Promotionen bzw. Promotionsversuche in der Vergangenheit durchgeführt habe und dass diese Arbeit von keiner anderen Fakultät/Fachbereich abgelehnt worden ist.

Essen, den _____

_____
Aniththa Thivakaran